AMS DAYS at CERN: 15 – 17 April 2015

Latest Results from the Pierre Auger Observatory and Future Prospects for Particle Physics and Cosmic Ray Studies

Alan Watson

University of Leeds

on behalf of the Pierre Auger Collaboration

a.a.watson@leeds.ac.uk

Outline

- The Auger Observatory – close to the end of phase 1
  - Events and analysis methods
  - Vertical and inclined showers

- Spectrum measurements

- Arrival directions – some recent results

- Mass: Recent results on Nuclei
  - Photon limit
  - Neutrino limit

- Insights into hadronic interactions

- The future for the Auger Observatory

Very little discussion of implications of data: stress measurements

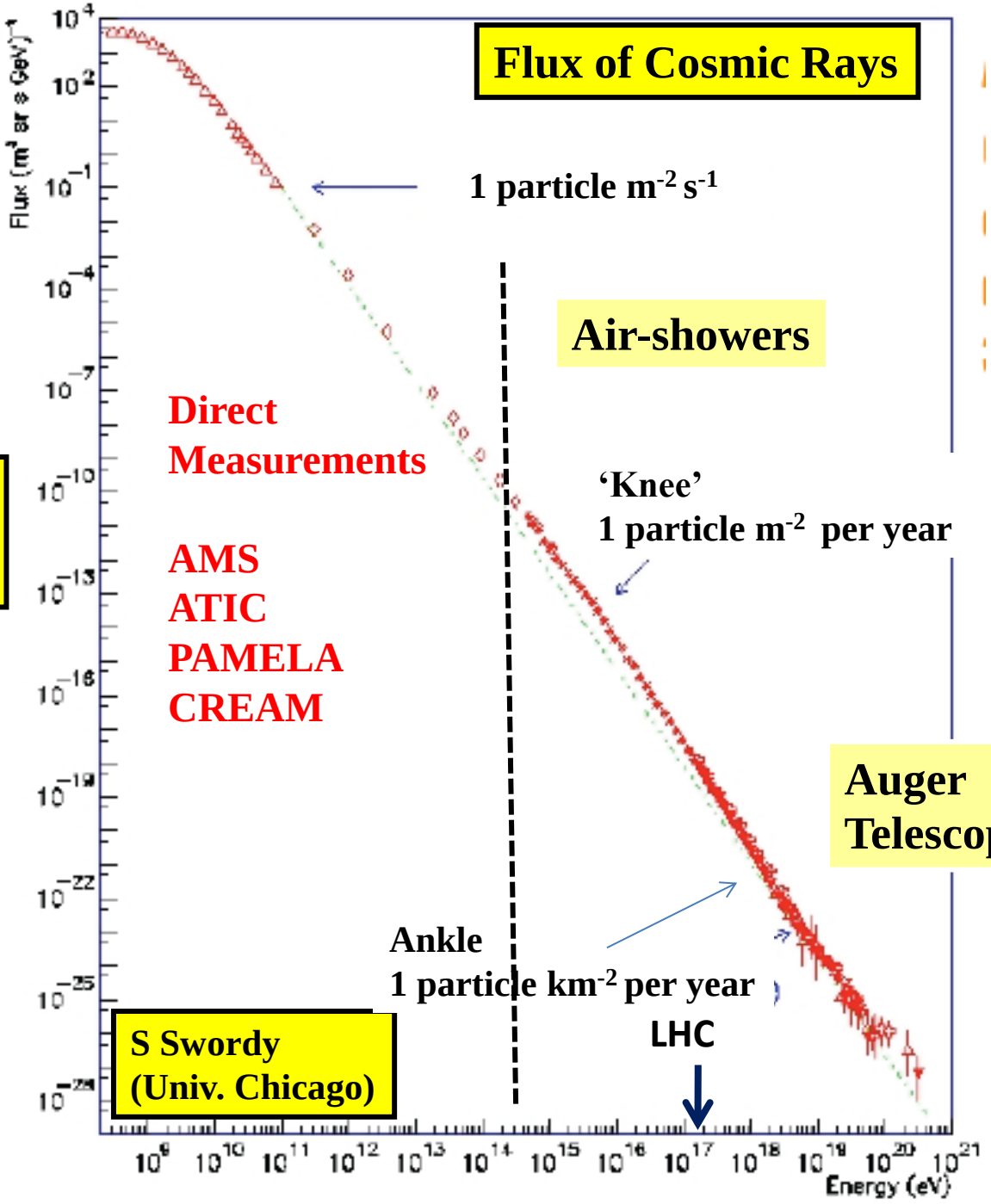

32 decades in intensity

12 decades in energy

Does the Cosmic Ray Energy Spectrum terminate?

Greisen-Zatsepin-Kuz'min – GZK effect (1966)

$$\gamma_{2.7\,K} + p \rightarrow \Delta^{+} \rightarrow n + \pi^{+} \quad \text{or} \quad p + \pi^{o}$$

and

$$\gamma_{IR/2.7\,K} + A \rightarrow (A - 1) + n$$

- **Sources must lie within ~ 100 Mpc at 100 EeV**
  - **Note that neutrinos - of different energies – come from the decay of π^{+} and n**
  - **Photons from decay of π^{o}**

The Pierre Auger Collaboration

Croatia*	**Argentina**
Czech Republic	**Australia**
France	**Brasil**
Germany	**Bolivia***
Italy	**Colombia***
Netherlands	**Mexico**
Poland	**USA**
Portugal	**Vietnam***
Rumania	***Associate Countries**
Slovenia	
Spain	**~ 400 PhD scientists from**
(United Kingdom)	**~ 100 Institutions in 17**

Aim: To measure properties of UHECR with unprecedented precision to discovery properties and origin of UHECR

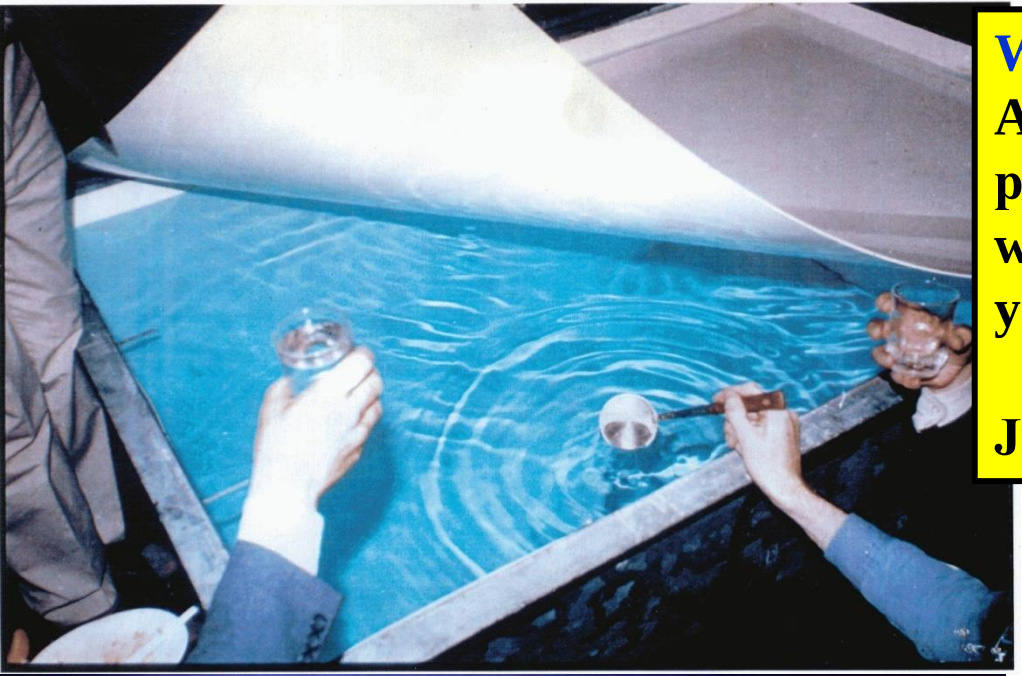

Water-Cherenkov, Haverah Park (UK):
A tank was opened at the 'end of project' party on 31 July 1987. The water shown had been in the tank for 25 years - but was quite drinkable

Jim Cronin: "An existence proof"

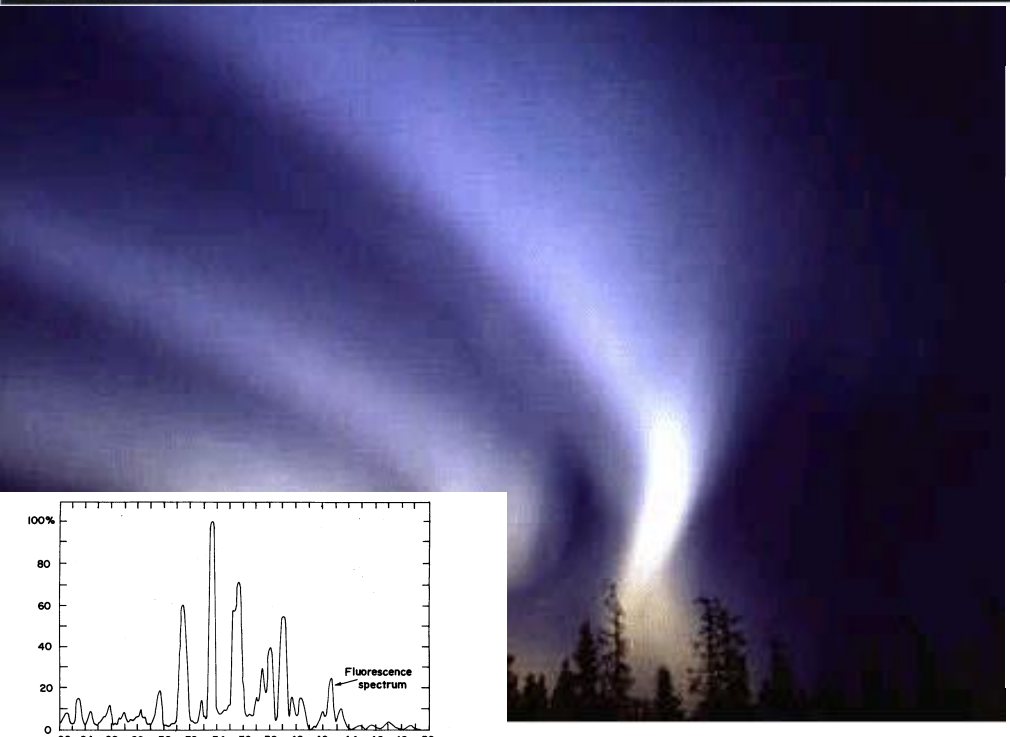

Schematic of the Fly's Eye Fluorescence Detector of University of Utah

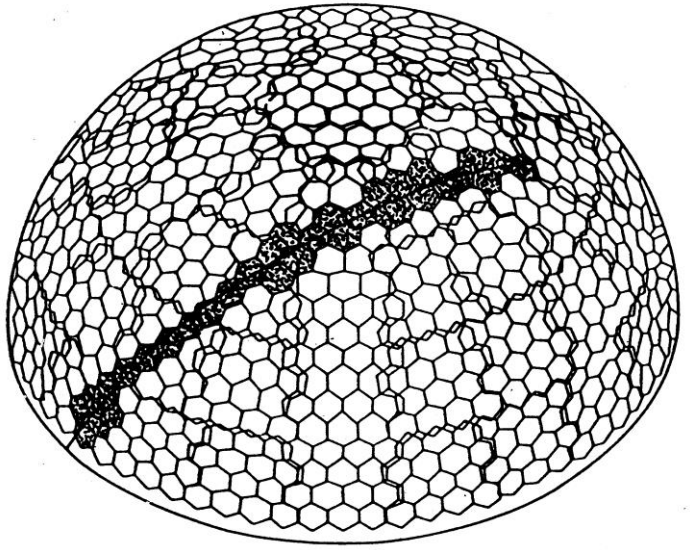

The Design of the Pierre Auger Observatory marries these two techniques in

the 'HYBRID' technique

Fluorescence →

AND

Array of water-Cherenkov detectors →

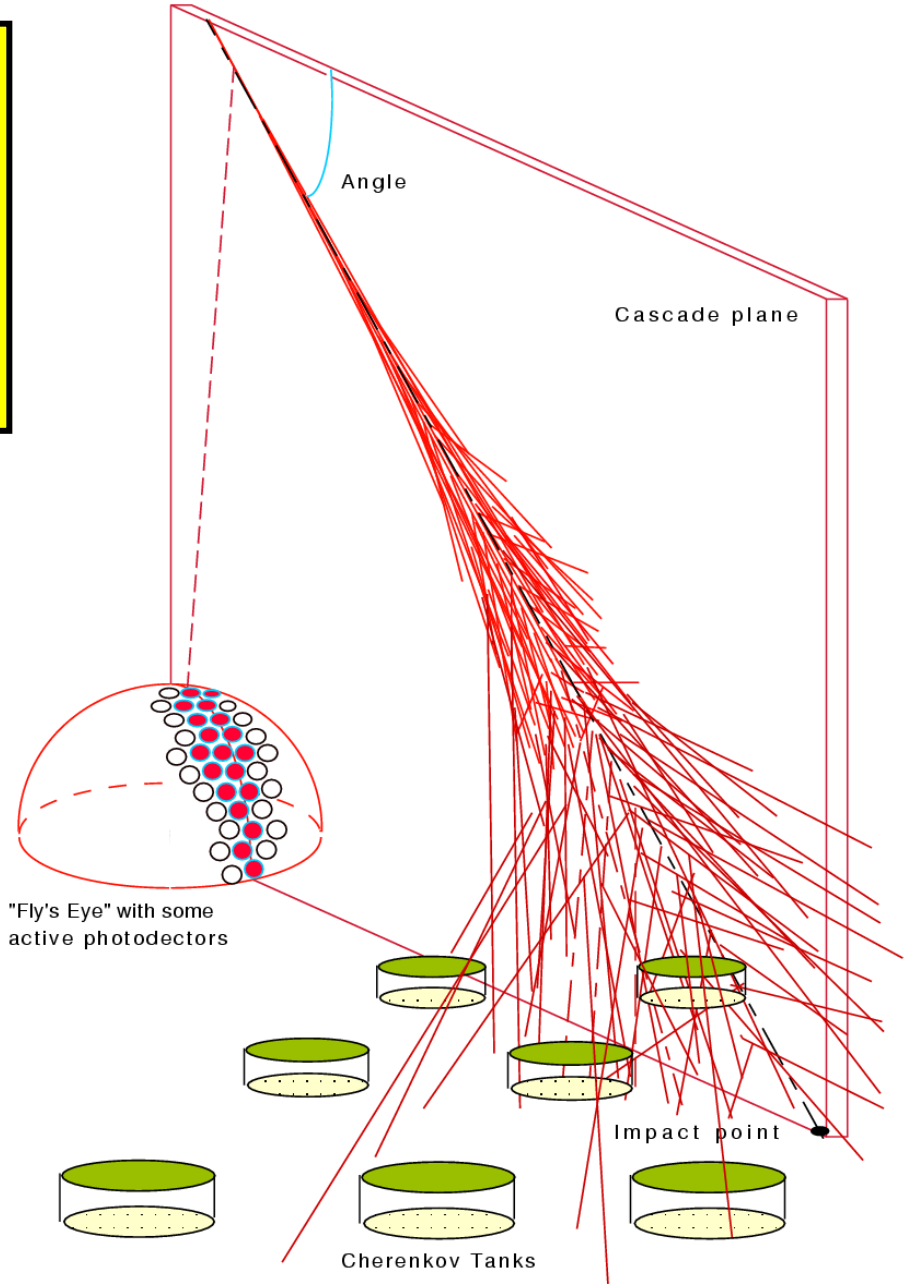

The Pierre Auger Observatory

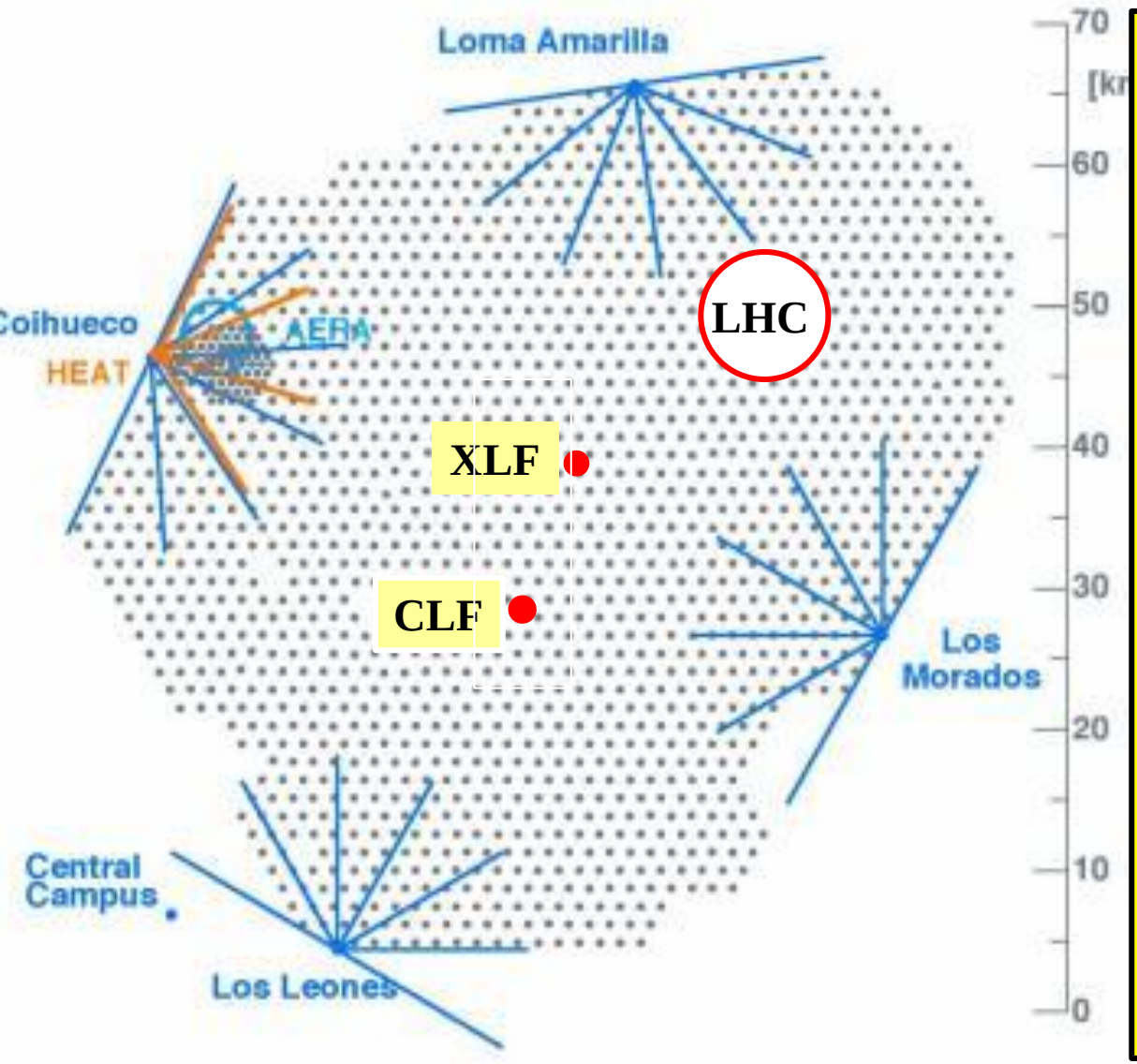

- 1600 water-Cherenkov detectors: 10 m^2 x 1.2 m
- 3000 km^2
- Fluorescence detectors at 4 locations
- Two laser facilities for monitoring atmosphere and checking reconstruction
- Lidars at each FD site
- Radio detection at AERA
- Muon detectors – buried

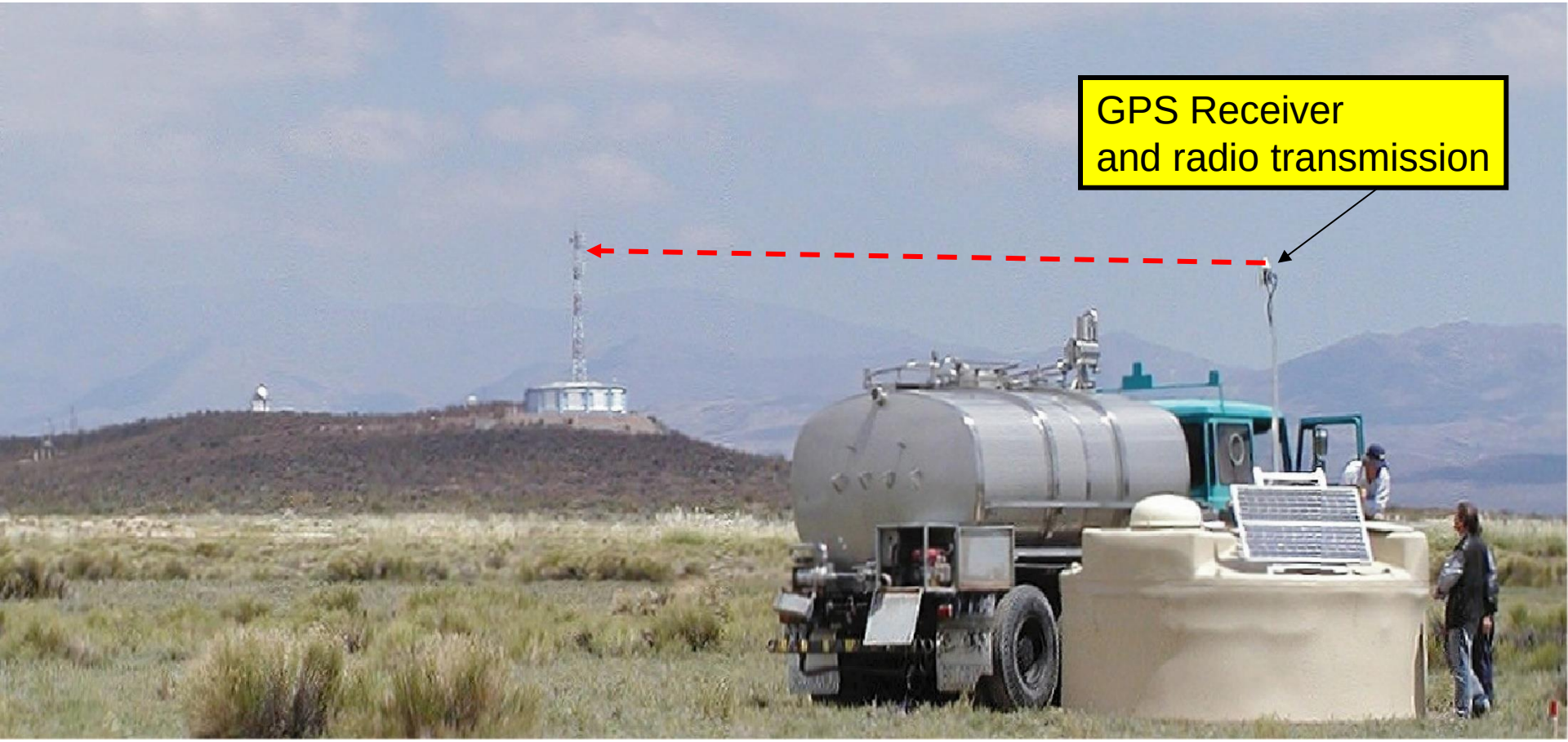
GPS Receiver
and radio transmission

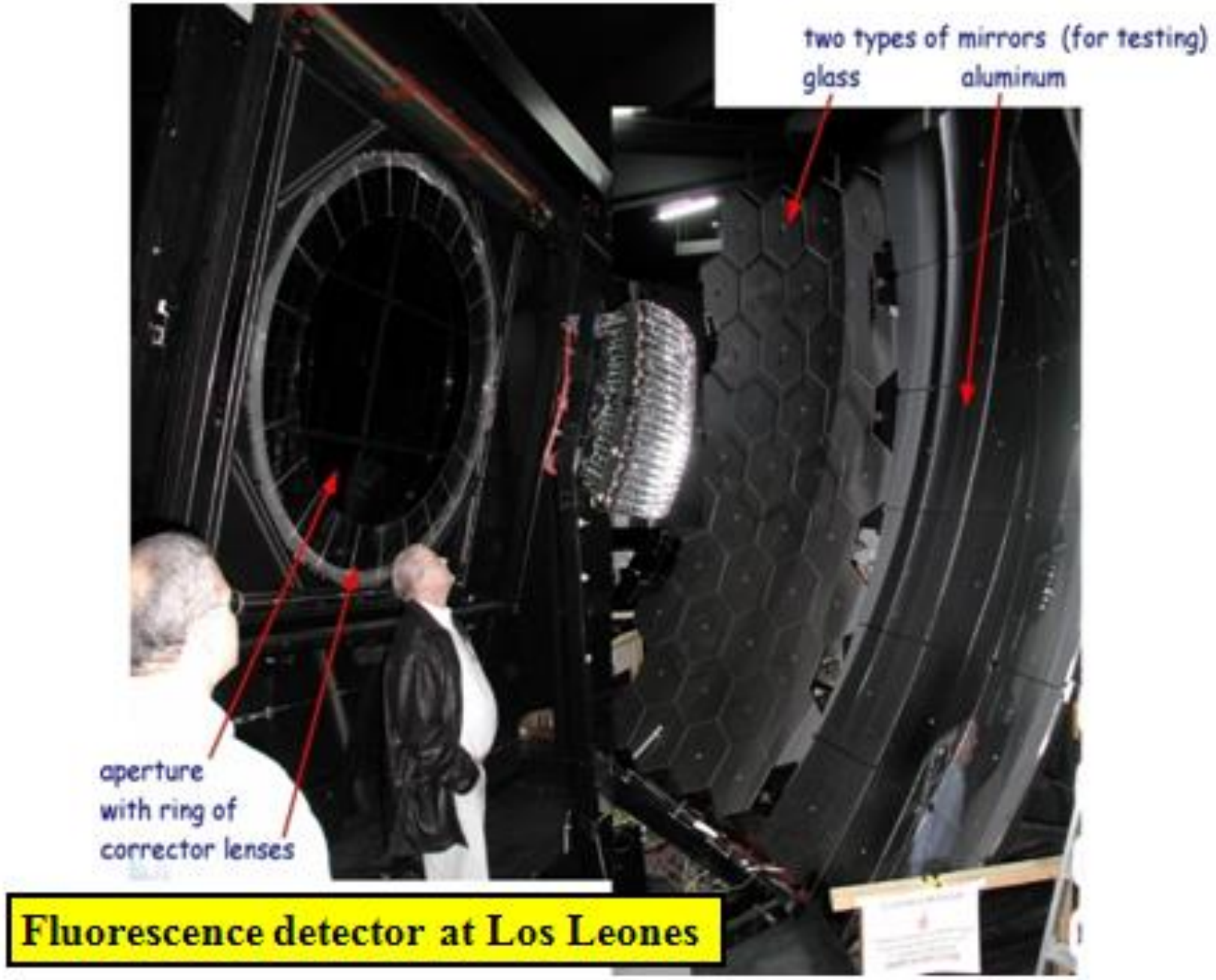

Fluorescence detector at Los Leones

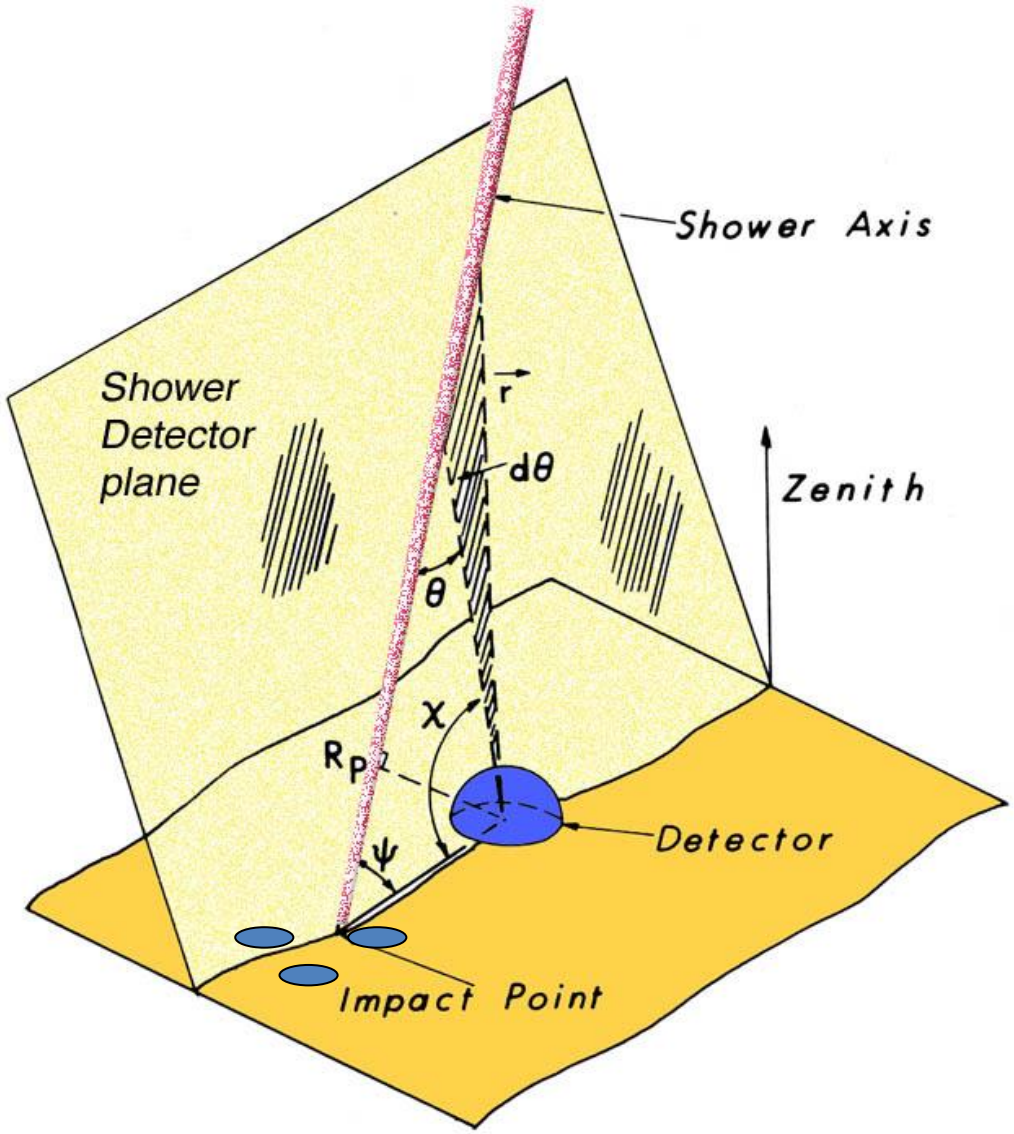

Important feature of the hybrid approach

Precise shower geometry from degeneracy given by SD timing

Essential step towards high quality energy and X_{max} resolution

Times at angles, χ , are key to finding R_p

Angular and core location resolution from Central Laser Facility

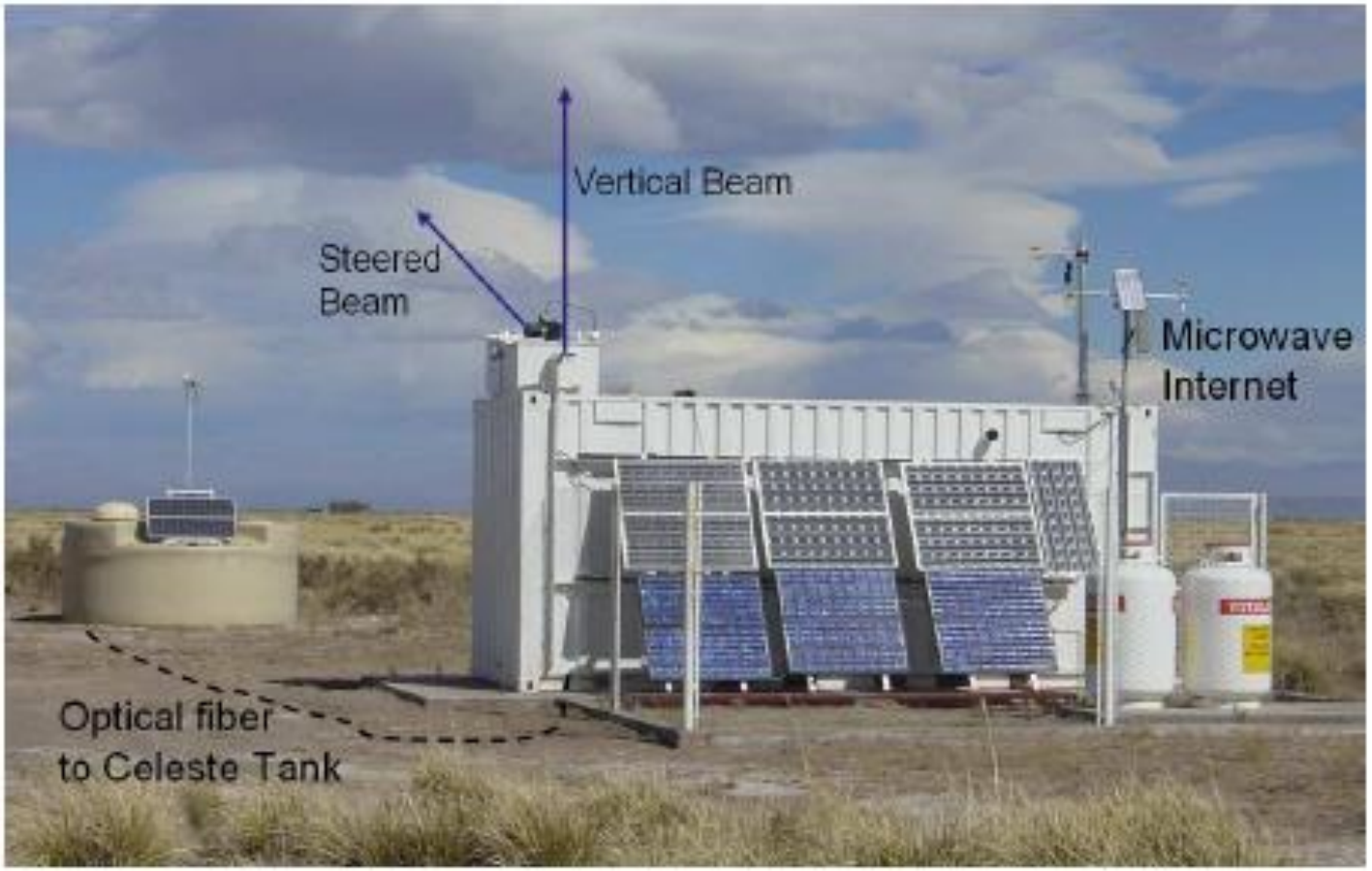

355 nm, frequency tripled, YAG laser, giving < 7 mJ per pulse: GZK energy

Angular Resolution

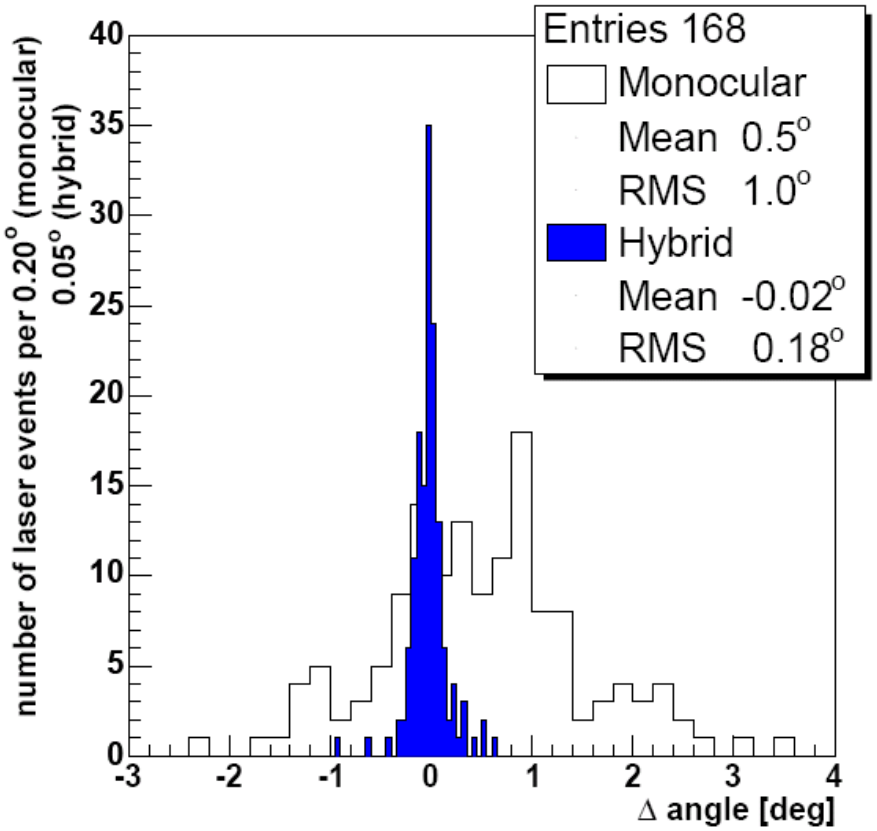

Core Location accuracy

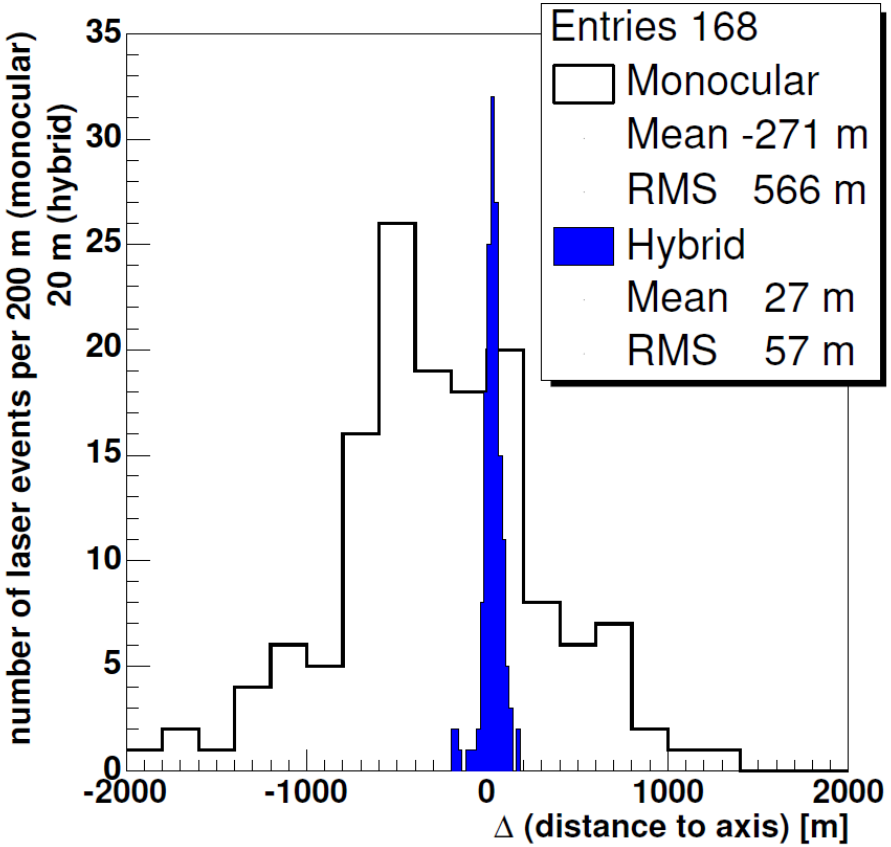

Reconstruction of an Auger Event using water-Cherenkov detectors

(i) Reconstruction of arrival direction

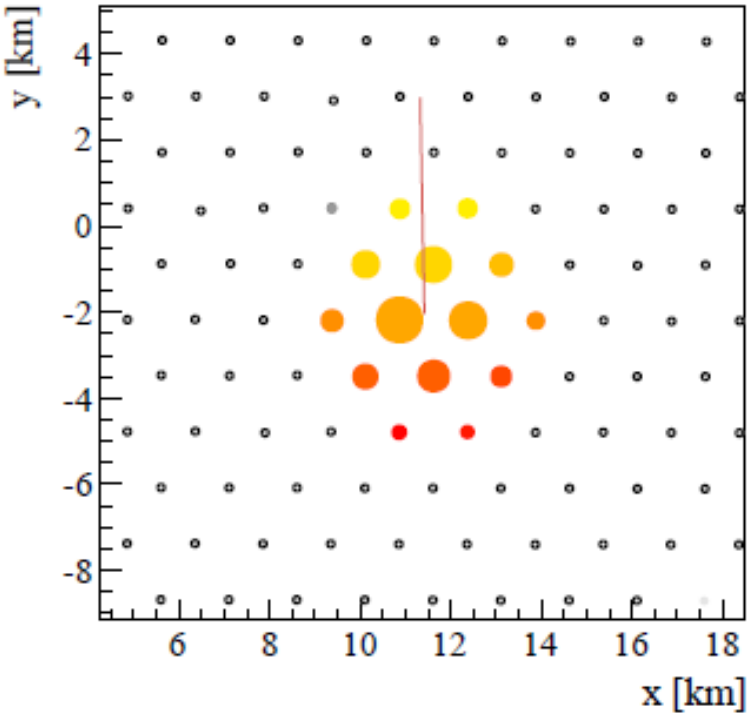

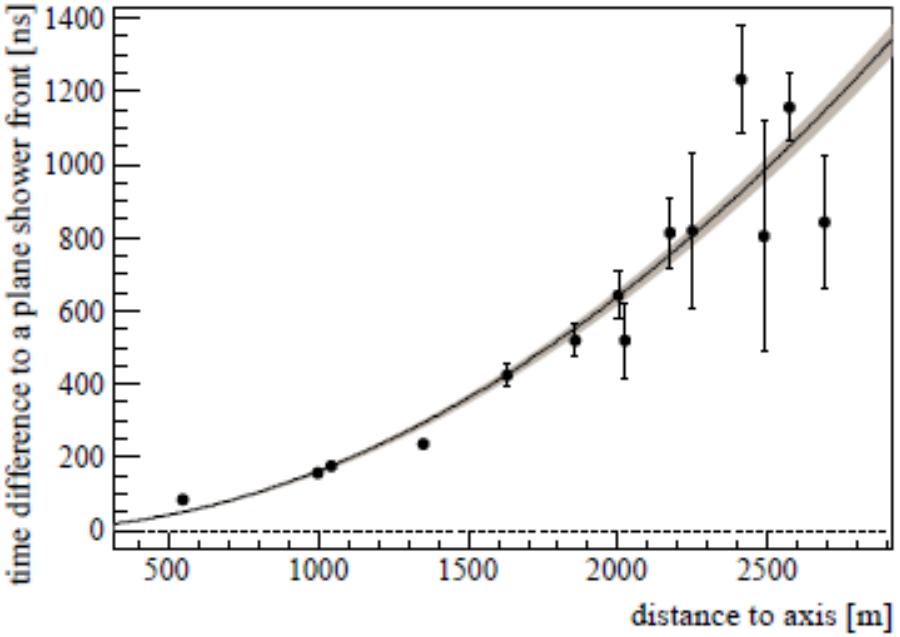

Angular Accuracy: better than 0.9° for more than 6 stations (arXiv 1502.01323)

(ii) Reconstruction of shower size, S(1000)

Signal in event, E = (104 ± 11) eV and θ = 25.1°

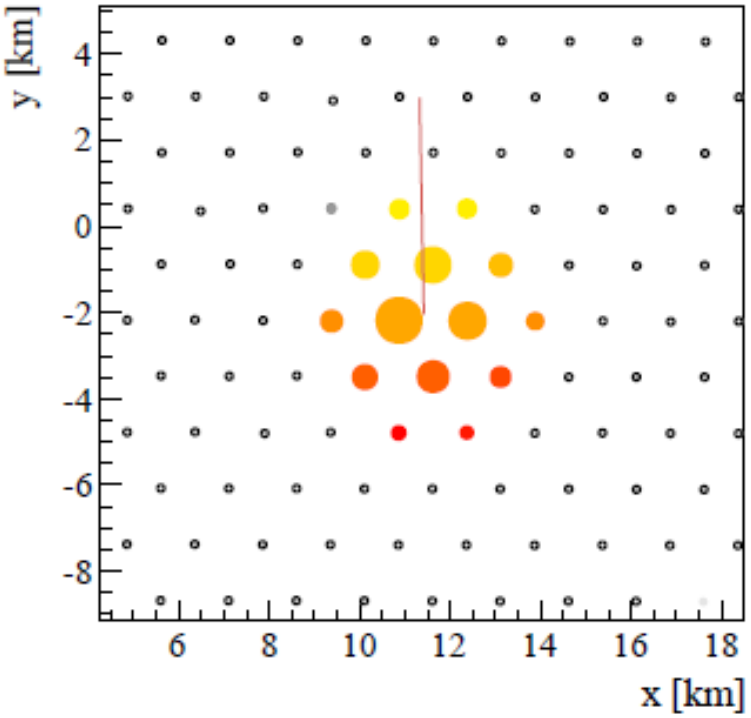

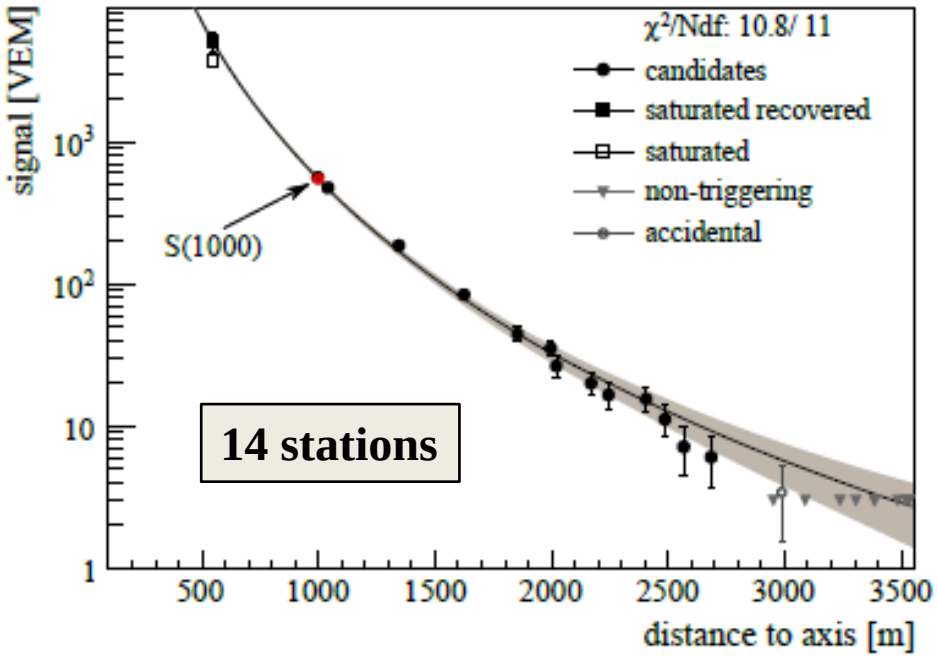

Choice of S(1000) as the 'shower size' is dictated by the spacing of the detectors

It is distance at which signal has minimum spread for a range of lateral distributions

Accuracy of S(1000) ~ 10%. **Details at arXiv 0709.2125 and 1502.01323**

(compare TA: 1.2 km spacing and parameter is S(800))

Reconstruction of fluorescence event

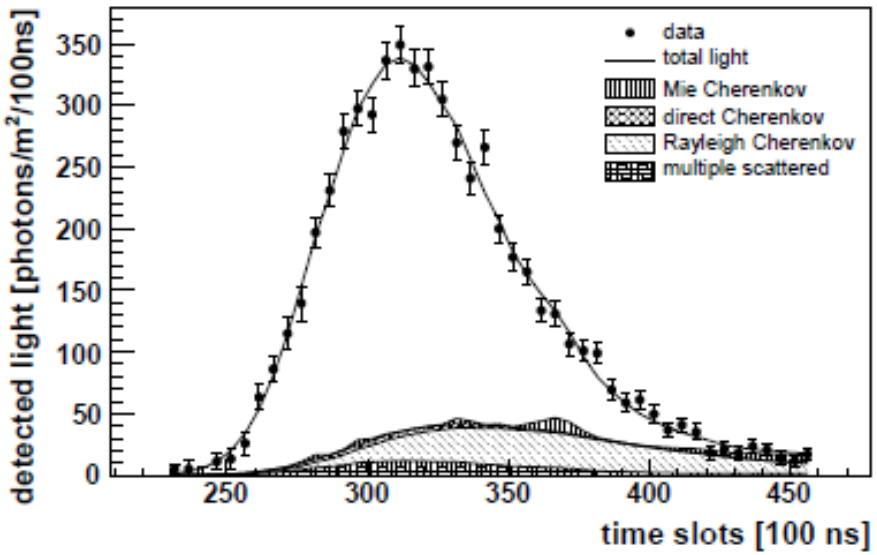

(a) Light at aperture.

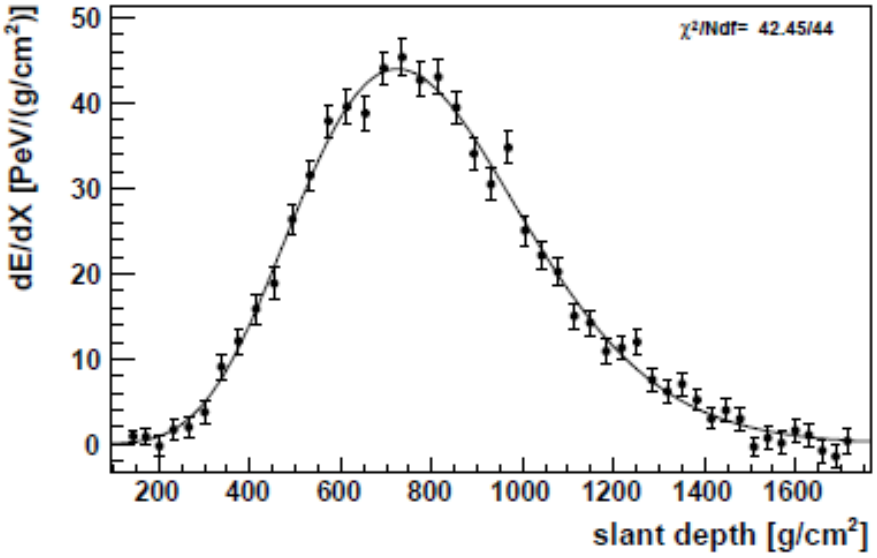

(b) Energy deposit.

A Hybrid Event

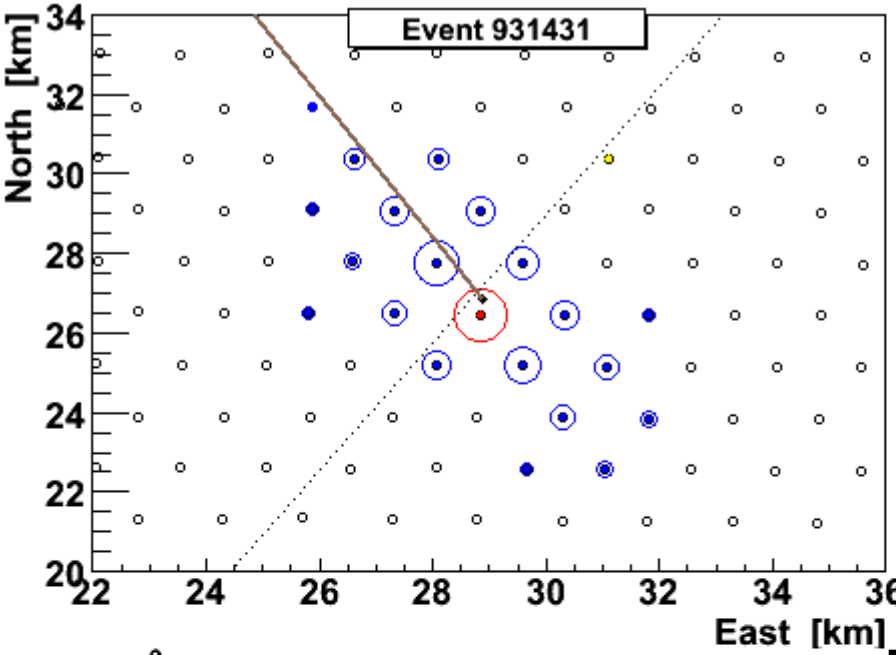

Core location

Easting 468693 ± 59

Northing 6087022 ± 80

Altitude = 1390 m a.s.l.

Shower Axis

$\theta = (62.3 \pm 0.2)^{\circ}$

$\phi = (119.7 \pm 0.1)^{\circ}$

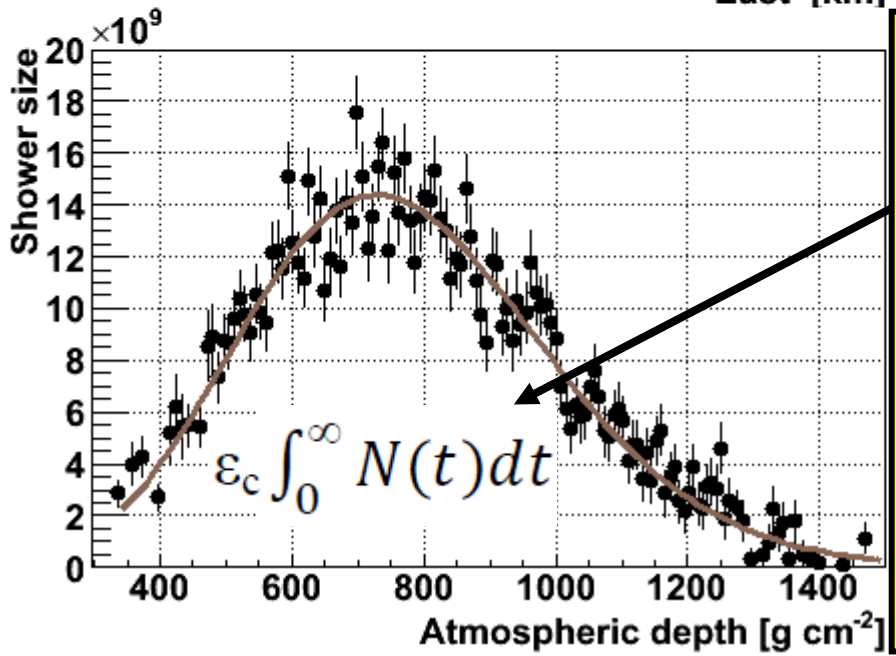

Energy Estimate
- from area under curve

$(2.1 \pm 0.5) \times 10^{19}$ eV

must also account for 'invisible energy'

$f = E_{tot}/E_{em}$

Invisible Energy

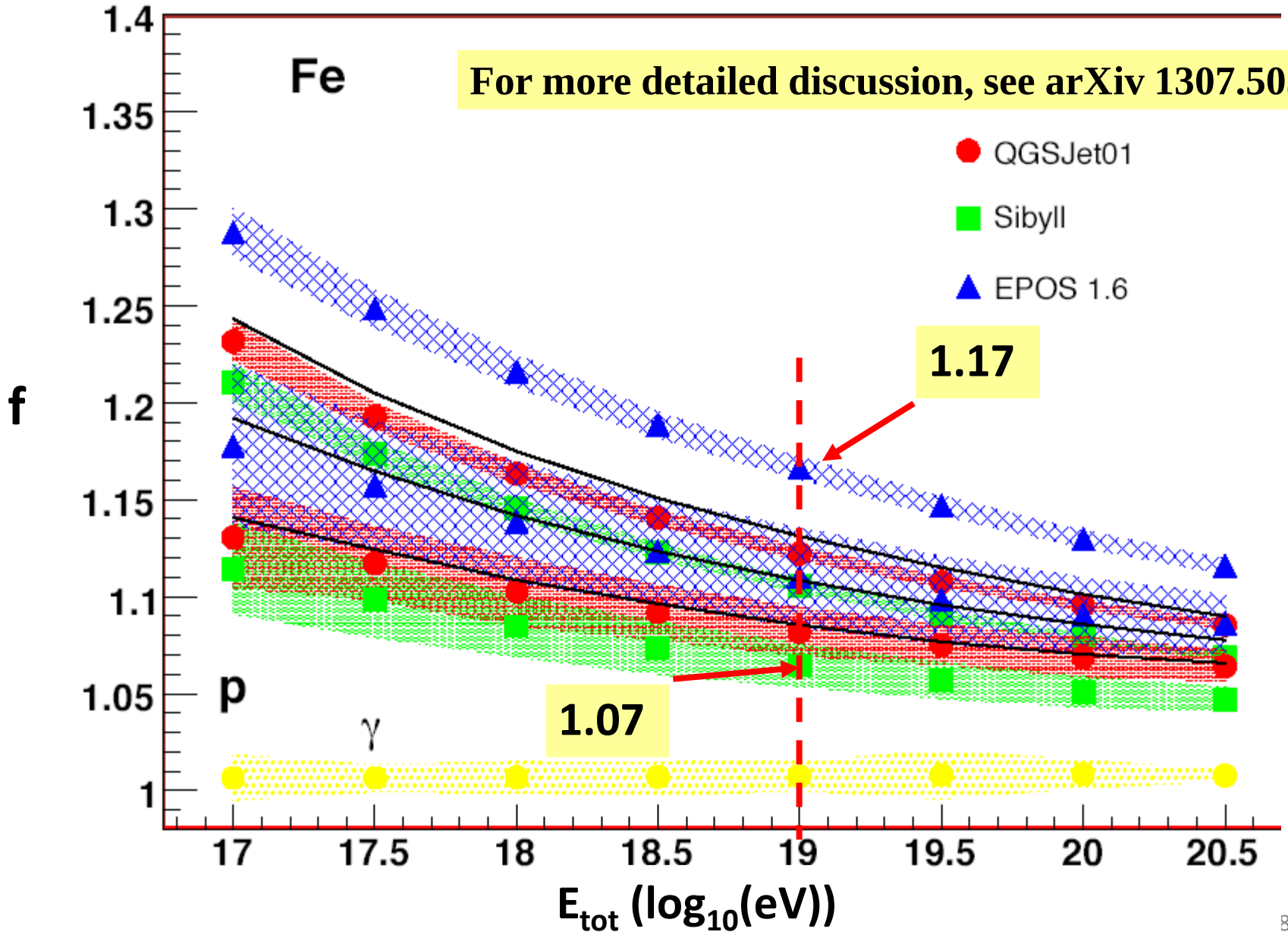

Spectrum determination: Minimal use of hadronic models

Vertical events (< 60°):

Uses fact that showers at different zenith angles but of the same energy come at same rate

Constant Intensity Cut: **$S(1000)_\theta$ is normalised to 38°, $S_{38°}$, and then compared with the calorimetric energy measured with the fluorescence detectors, E_{FD}**

Inclined events: **increased declination spread and event number (by ~ 30%) but requires a different analysis approach**

Checking the energy and X_{max} resolution

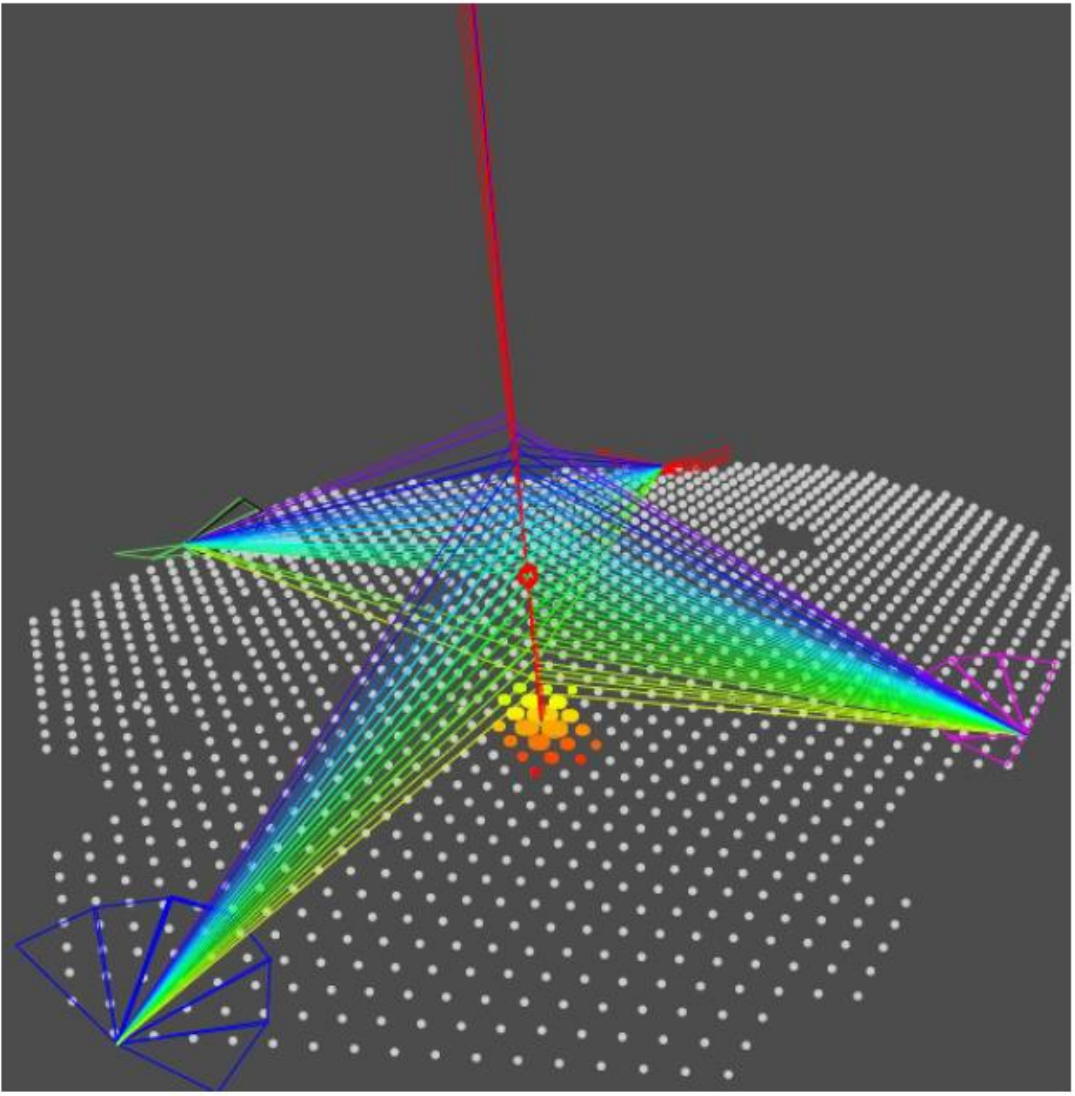

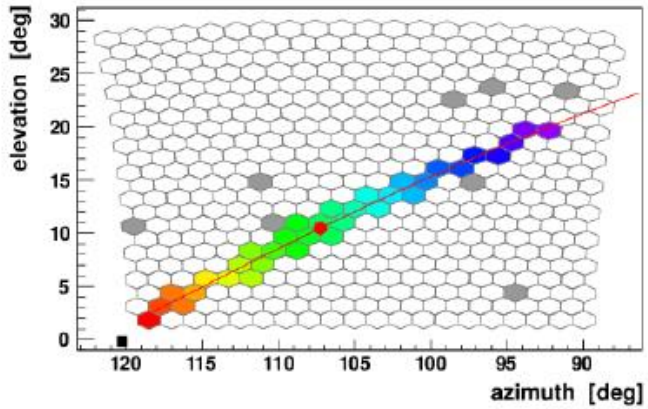

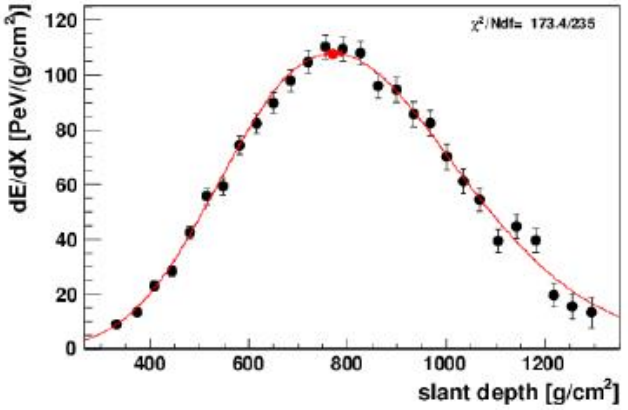

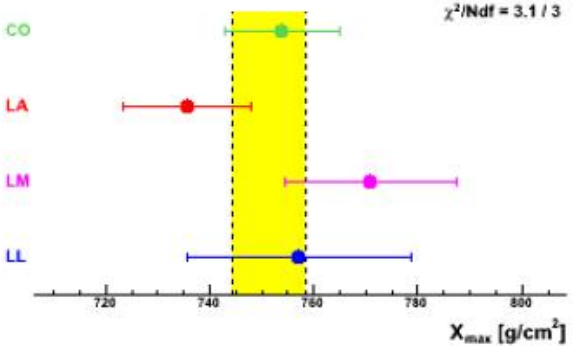

E = 7.1± 0.2 10^{19} eV - X_{max} = 752 ± 7 g/cm²

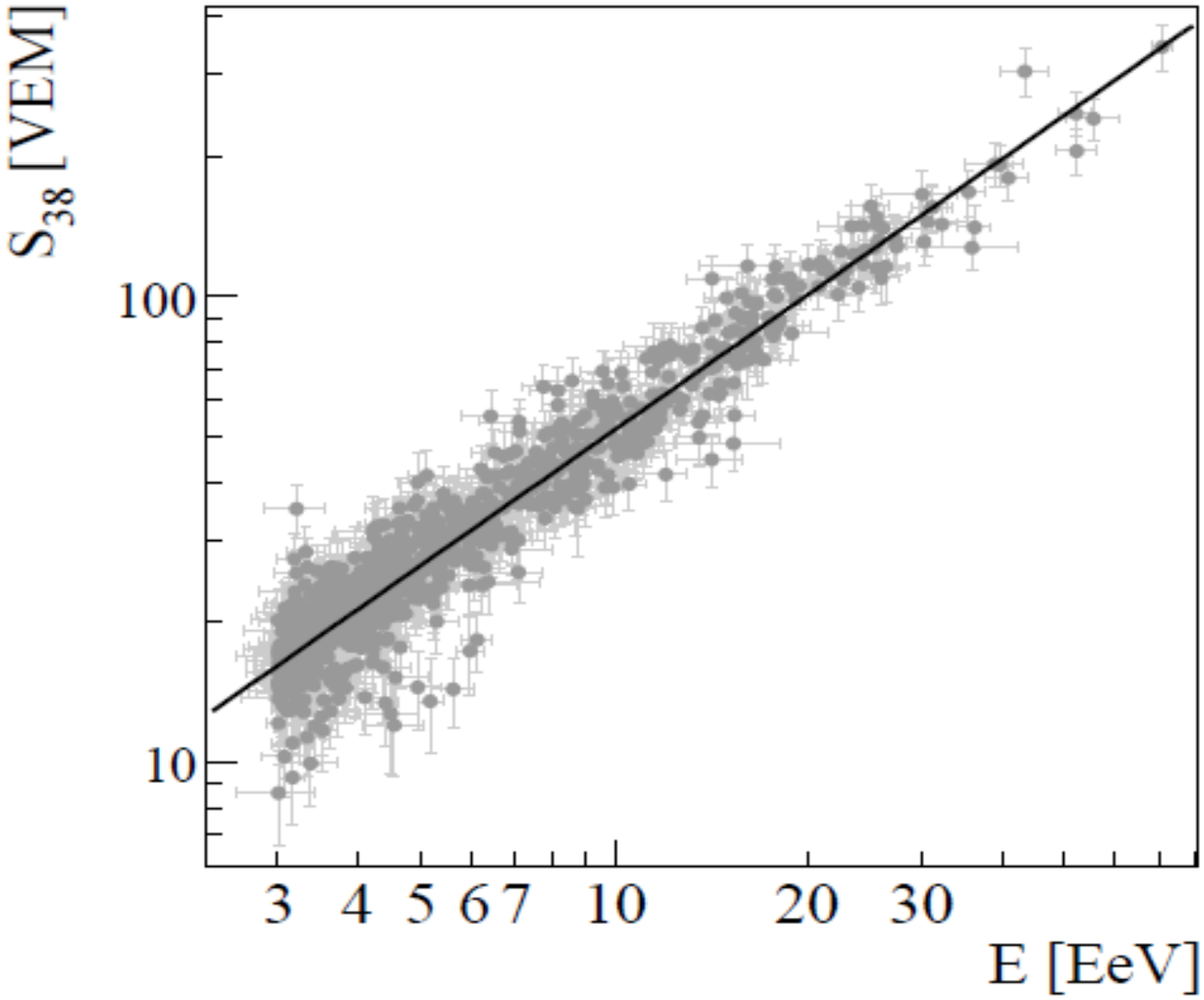

839 events

7.5 x 10^{19} eV

Auger Energy Calibration for Vertical Showers

Auger Energy Spectrum from Vertical Events:2013

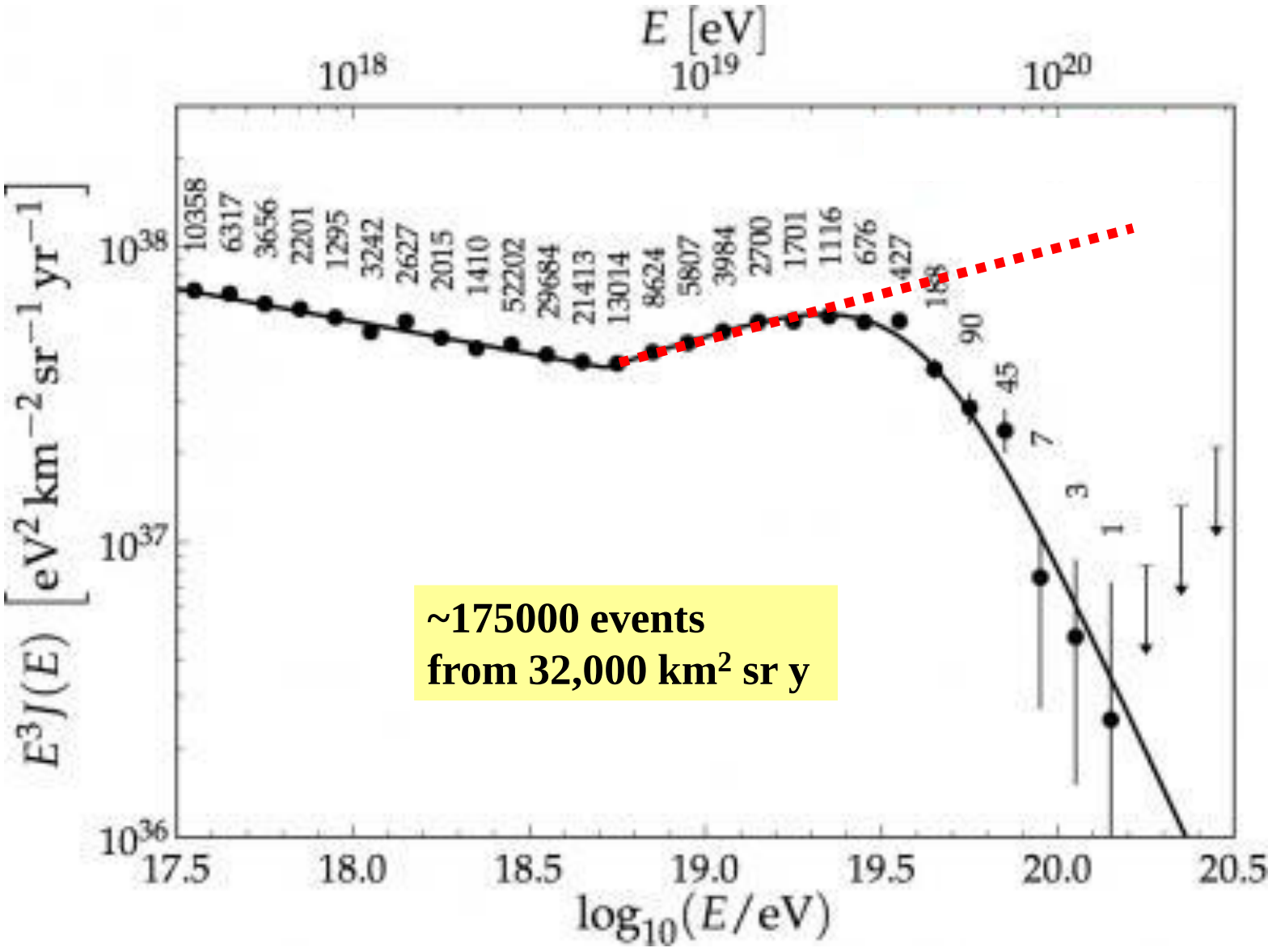

Analysis of inclined showers (> 60°)

- **Particles must penetrate more atmosphere and at observation level the signals are almost entirely muons – with contemporaneous component of electromagnetic radiation from μ-decay and knock-on electrons**

- **Muons are energetic but strongly deflected in geomagnetic field**

- **Shower loses circular symmetry**

FADC traces are short in inclined events

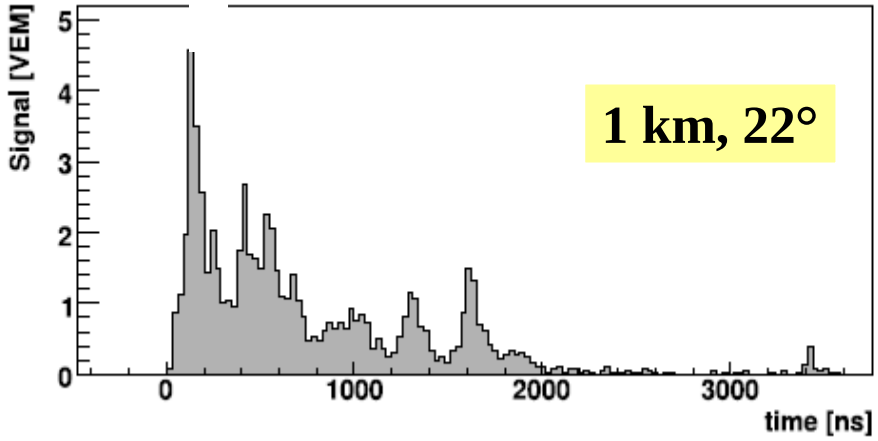

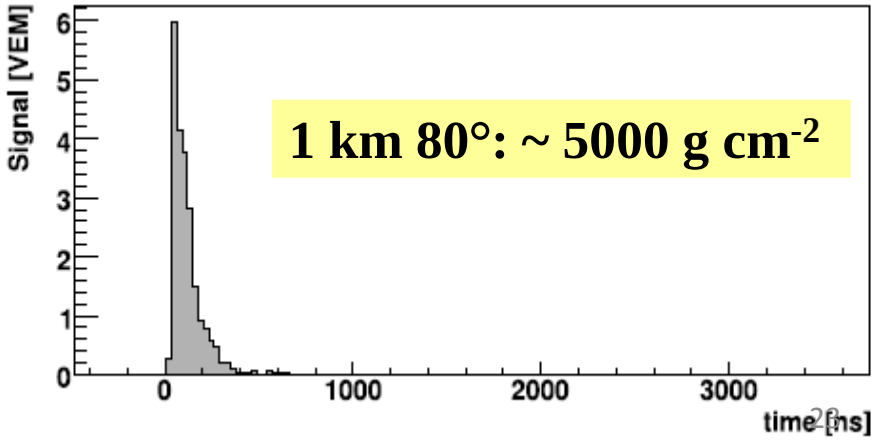

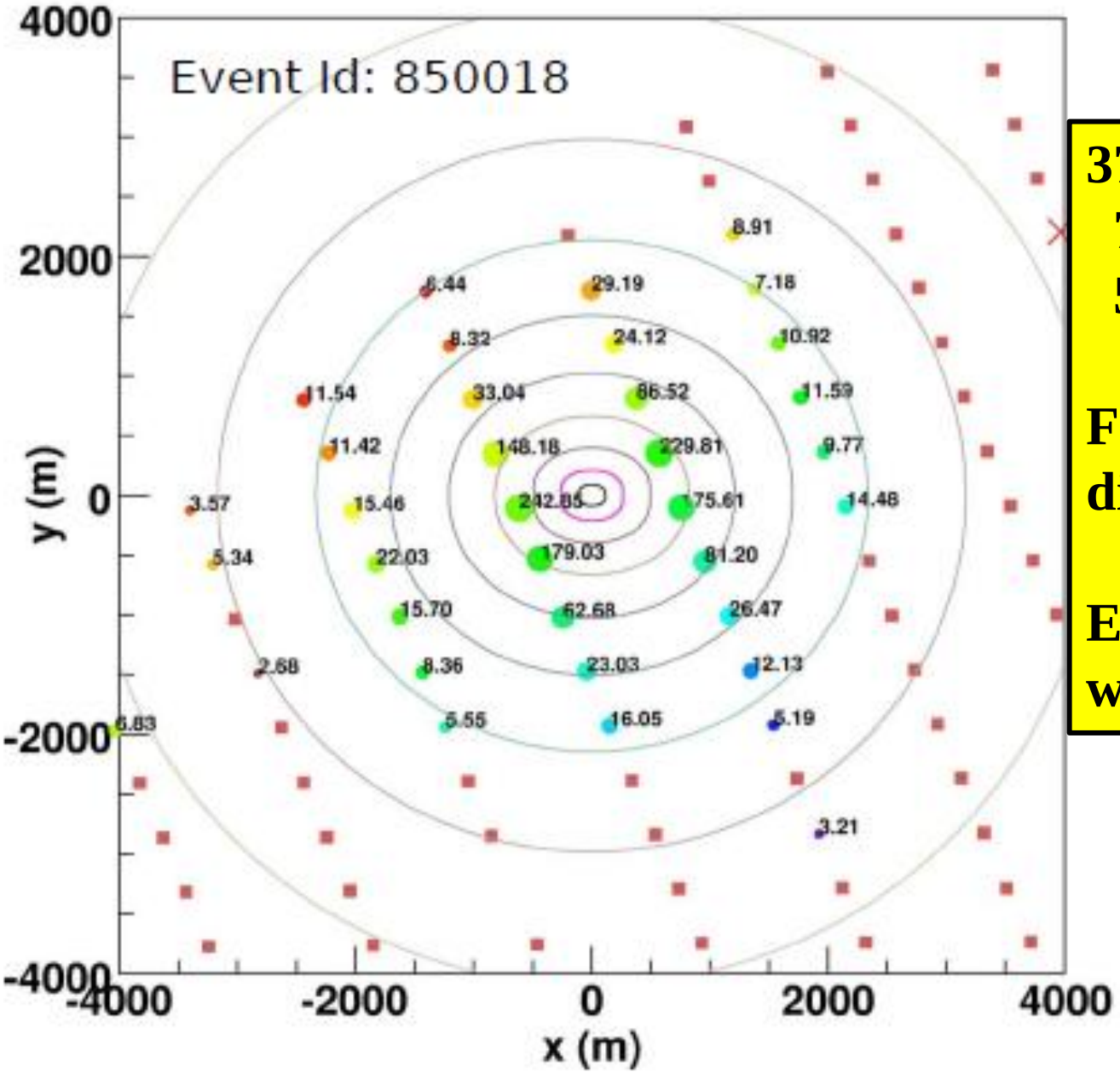

37 stations
71°
54 EeV

Fit made to density distribution

Energy measured with ~20 % accuracy

MC: proton, QGSJet II-03
$E = 10^{19}$ eV
$\theta = 80°$
$\phi = 0°$

$$\rho_\mu(\vec{r}) = N_{19}\rho_{\mu,19}(\vec{r};\theta,\phi)$$

Average muon density profile of simulated-proton of 10^{19}eV

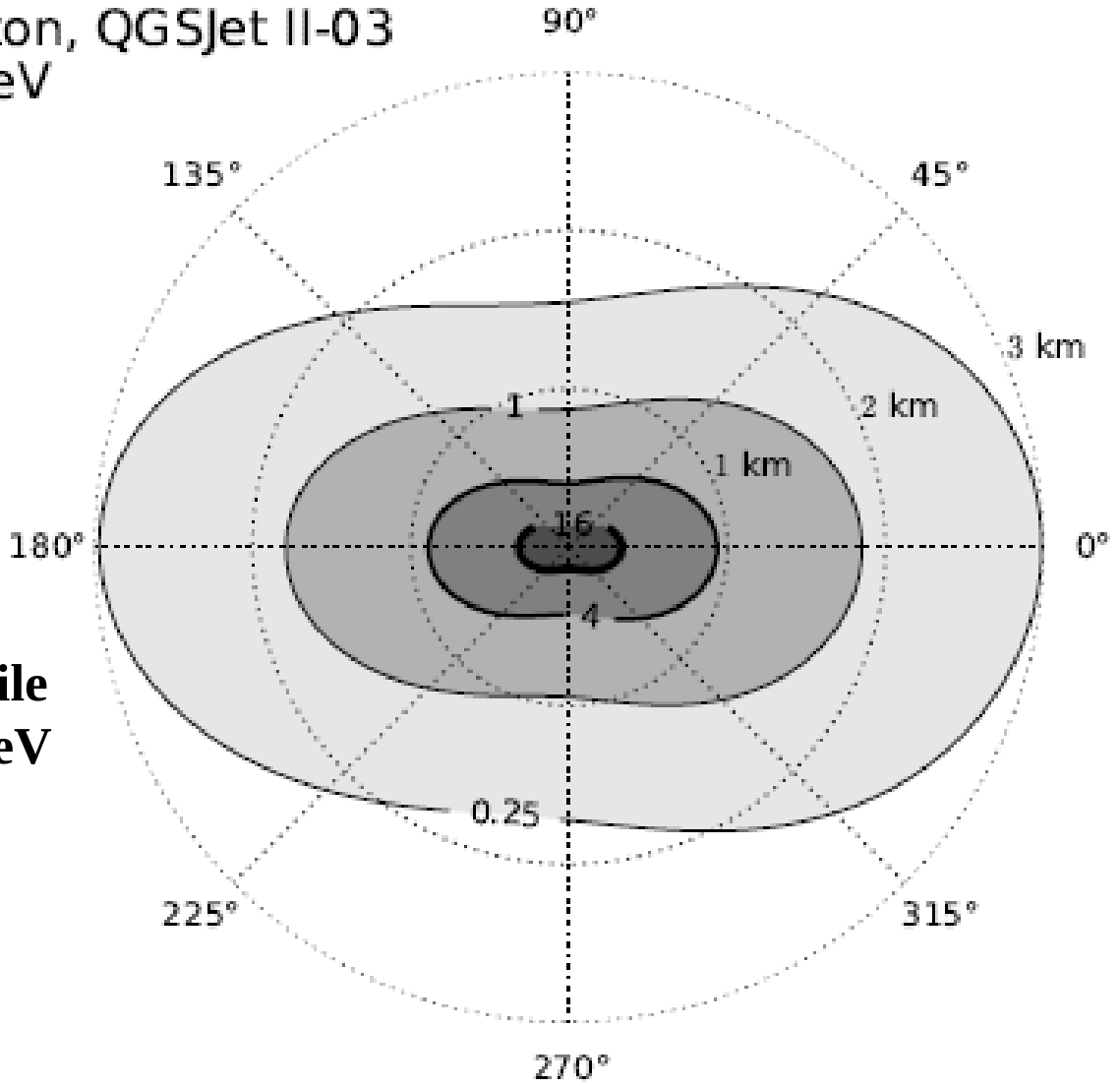

Maps such as these are compared and fitted to the observations so that the number of muons, N_μ, can be obtained

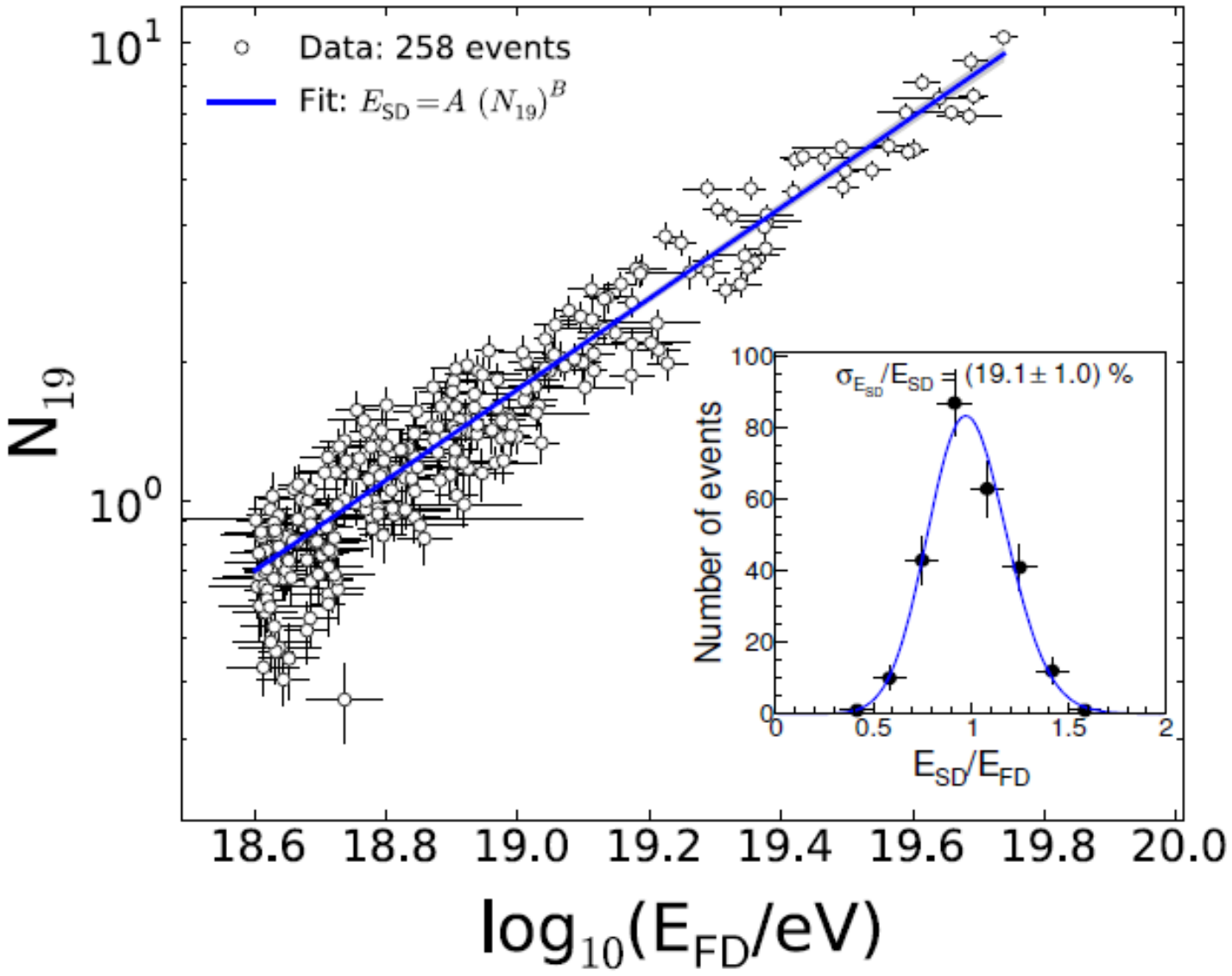
Data: 258 events
Fit: $E_{SD} = A\ (N_{19})^B$
N_{19}
10^1
10^0
18.6 18.8 19.0 19.2 19.4 19.6 19.8 20.0
$\log_{10}(E_{FD}/eV)$
$\sigma_{E_{SD}}/E_{SD} = (19.1 \pm 1.0)$ %
Number of events
100
80
60
40
20
0
0 0.5 1 1.5 2
E_{SD}/E_{FD}

Spectrum from events 60 < θ < 80°: arXiv: 1503.00786

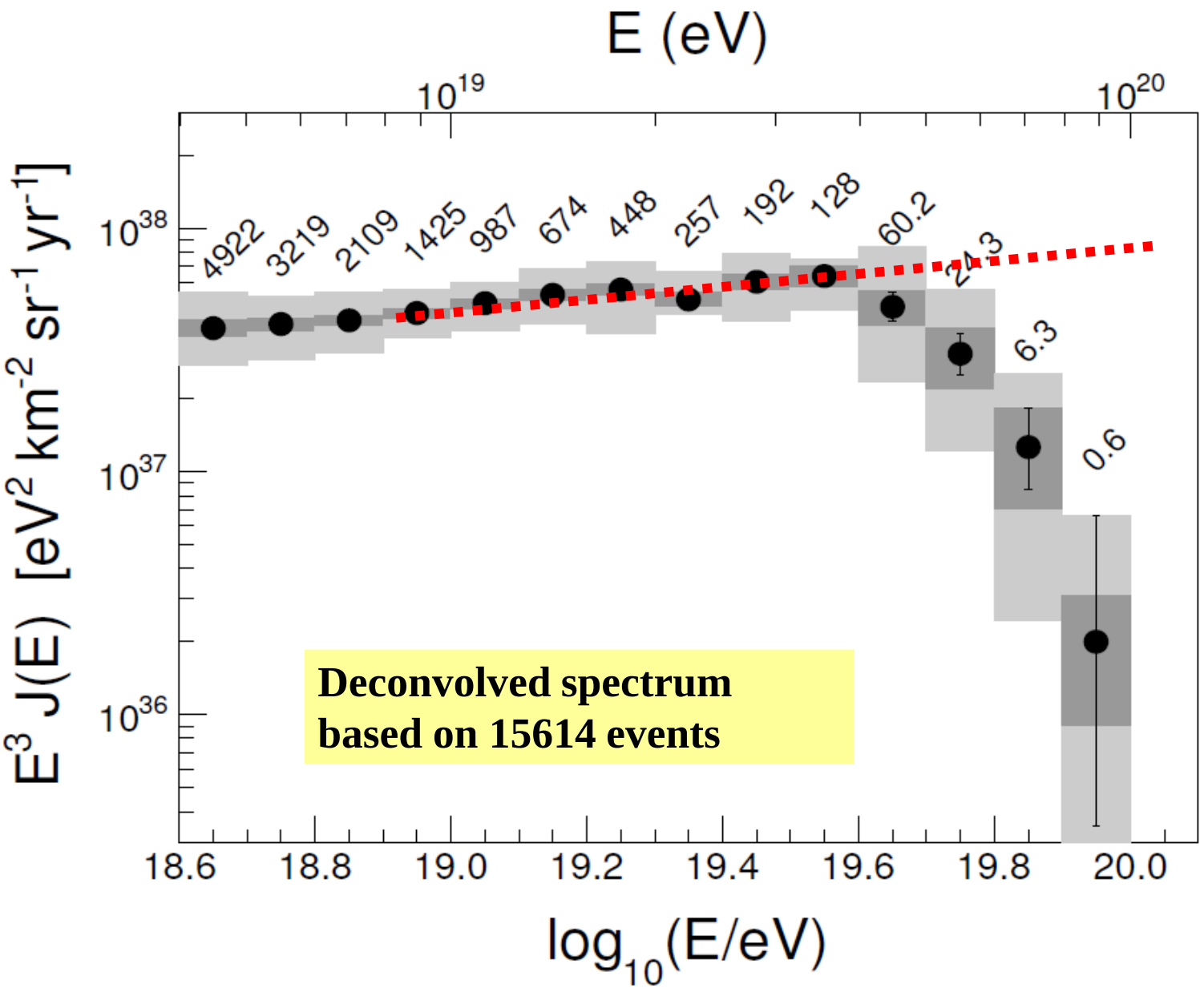

Comparison of two Auger Spectra with Telescope Array

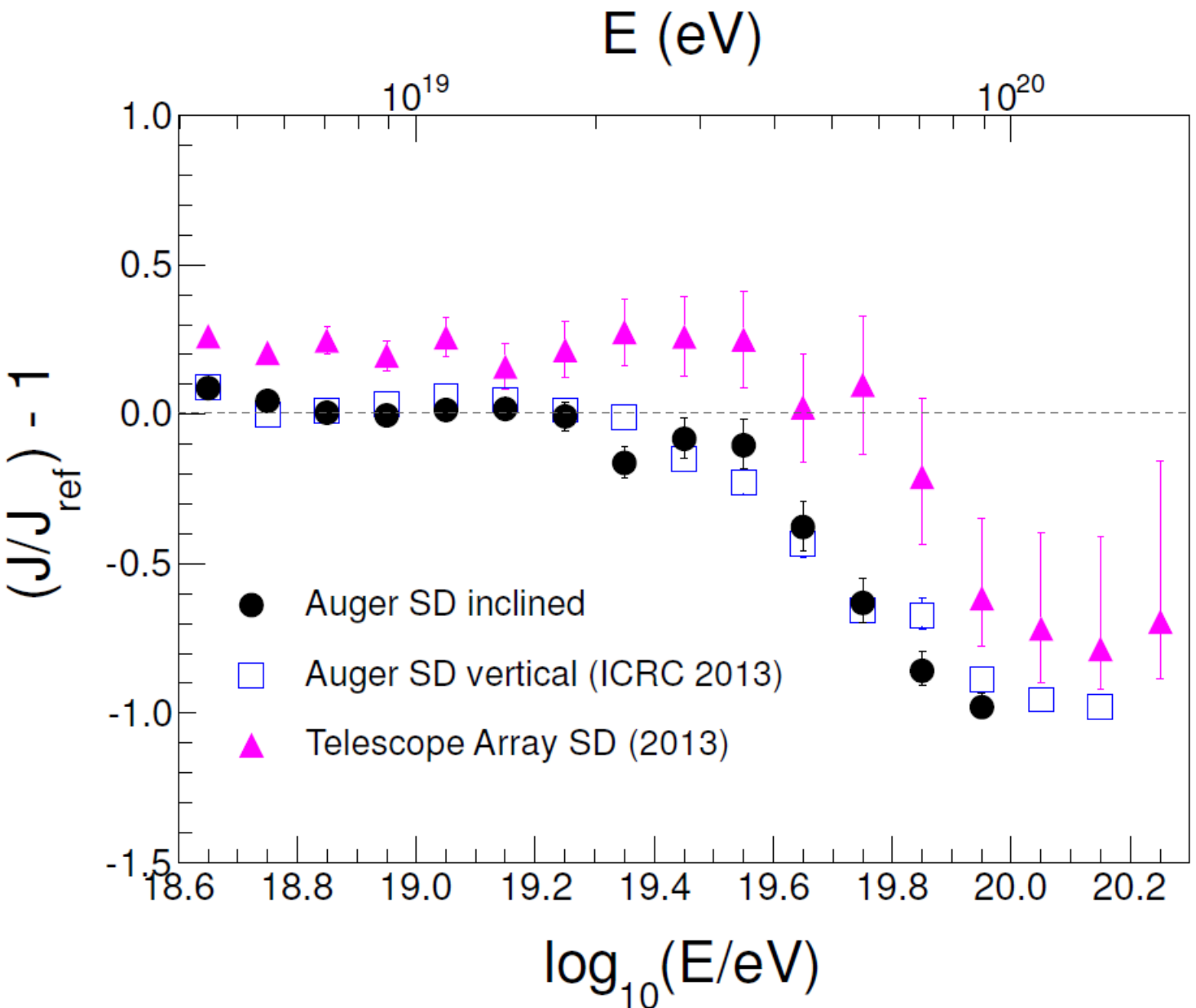

Comparison with Telescope Array

- **Auger spectrum is now measured up to a declination of 25.3°N, well into Telescope Array range**

- **Up to suppression region, TA and Auger spectra agree well**
  Average TA residual is 23%.

- **In suppression region the differences are large and may be due to**

  Anisotropy effects

  Atmospheric (Vertical aerosol depth as function of height)

  Detector effects: energy dependence of systematic uncertainties

  Different assumptions about composition
  invisible energy
  fluorescence yield

The well-established steepening of the spectrum itself is INSUFFICIENT for us to claim that we have seen the Greisen-Zatsepin-Kuz'min effect

It might simply be that the sources cannot raise particles to energies as high as 10^{20}eV

It would be enormously helpful if the arrival directions were Anisotropic and sources could be identified

Deflections in magnetic fields:

at **~ 10^{19} eV: still ~ 10° in Galactic magnetic field**
- depending on the direction

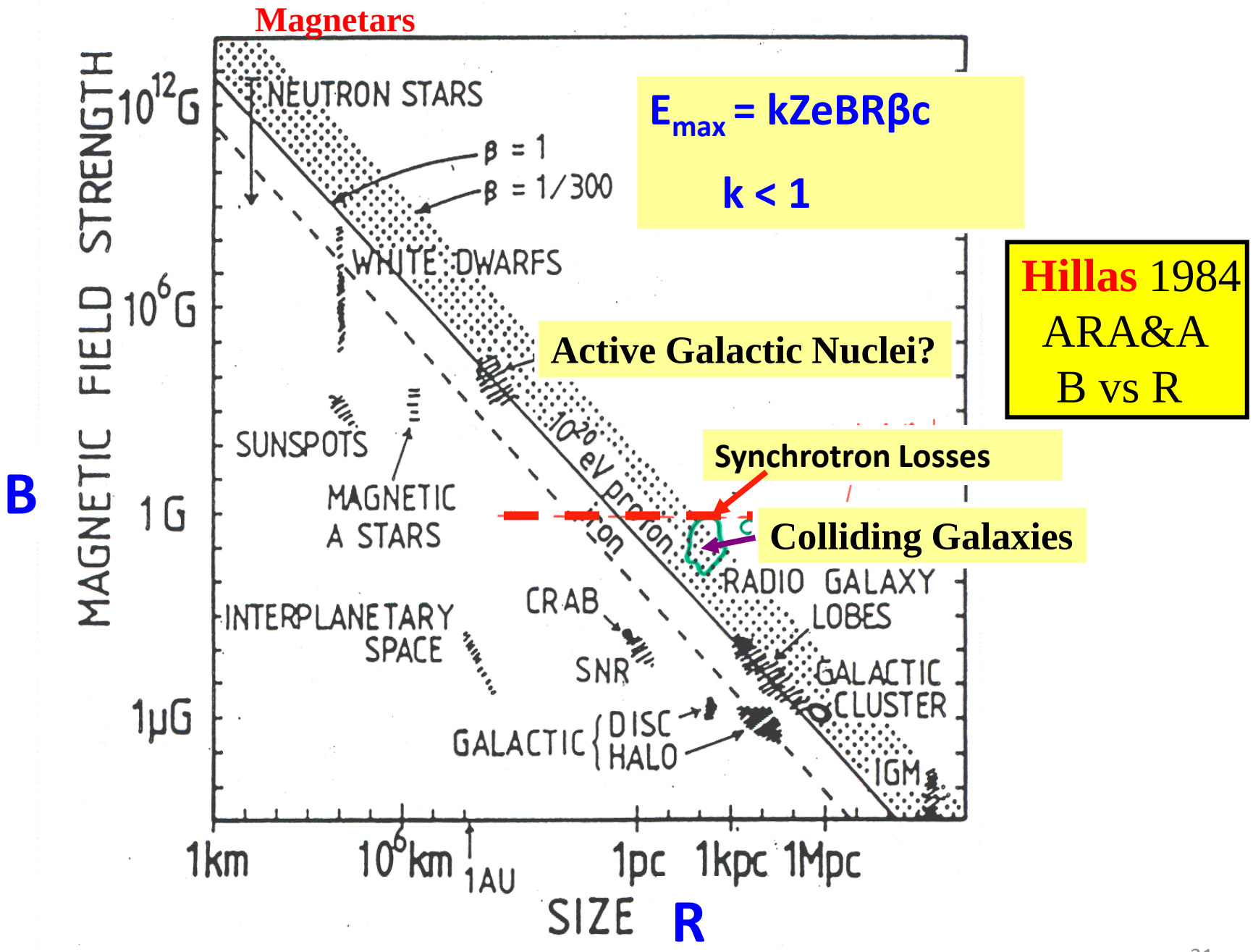
Magnetars
MAGNETIC FIELD STRENGTH
10^{12}G
10^{6}G
1G
1μG
B
NEUTRON STARS
β = 1
β = 1/300
WHITE DWARFS
SUNSPOTS
MAGNETIC A STARS
INTERPLANETARY SPACE
CRAB
SNR
GALACTIC DISC HALO
10^{20} eV proton
RADIO GALAXY LOBES
GALACTIC CLUSTER
IGM
1km
10^{6}km
1AU
1pc
1kpc
1Mpc
SIZE
R
$E_{max} = kZeBR\beta c$
k < 1
Active Galactic Nuclei?
Synchrotron Losses
Colliding Galaxies
Hillas 1984
ARA&A
B vs R

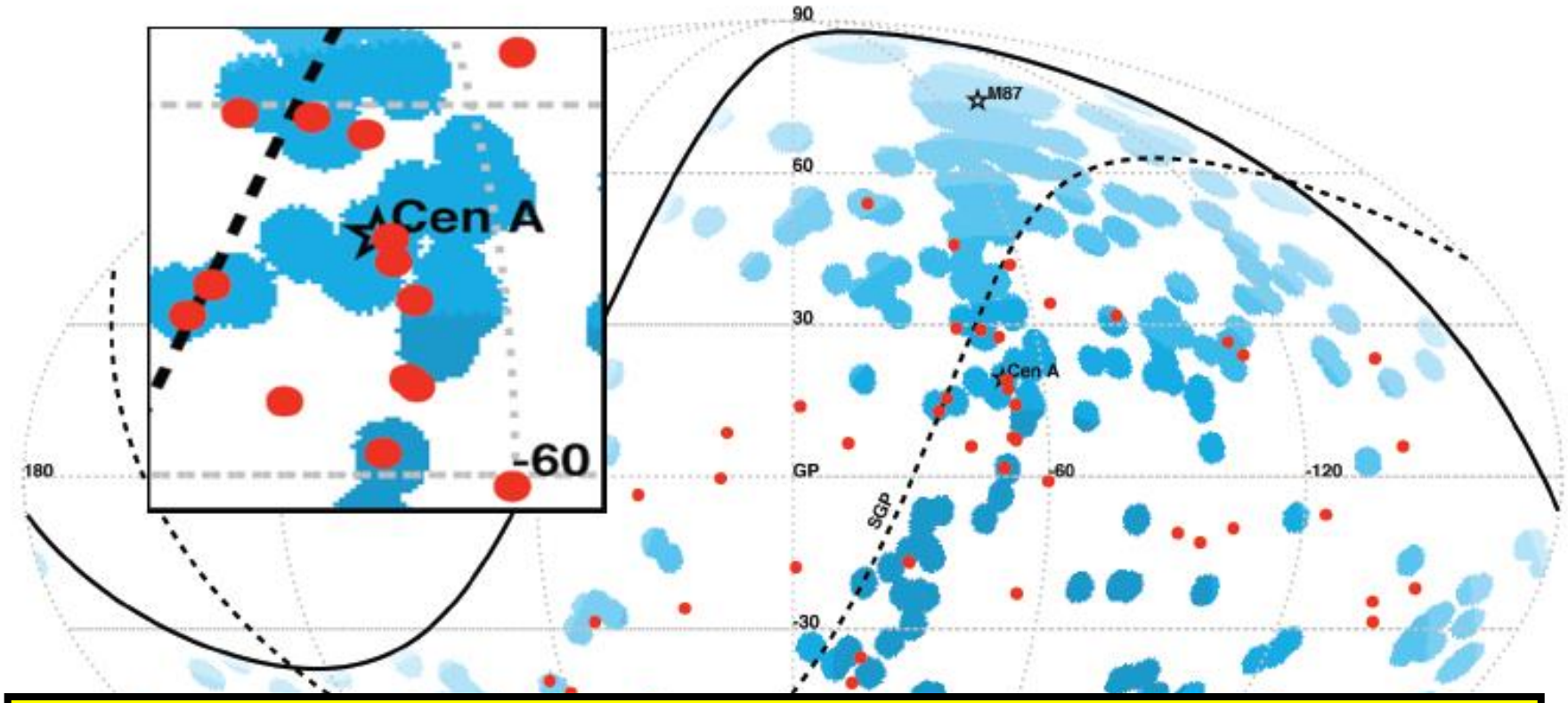

Correlation has fallen from ~ 68% to ~ 28% (2007 –> 2014) compared with 21% for isotropy: about 1.4% probablity

Cen A may be a source: in 13° circle around: 12 seen/1.7

A clear message from the Pierre Auger Observatory:-

We made it too small (2 per month at energy of interest)

Auger and Telescope Array Hot-Spots

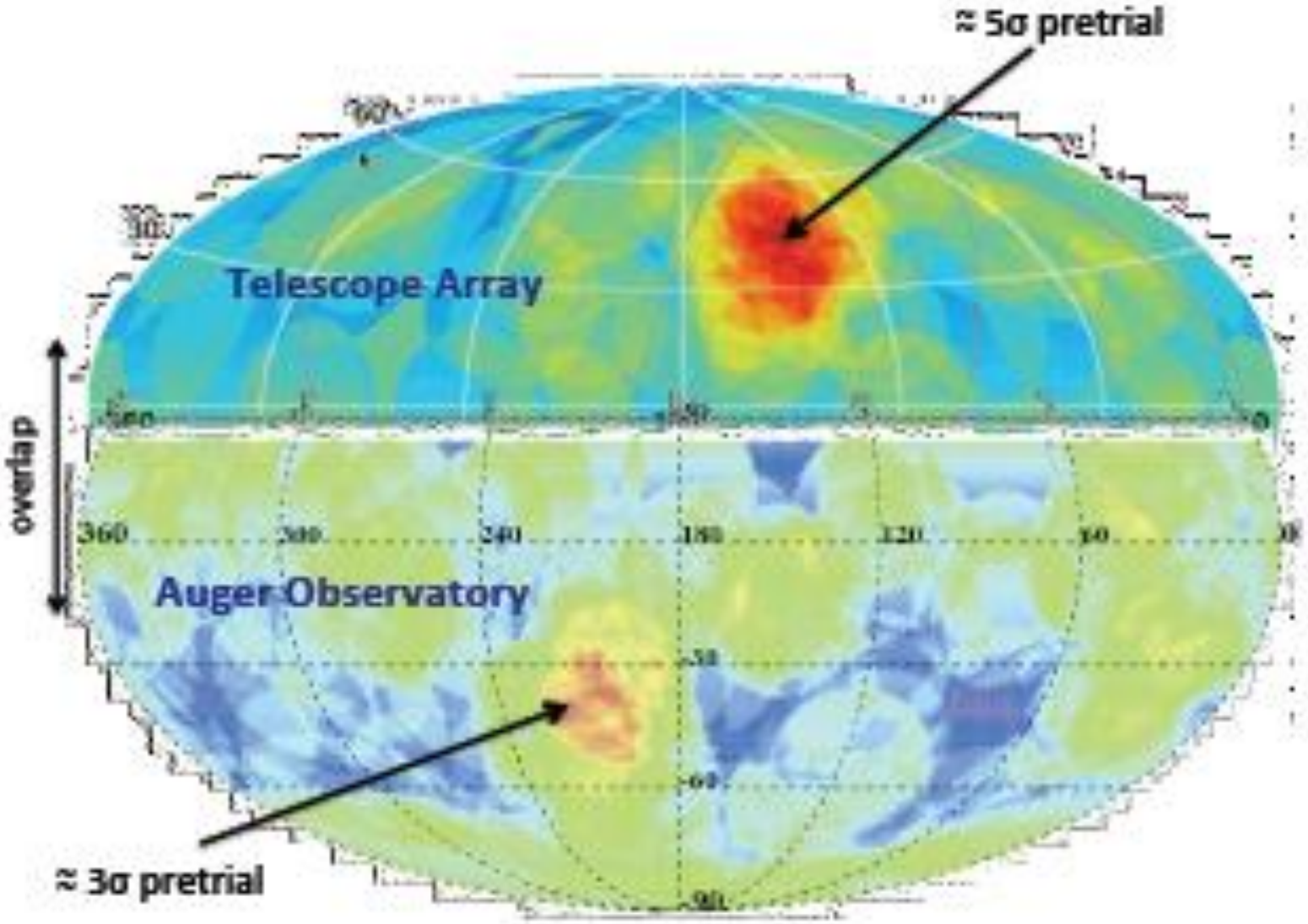

Broad anisotropy search in right ascension

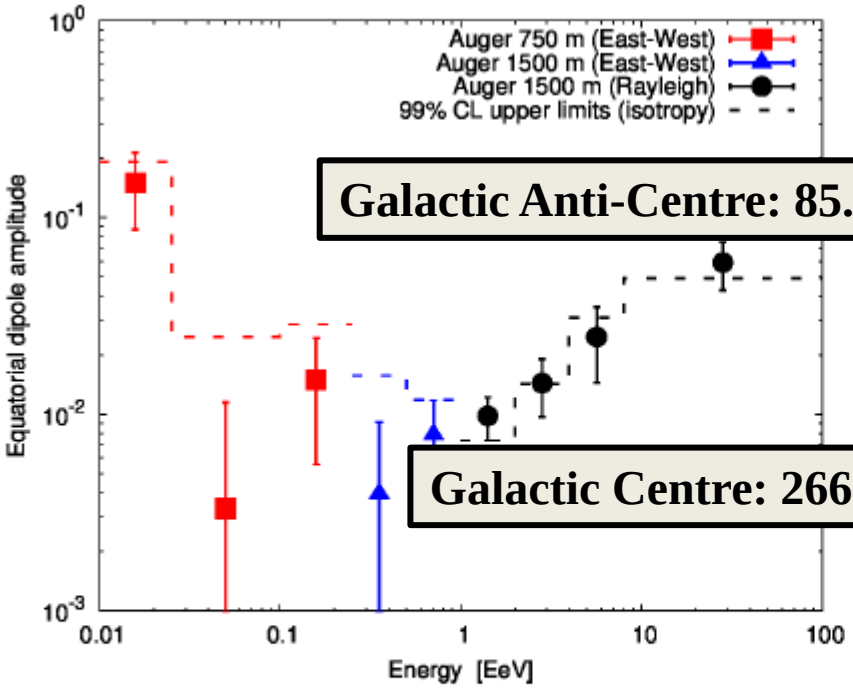

Figure 5. Amplitude of the first term in the Fourier expansion of the flux measured at the Auger Observatory in terms of R.A. as a function of energy. It can be related to

Galactic Anti-Centre: 85.5°

Galactic Centre: 266°

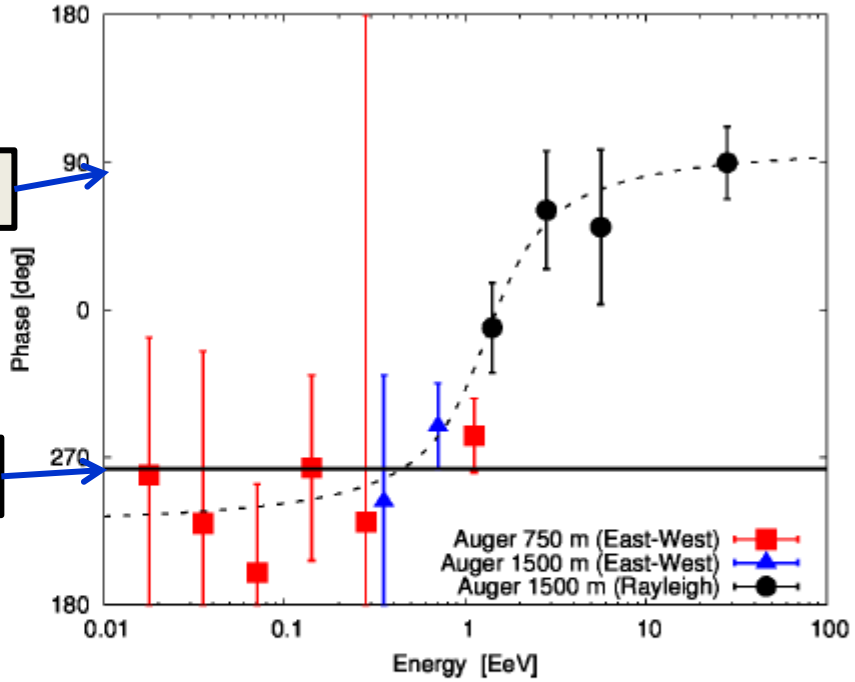

Figure 6. Phase of the first harmonic in R.A. as a function of energy using data from the Pierre Auger Observatory from January 1 2004 to December 31 2010 for the larger array,

Latest News (ApJ in press: arXiv 1411.6111)

Recently we have completed analysis of inclined events above 4 EeV and the addition of 30% more data from inclined events.

This has:-

(i) given a broader sky coverage – up to declination 25.3°
and
(ii) improved the significance of anisotropy the largest energy bin

Note that the phase is in good agreement with previous work

Table 1: Rayleigh analysis in right ascension

E [EeV]	N	k	a_k^α	b_k^α	r_k^α	φ_k^α	$P(\geq r_k^\alpha)$
4 - 8	50,417	1	0.0030 ± 0.0063	0.0008 ± 0.0063	0.0031	15°	0.88
		2	-0.0012 ± 0.0063	-0.0004 ± 0.0063	0.0013	99°	0.98
> 8	19,797	1	-0.004 ± 0.010	0.044 ± 0.010	0.044	95°	6.4×10^{-5}
		2	0.009 ± 0.010	0.027 ± 0.010	0.028	36°	0.021

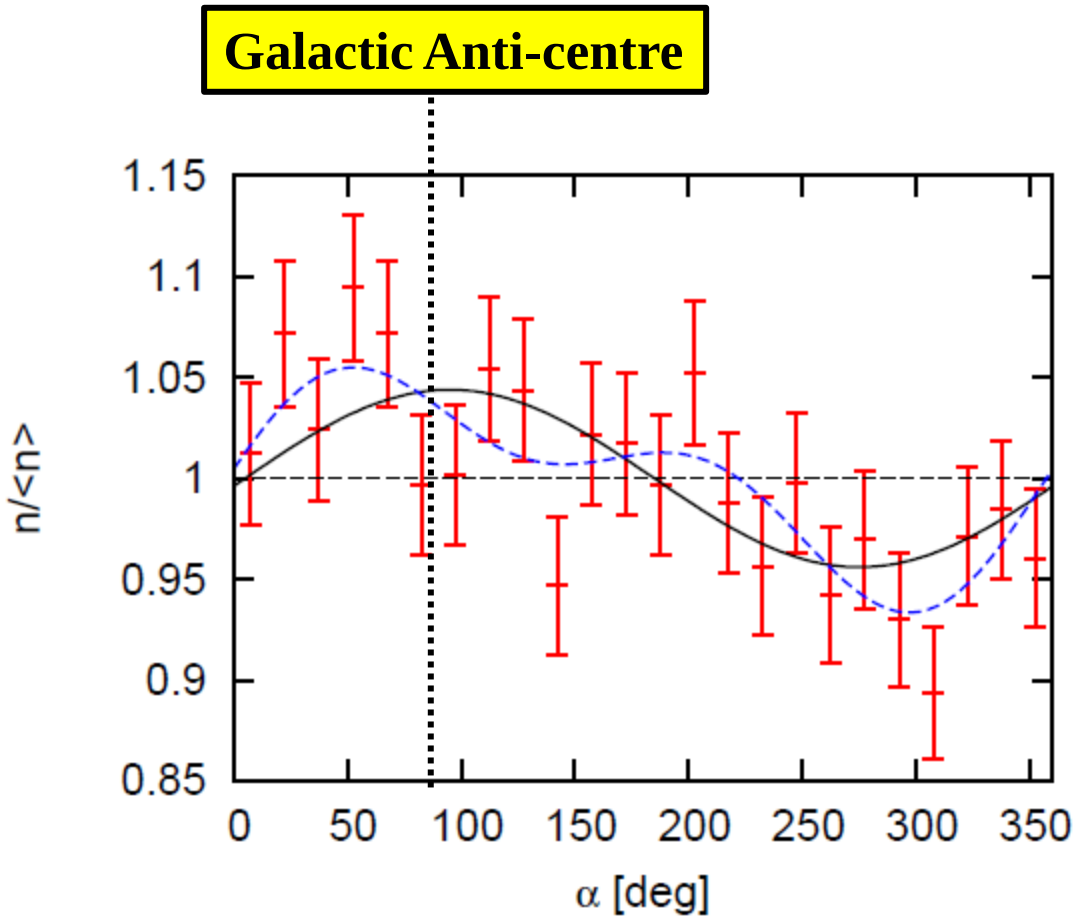

Fig. 2.— Observed number of events over the mean as a function of the right ascension with 1 σ error bars for $E > 8$ EeV. The black solid line shows the first harmonic modulation from Table 1, while the blue dashed line shows the combination of the first and second harmonics.

To interpret the arrival direction data a crucial question is

"What is the mass of the cosmic ray primaries at the highest energies?"

- **Answer is dependent on unknown hadronic interaction physics at energies up to ~ 30 times CM energy at LHC**

- **In particular, cross-section, inelasticity and multiplicity and, in addition , pion-nucleus and nucleus- nucleus interactions**

- **Here is an important link between particle physics and astroparticle physics**

How we try to infer the variation of mass with energy

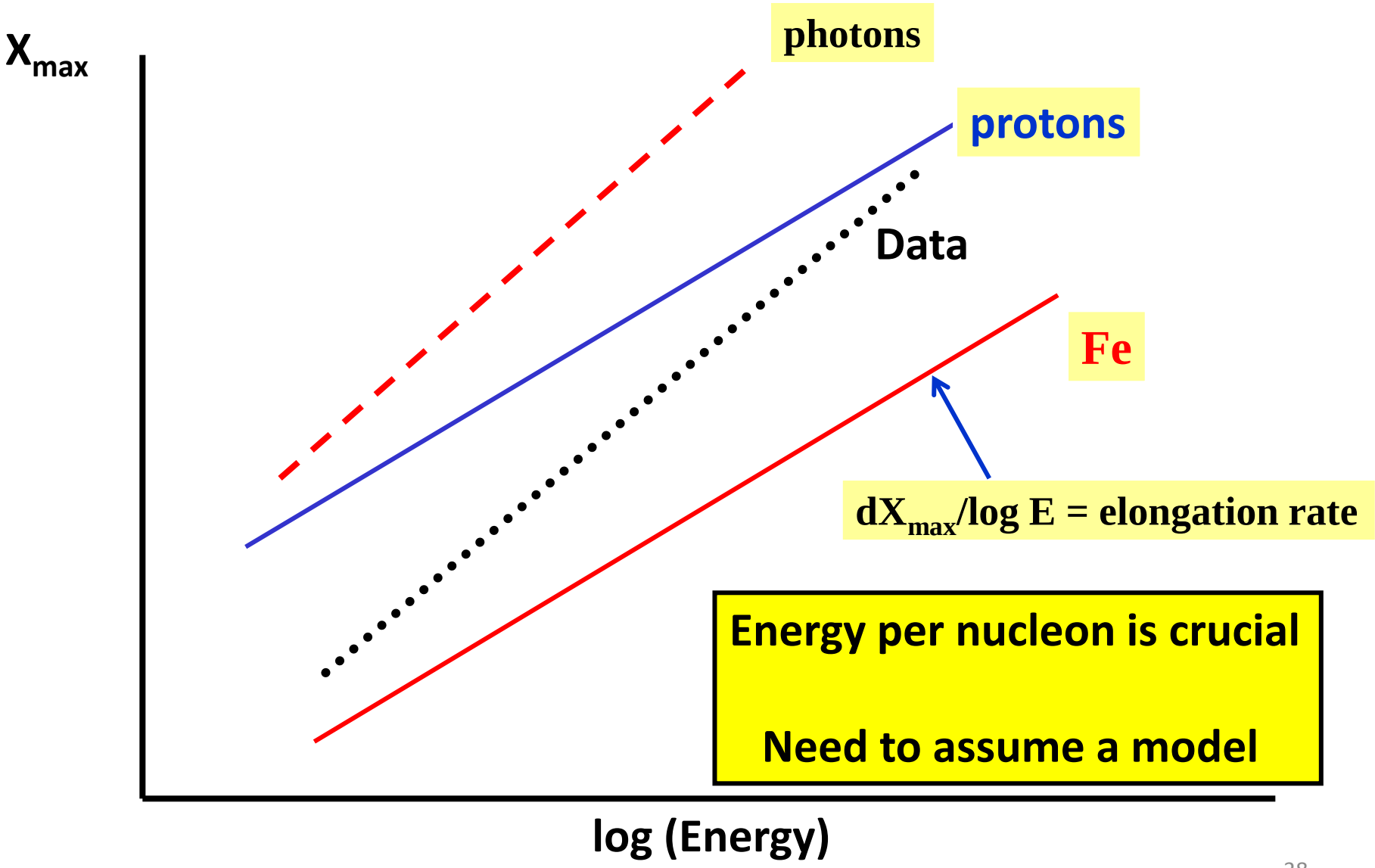

Energy per nucleon is crucial

Need to assume a model

Some Longitudinal Profiles measured with Auger

1000 g cm^{-2} = 1 Atmosphere ~ 1000 mb

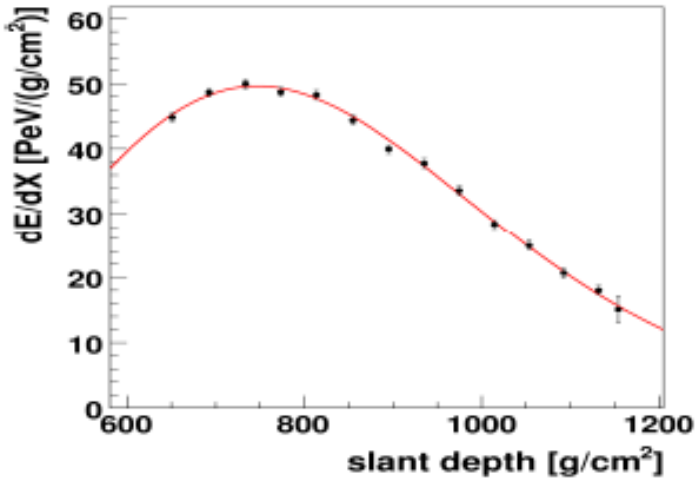

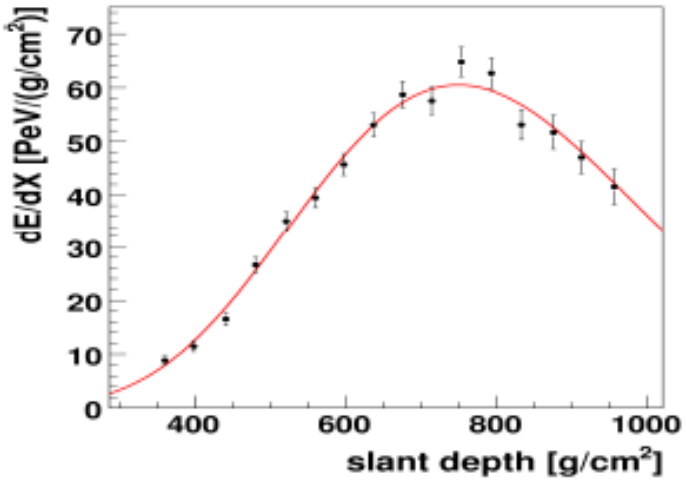

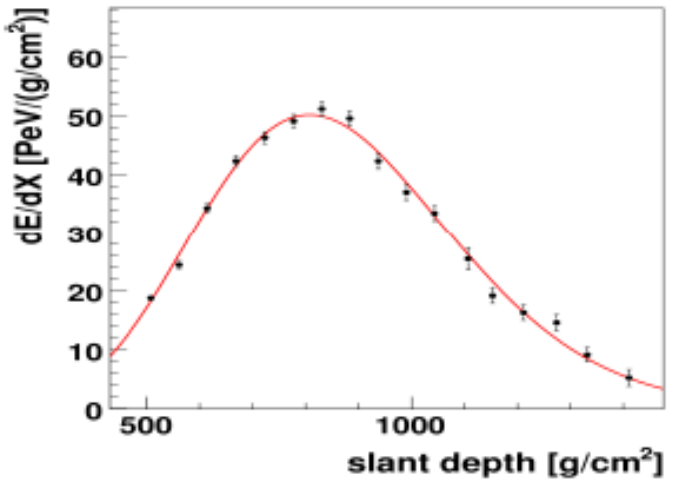

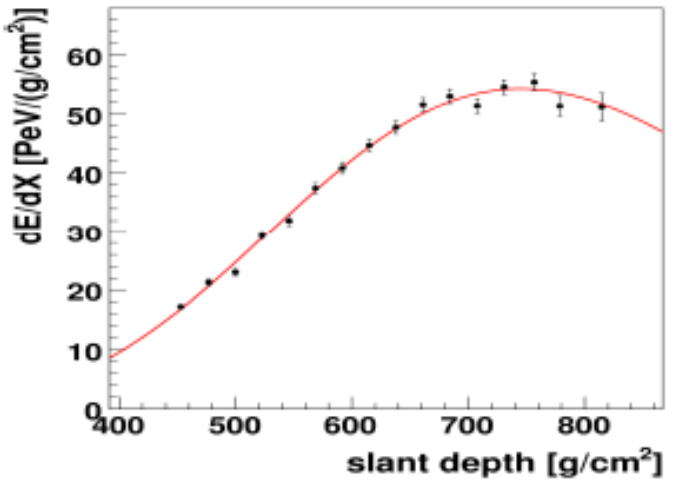

rms uncertainty in X_{max} < 20 g cm^{-2} - from stereo-measurements

X_{max} and RMS(X_{max}) compared to Pre-LHC models

<X_{max}>

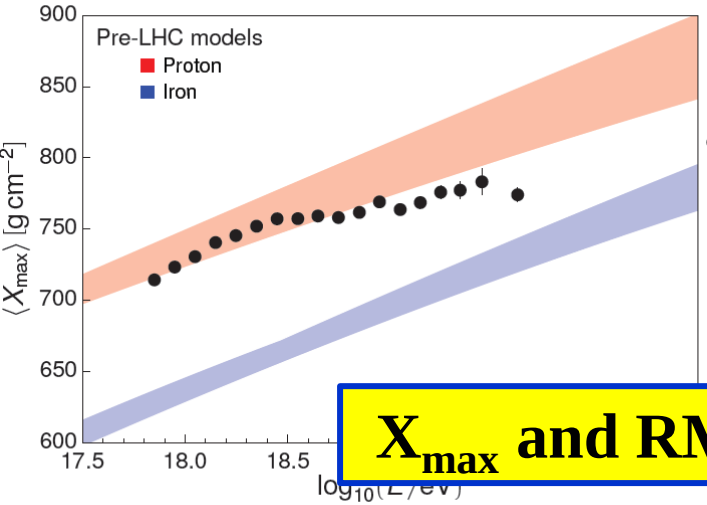

RMS(X_{max})

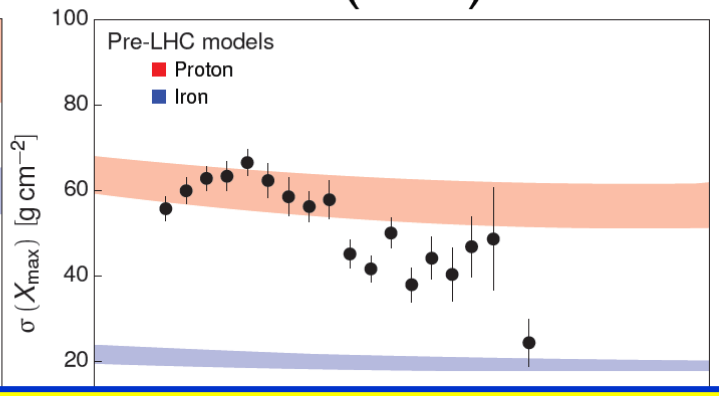

X_{max} and RMS (Xmax)compared to Post-LHC models

<X_{max}>

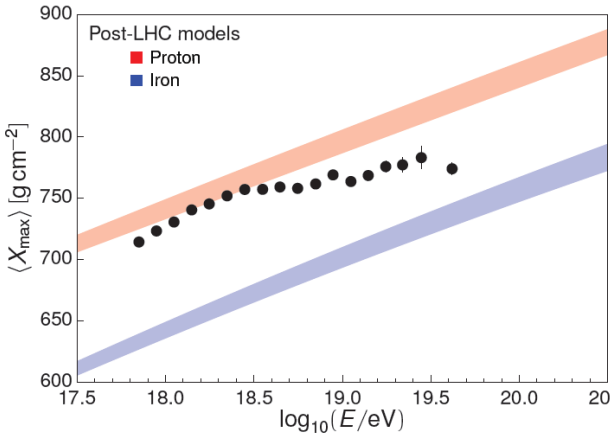

RMS(X_{max})

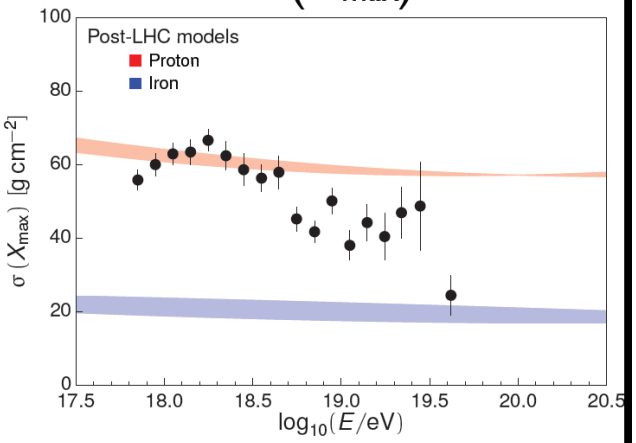

LHC data have been very useful for tuning of interaction models

Distribution of X_{max} as function of energy

PRD 90 1220005 2014

19759 events above 6 x 10^{17} eV

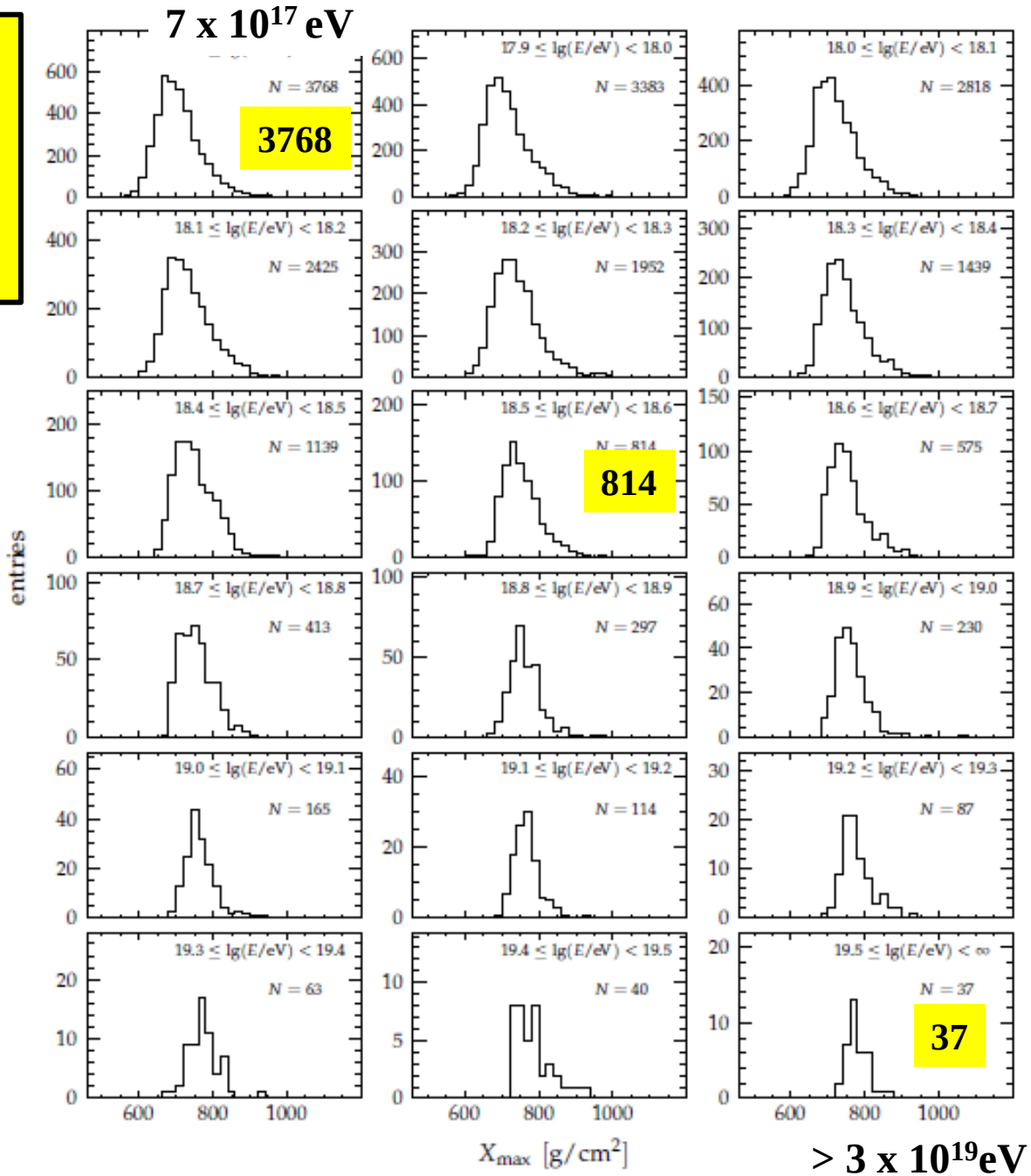

Figure 8: X_{max} distributions for different energy intervals.

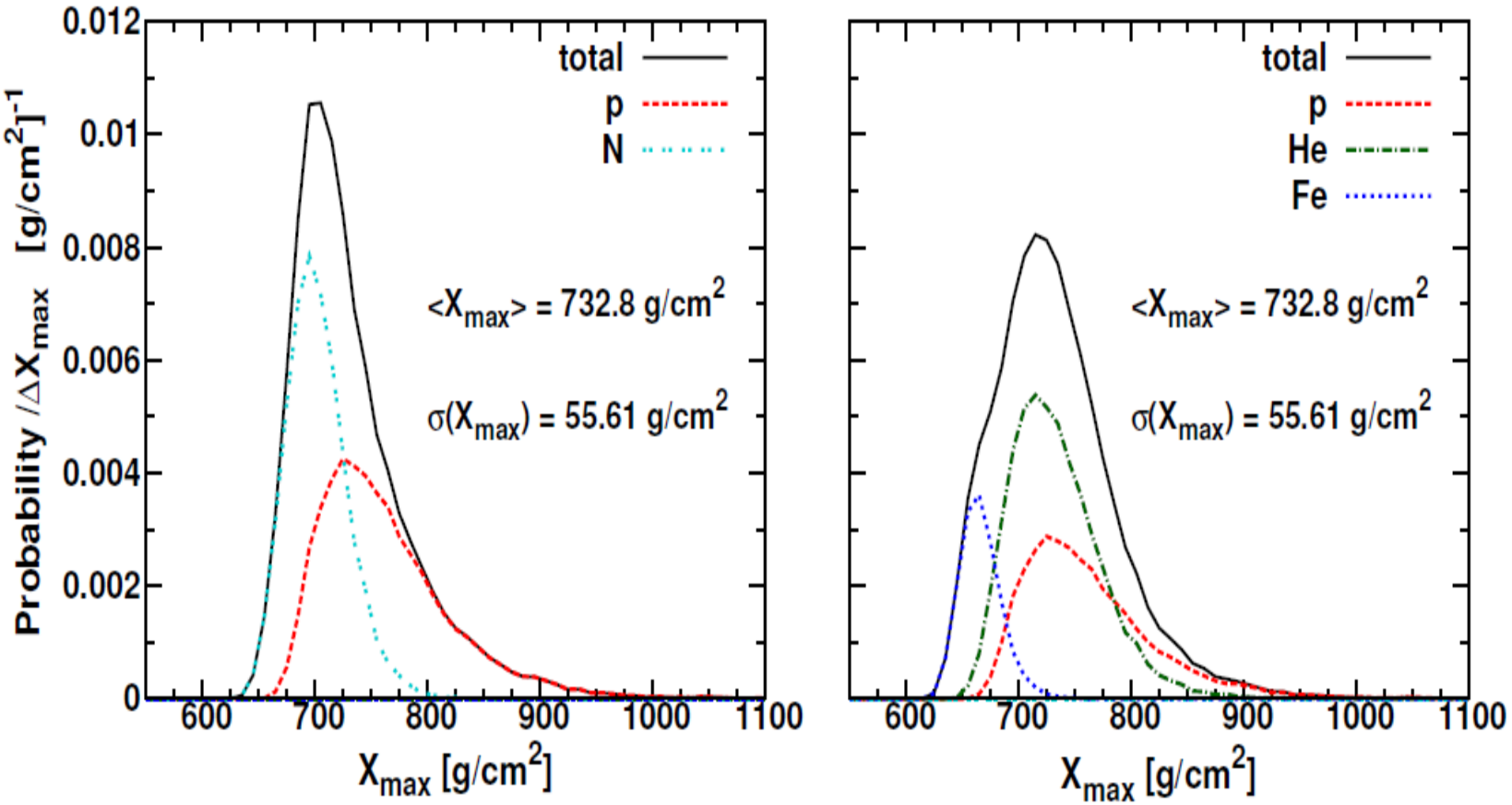

FIG. 1. Two $X_{\max}$ distributions generated with identical mean and dispersion but with different composition. The hadronic interaction model EPOS-LHC was used to generate 10^4 events between

Detailed study of X_{max} distributions are required

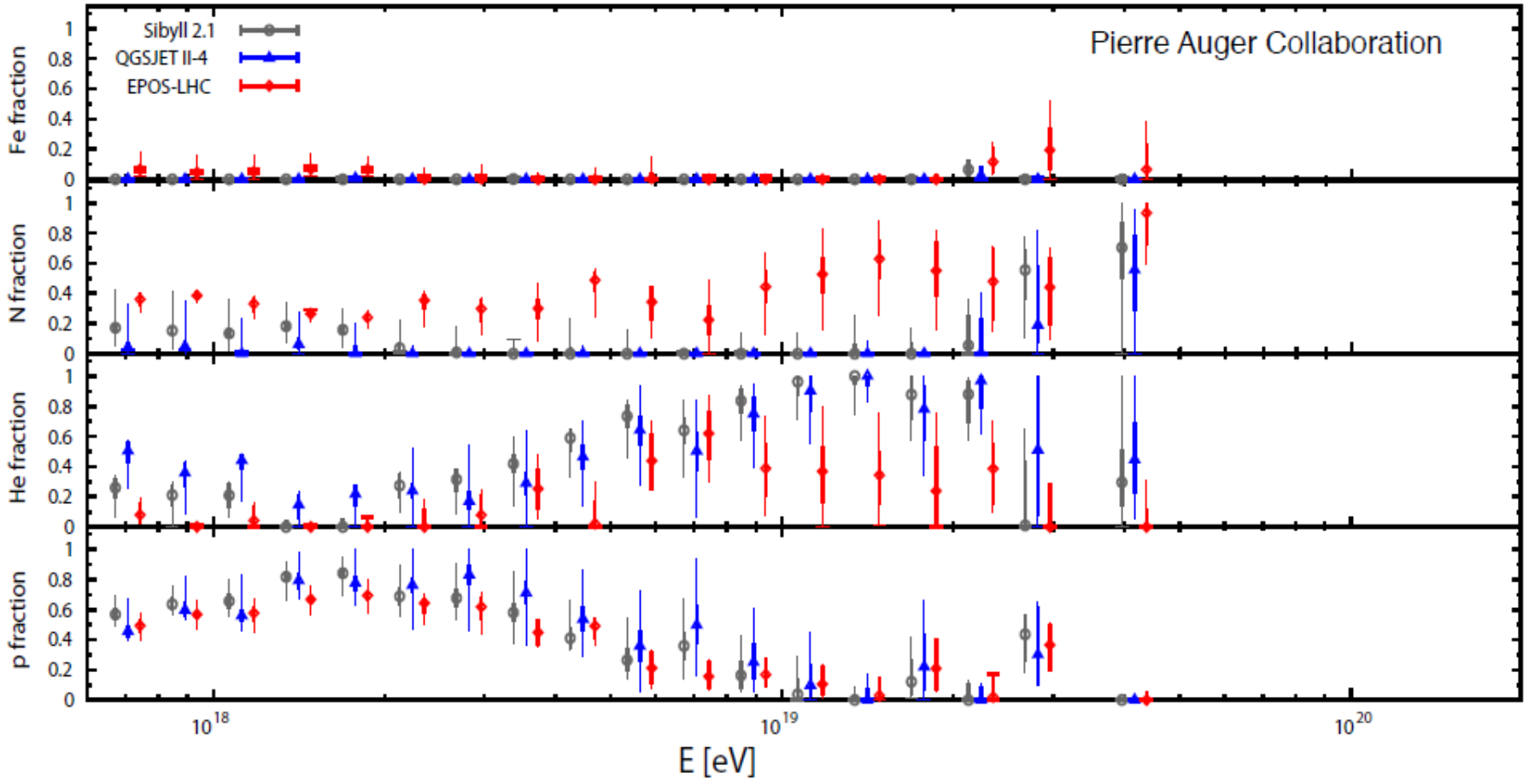
Sibyll 2.1
QGSJET II-4
EPOS-LHC
Pierre Auger Collaboration
Fe fraction
N fraction
He fraction
p fraction
0
0.2
0.4
0.6
0.8
1
10^{18}
10^{19}
10^{20}
E [eV]

Auger Interpretation: Phys Rev D 90 1222006 2014 (arXiv 1409.5083)

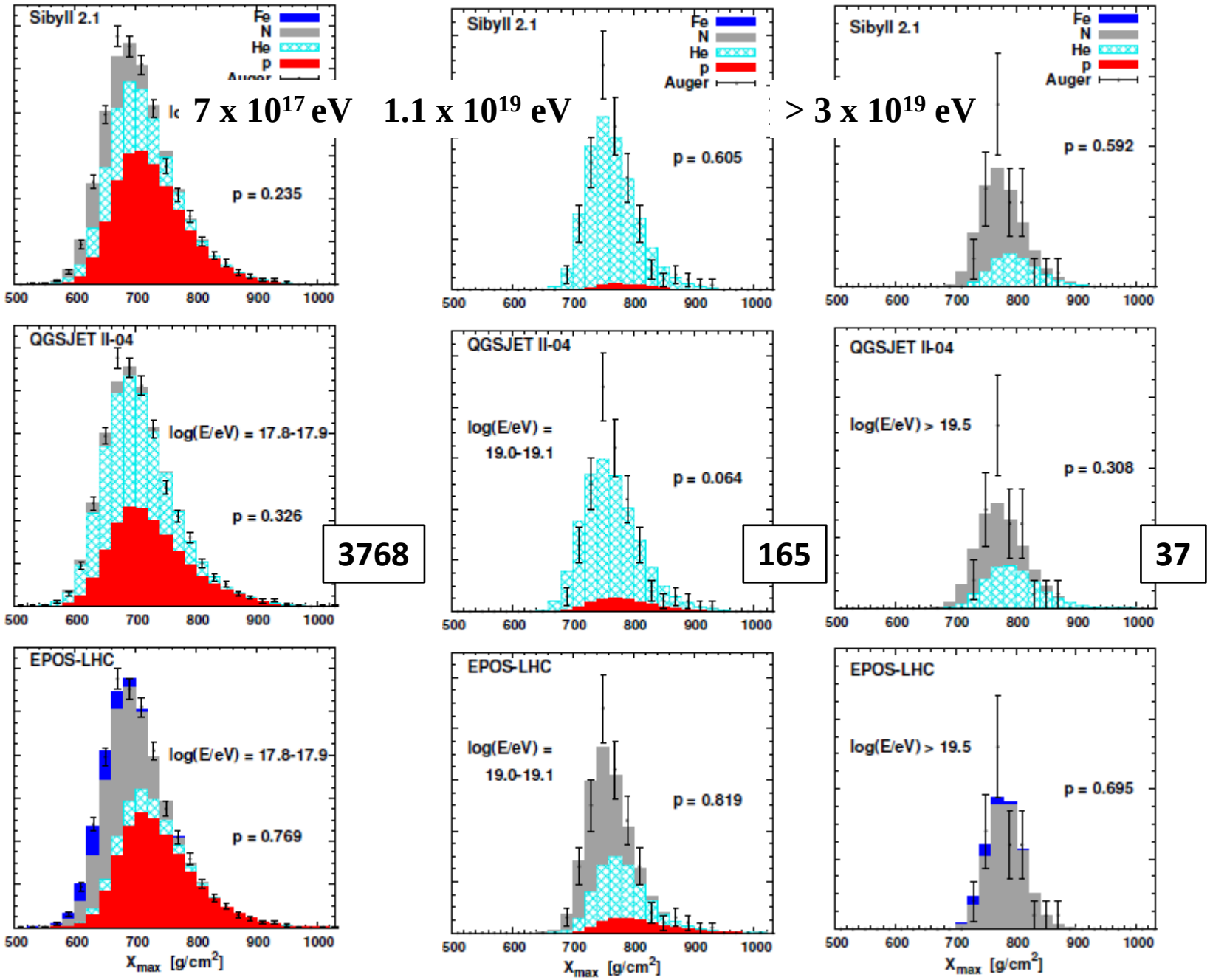

Discussion of Auger/Telescope array data: arXiv 1503.07540
Report of Joint Analysis Working Group

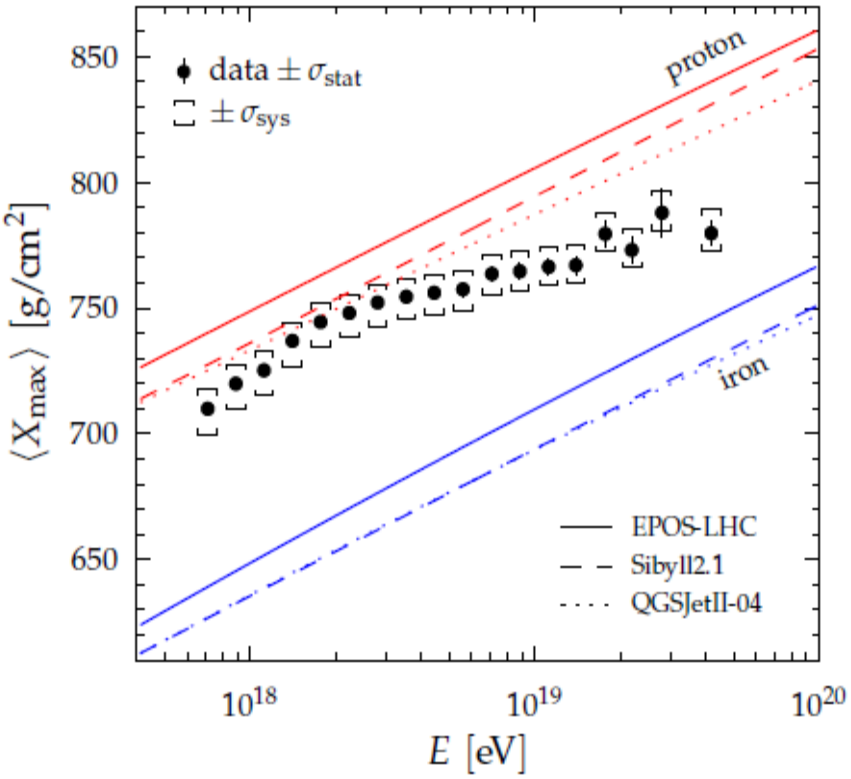

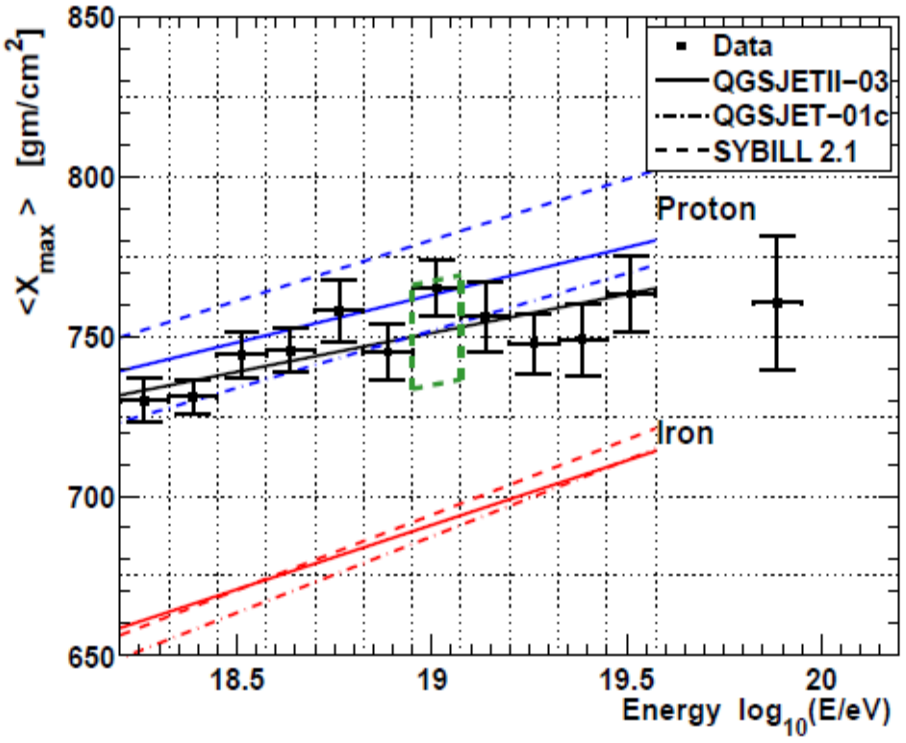

Auger: 19759 events

Telescope Array: 822 events

Direct comparison is not possible because of different approaches to analysis

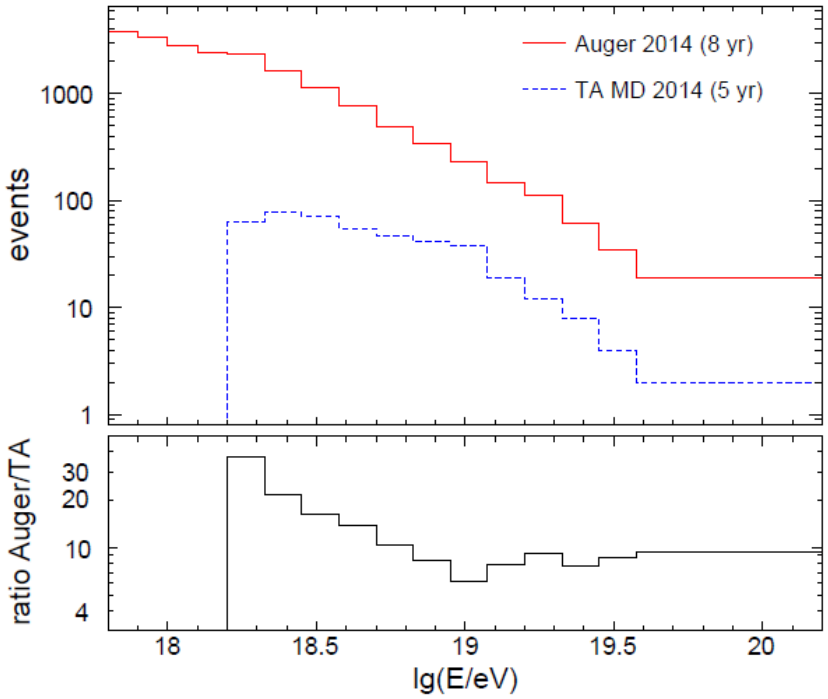

The TA approach has been to fold the detector resolution and the efficiency into the raw data and into Monte Carlo comparisons.

The large Auger sample has allowed a more data-driven approach with only certain geometries being selected that give an almost-unbiased X_{max} distribution:

Fiducial Selection

A joint TA/Auger working group has studied this problem

The mass composition inferred from the Auger measurements, in terms of p, He, N and Fe has been simulated with the TA fluorescence analysis methods.

X_{max} measured by TA is consistent with that found with Auger mass distribution

$$\Delta X_{max} = 2.9 \pm 2.7 \text{ (statistical)} \pm 18 \text{ (syst) g cm}^{-2}$$

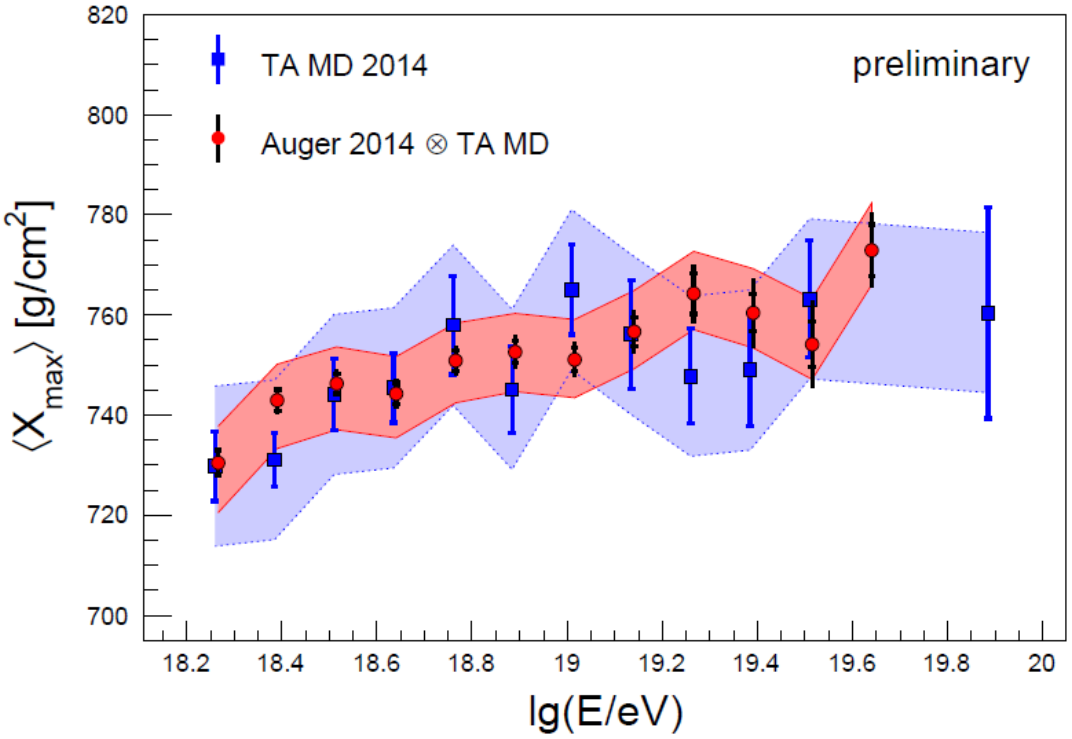

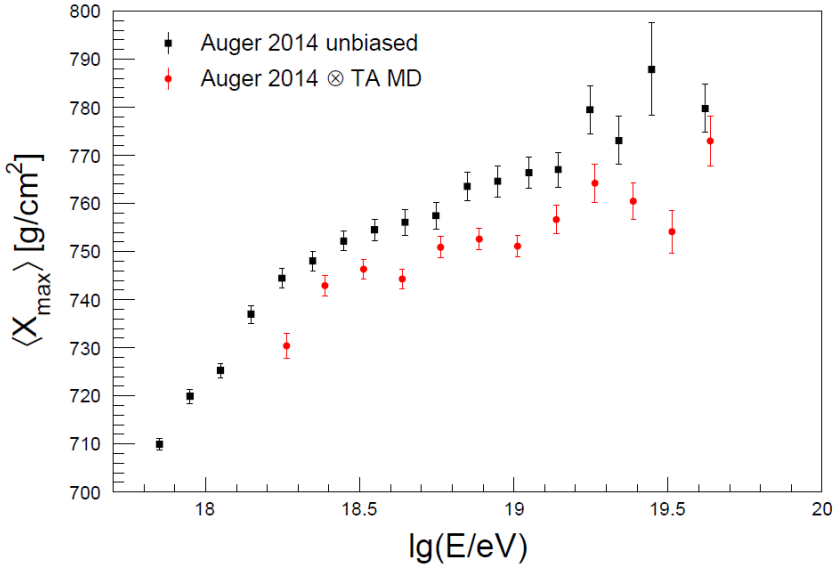
Auger 2014 unbiased
Auger 2014 ⊗ TA MD
⟨X_max⟩ [g/cm²]
lg(E/eV)

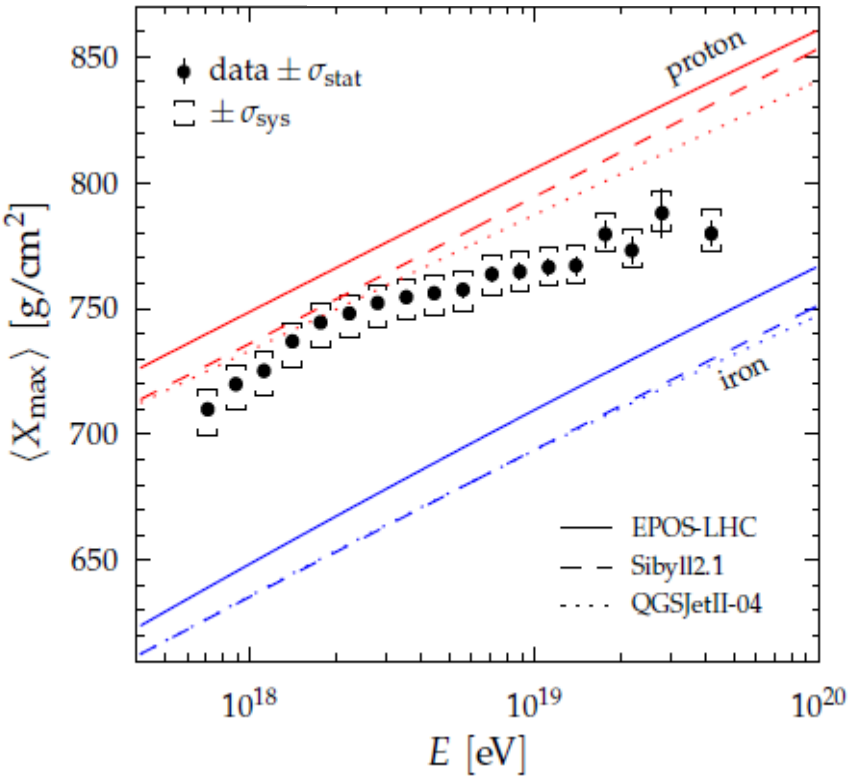
data ± σ_stat
± σ_sys
proton
iron
EPOS-LHC
Sibyll2.1
QGSJetII-04
⟨X_max⟩ [g/cm²]
E [eV]

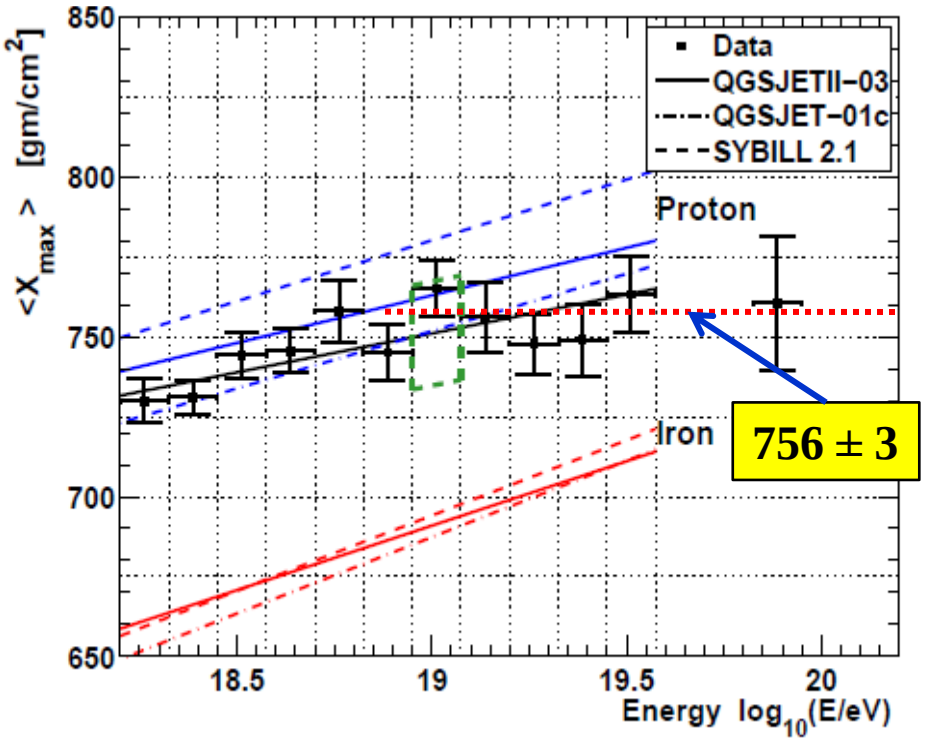
Data
QGSJETII-03
QGSJET-01c
SYBILL 2.1
Proton
Iron
756 ± 3
<X_max> [gm/cm²]
Energy log10(E/eV)

Photon Limit:
new results – to be reported at ICRC 2015

Searches for photons make use of anticipated differences in showers arising from:-

- **the steeper fall-off of signal with distance**
- **the slower risetime of the signals in the water-Cherenkov detectors**
- **the larger curvature of the shower front**
- **the deeper development in the atmosphere resulting in greater X_{max}**

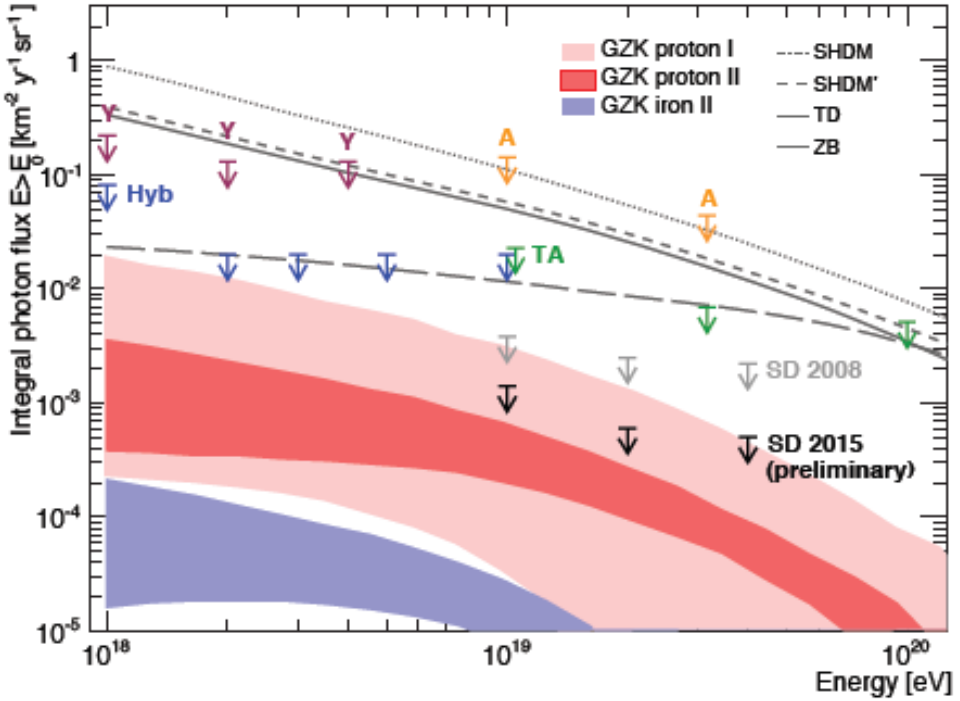

The limits rule out exotic, super-heavy relic models

Search for High-energy Neutrinos

ApP 3 321 1988

On the detection of ultra high energy neutrinos with the Auger observatory

K.S. Capelle [a], J.W. Cronin [a], G. Parente [b], E. Zas [b]

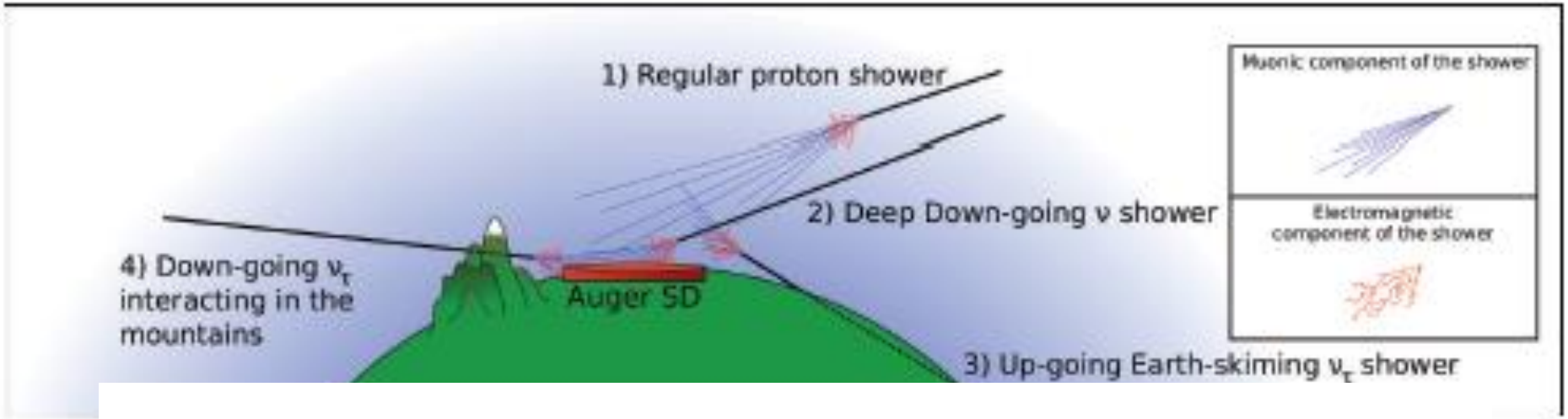

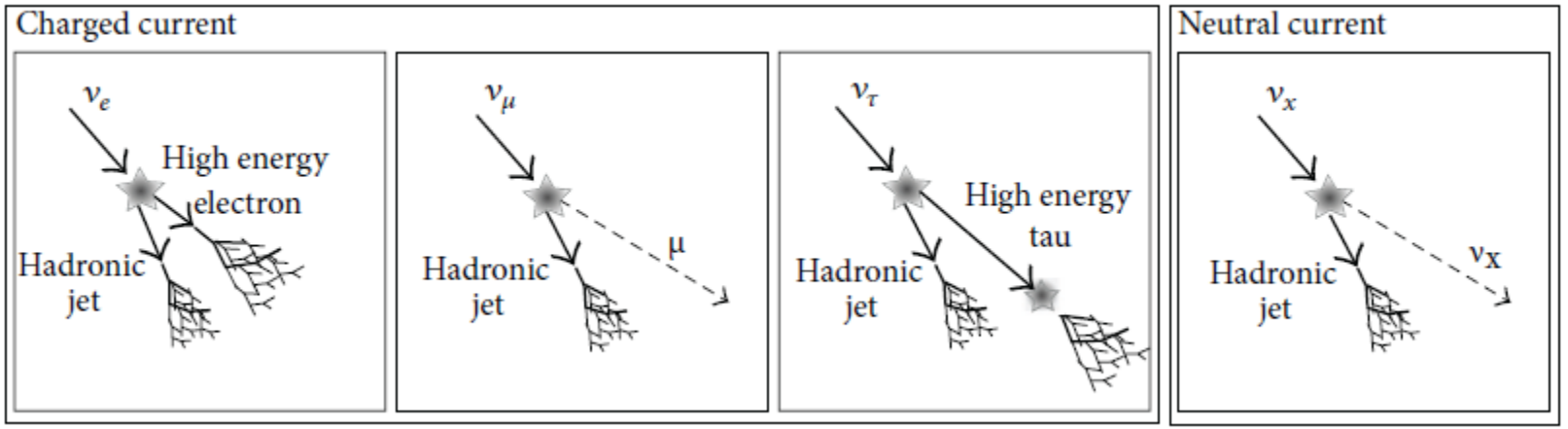

Details in Advances in High Energy Physics 708680 2013

The neutrino search strategy

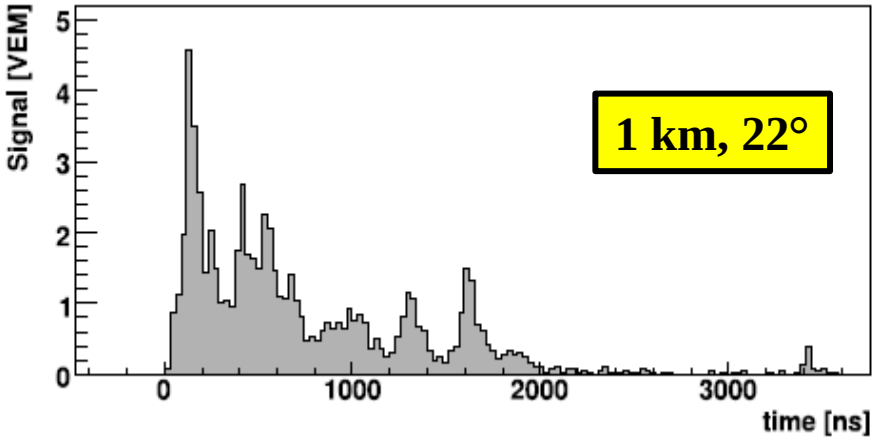

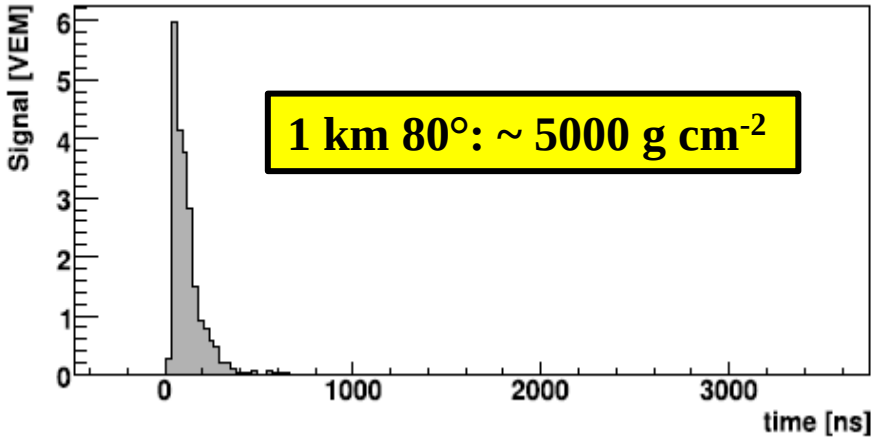

Are showers seen at very large zenith angles with the characteristics of vertical showers?

The right-hand type of event is the hadronic background: the left-hand type of event is what is expected from the signal

No candidates yet found

Latest result on search for neutrinos: submitted to Phys Rev D

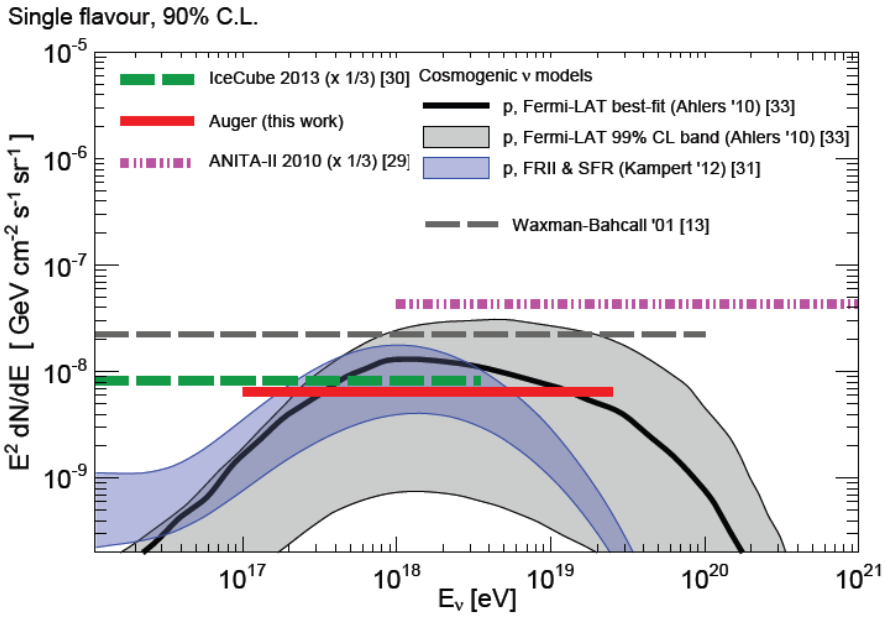

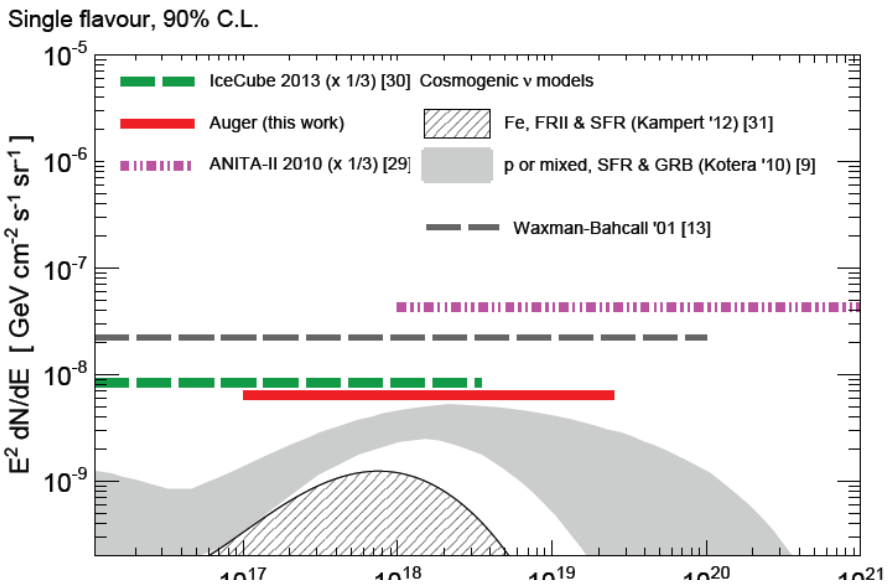

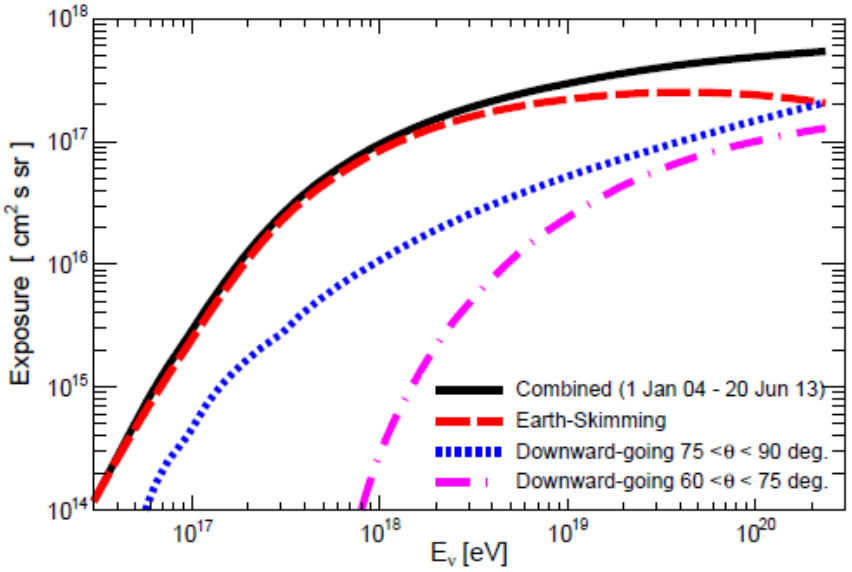

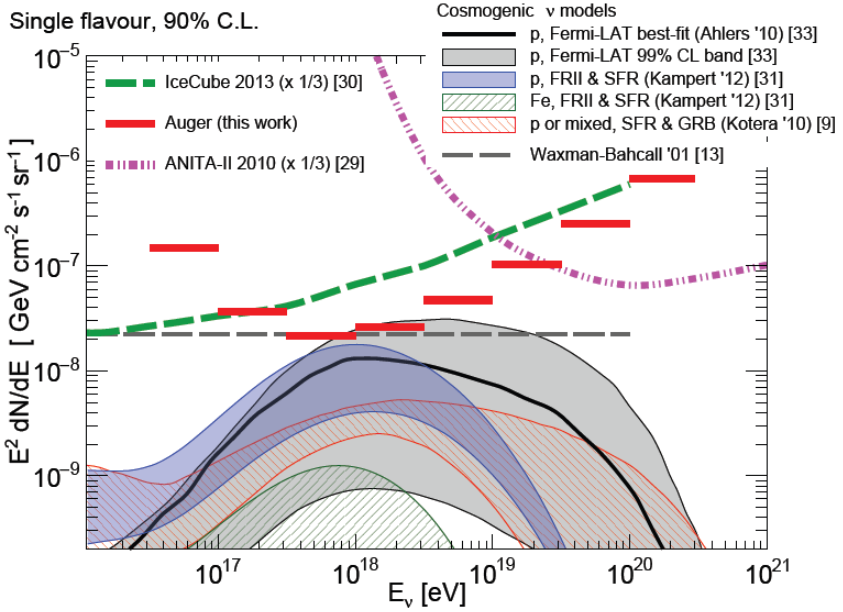

Hadronic Interactions

Demonstrations of some successes - and of some problems

Models developed by the Cosmic Ray community fitted early LHC data quite well

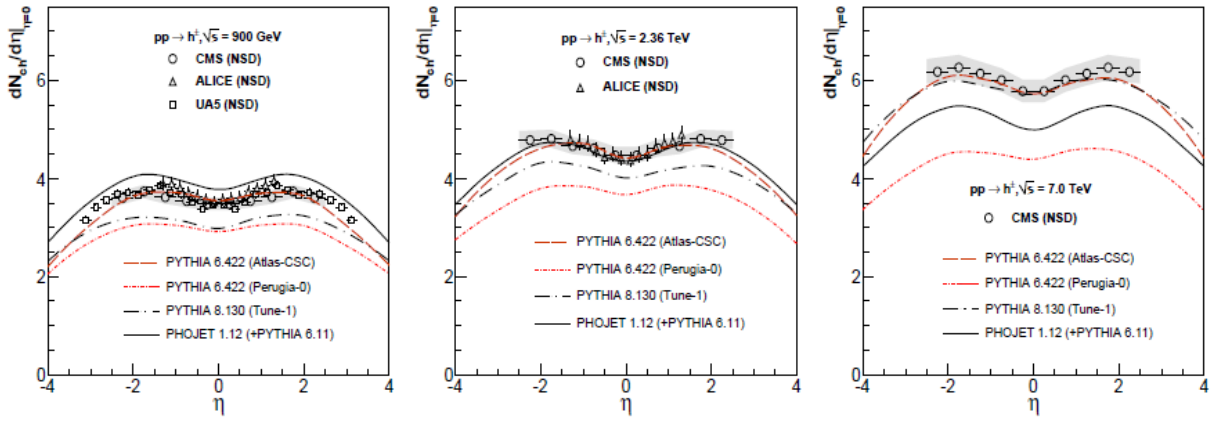

FIG. 2: Pseudorapidity distributions of charged hadrons, $h^{\pm} \equiv (h^+ + h^-)/2$, measured in NSD p-p events at the LHC ($\sqrt{s} = 0.9$, 2.36 and 7 TeV) by ALICE [34, 35] and CMS [36, 37] (and by UA5 [41] in p-$\bar{p}$ at 900 GeV) compared to three different versions of the PYTHIA and PHOJET MCs. The dashed band is the systematic uncertainty of the CMS experiment which is similar to those of the two other measurements.

Accelerator Models

900 GeV **2.36 TeV** **7 TeV**

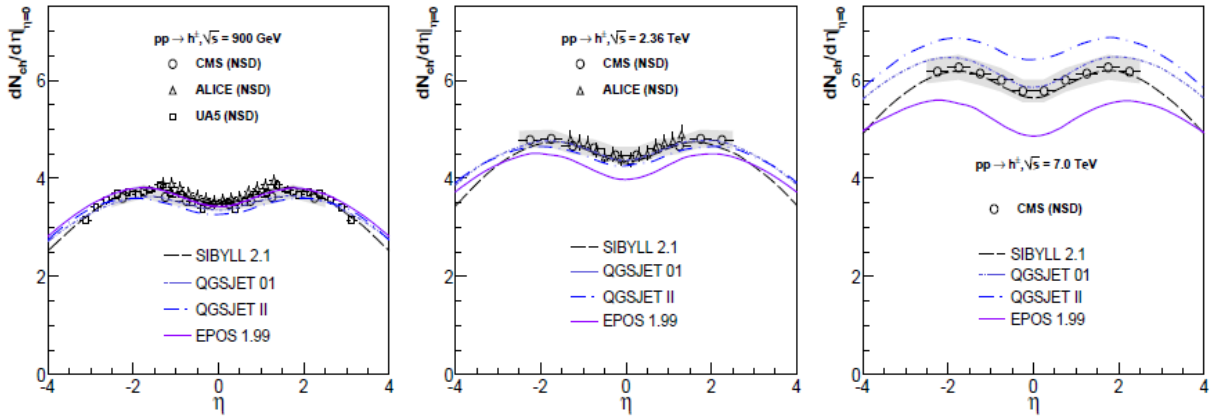

FIG. 3: Pseudorapidity distributions of charged hadrons, $h^{\pm} \equiv (h^+ + h^-)/2$, measured in NSD p-p events at the LHC (0.9, 2.36 and 7 TeV) by ALICE [34, 35] and CMS [36, 37] (and by UA5 [41] in p-$\bar{p}$ at 900 GeV) compared to the predictions of QGSJET01 and II, SIBYLL, and EPOS. The dashed band is the systematic uncertainty of the CMS experiment which is similar to those of the two other measurements.

Cosmic ray models

d'Enterria, Engel, Pierog, Ostapchenko and Werner (2011)

Cross-section measurements from Auger Observatory: PRL 109 062002 2012

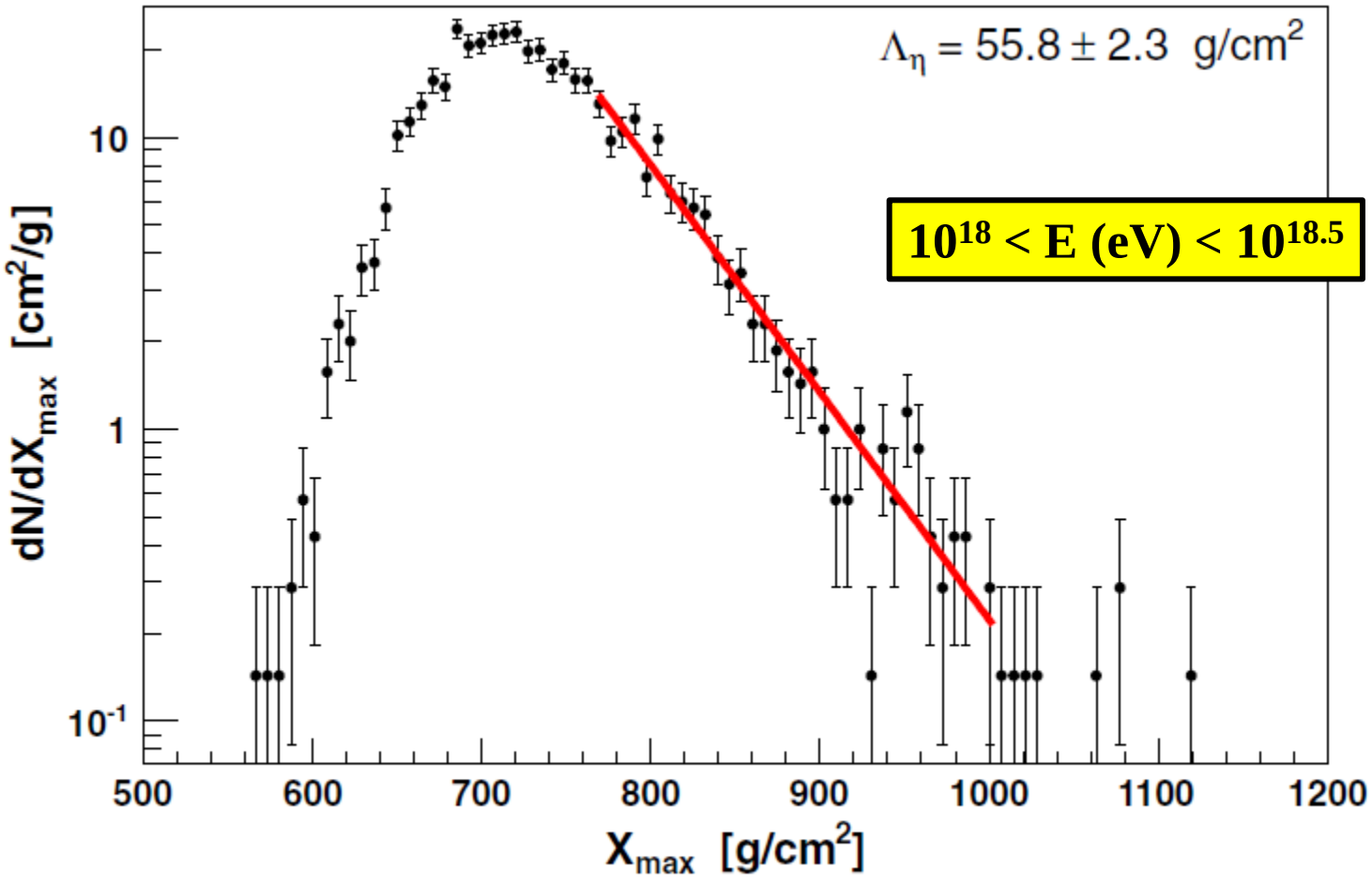

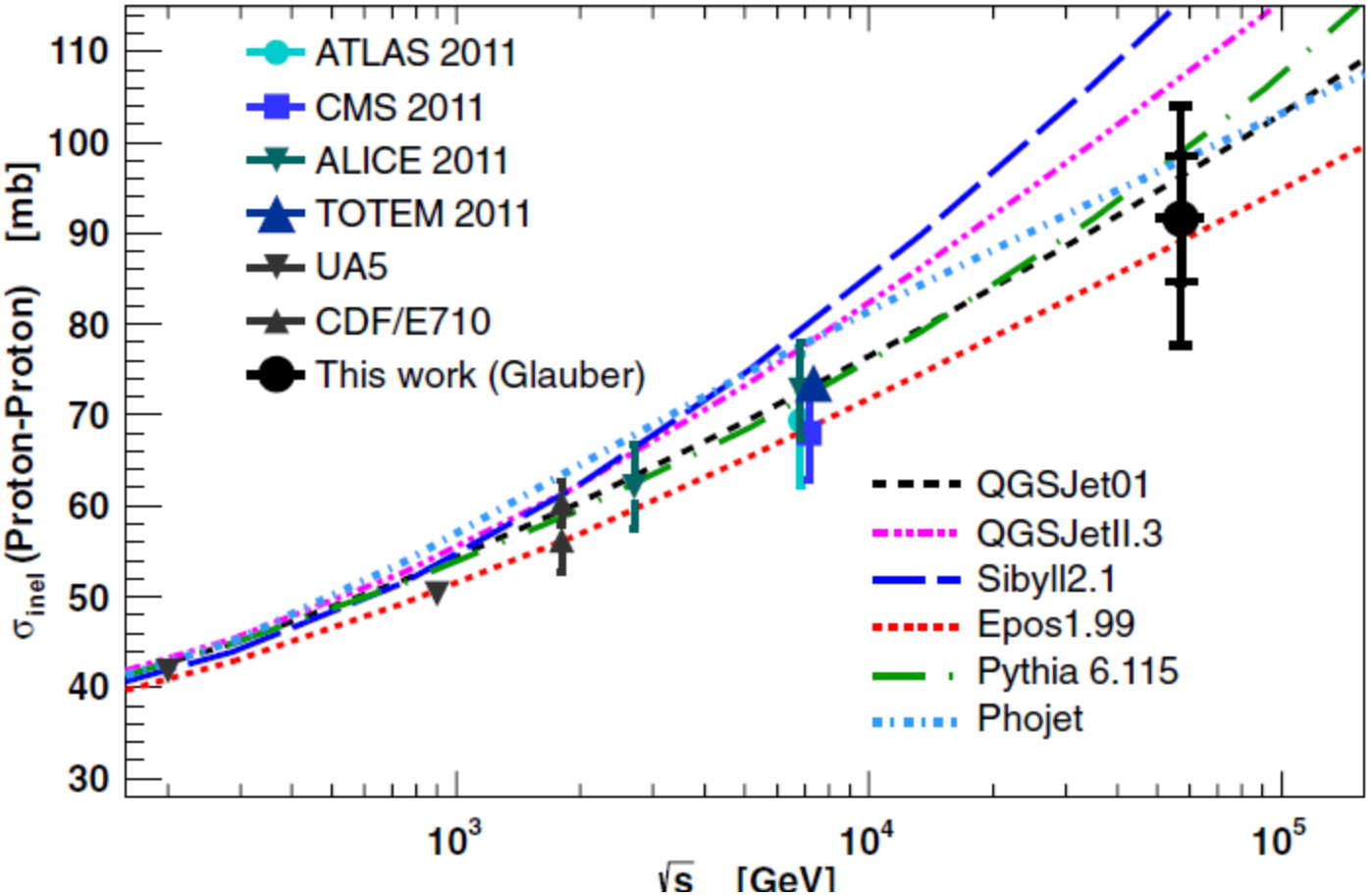

$$\sigma_{pp}^{\text{inel}} = [92 \pm 7(\text{stat})^{+9}_{-11}(\text{syst}) \pm 7(\text{Glauber})]\ \text{mb},$$

$$\sigma_{pp}^{\text{tot}} = [133 \pm 13(\text{stat})^{+17}_{-20}(\text{syst}) \pm 16(\text{Glauber})]\ \text{mb}.$$

Updated results on cross-section will be reported at ICRC 2015

- **Significant increase in number of events**
- **Two energy ranges: $10^{17.8} < E(eV) < 10^{18.0}$ and $10^{18} < E(eV) < 10^{18.5}$**
- **Systematic Uncertainties from mass better understood**
- **Only 20% of most proton-like events are being used**
- **Taking advantage of model updates from LHC**

Inclined showers are proving very useful to test models

We find that there are problems with models at high energies and large angles where muon number in showers can be studied cleanly

Summary of following papers:-

Inclined Reconstruction: JCAP 08 019 2014

Inclined Muon Number: PRD 91 032003 2015

Muon Production Depth: Phys Rev D 90 (2014) 012012

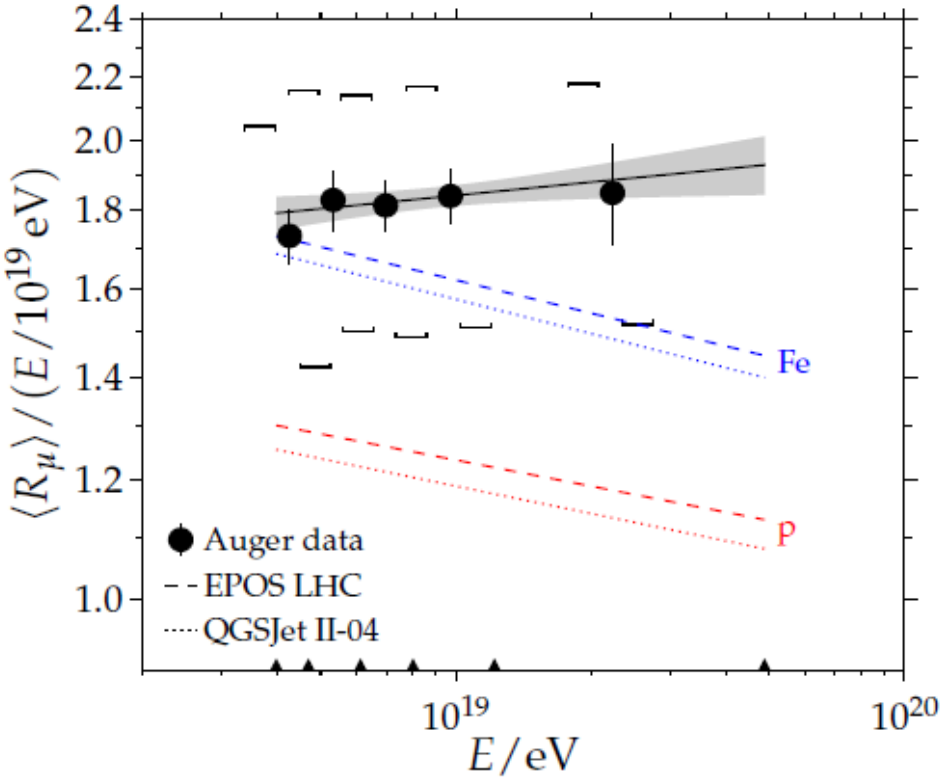

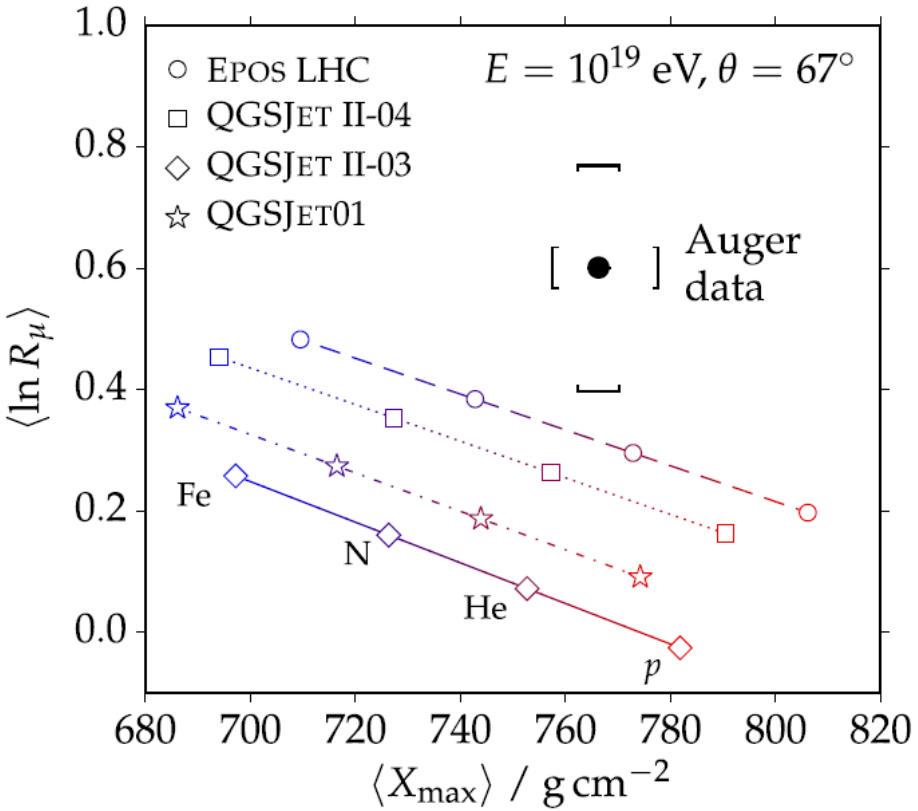

Muon numbers predicted by models are under-estimated by 30 to 80% (20% systematic)

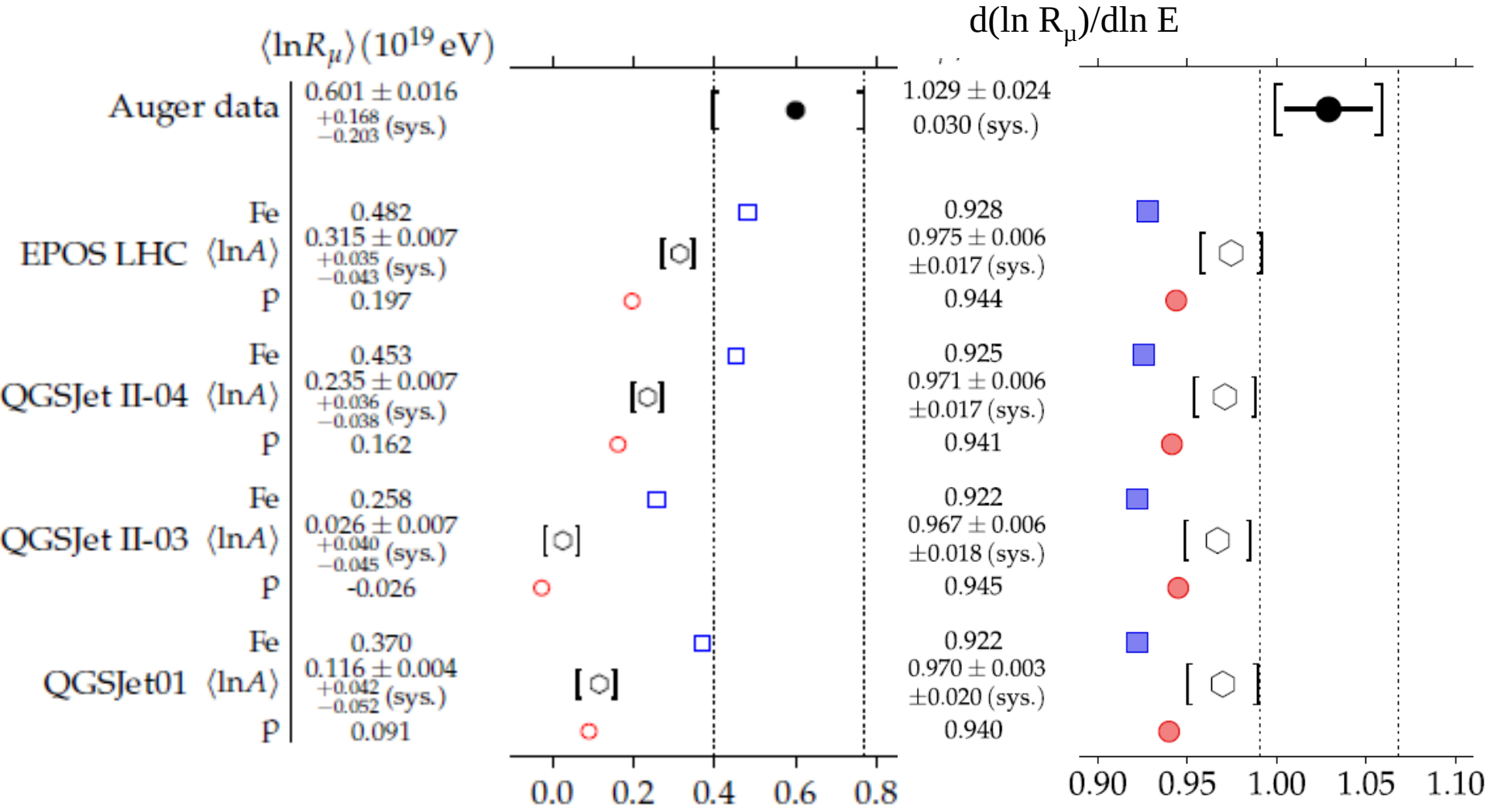
$\langle \ln R_\mu \rangle (10^{19}\,\mathrm{eV})$
d(ln R_μ)/dln E
Auger data
0.601 ± 0.016 $^{+0.168}_{-0.203}$ (sys.)
1.029 ± 0.024 0.030 (sys.)
EPOS LHC
Fe
0.482
$\langle \ln A \rangle$
0.315 ± 0.007 $^{+0.035}_{-0.043}$ (sys.)
0.975 ± 0.006 ± 0.017 (sys.)
p
0.197
0.944
0.928
QGSJet II-04
Fe
0.453
$\langle \ln A \rangle$
0.235 ± 0.007 $^{+0.036}_{-0.038}$ (sys.)
0.971 ± 0.006 ± 0.017 (sys.)
p
0.162
0.941
0.925
QGSJet II-03
Fe
0.258
$\langle \ln A \rangle$
0.026 ± 0.007 $^{+0.040}_{-0.045}$ (sys.)
0.967 ± 0.006 ± 0.018 (sys.)
p
-0.026
0.945
0.922
QGSJet01
Fe
0.370
$\langle \ln A \rangle$
0.116 ± 0.004 $^{+0.042}_{-0.052}$ (sys.)
0.970 ± 0.003 ± 0.020 (sys.)
p
0.091
0.940
0.922
0.0
0.2
0.4
0.6
0.8
0.90
0.95
1.00
1.05
1.10

Second method of testing models:
Muon Production Depth (MPD)
PRD 90 012012 2014

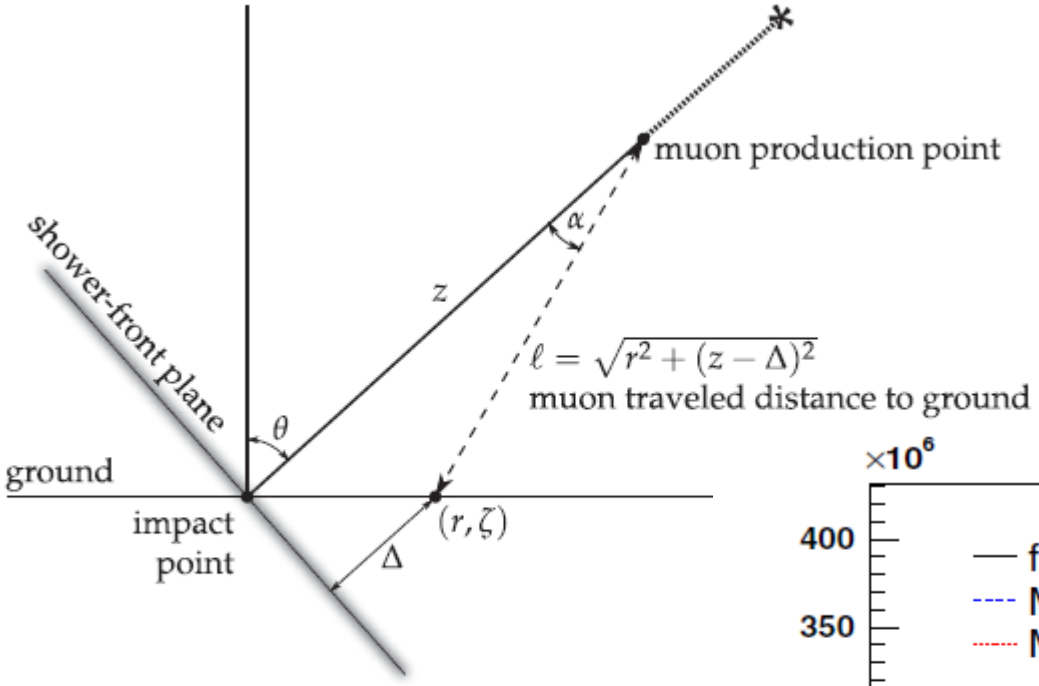

FIG. 1. Geometry used to obtain the muon t
the time delay.

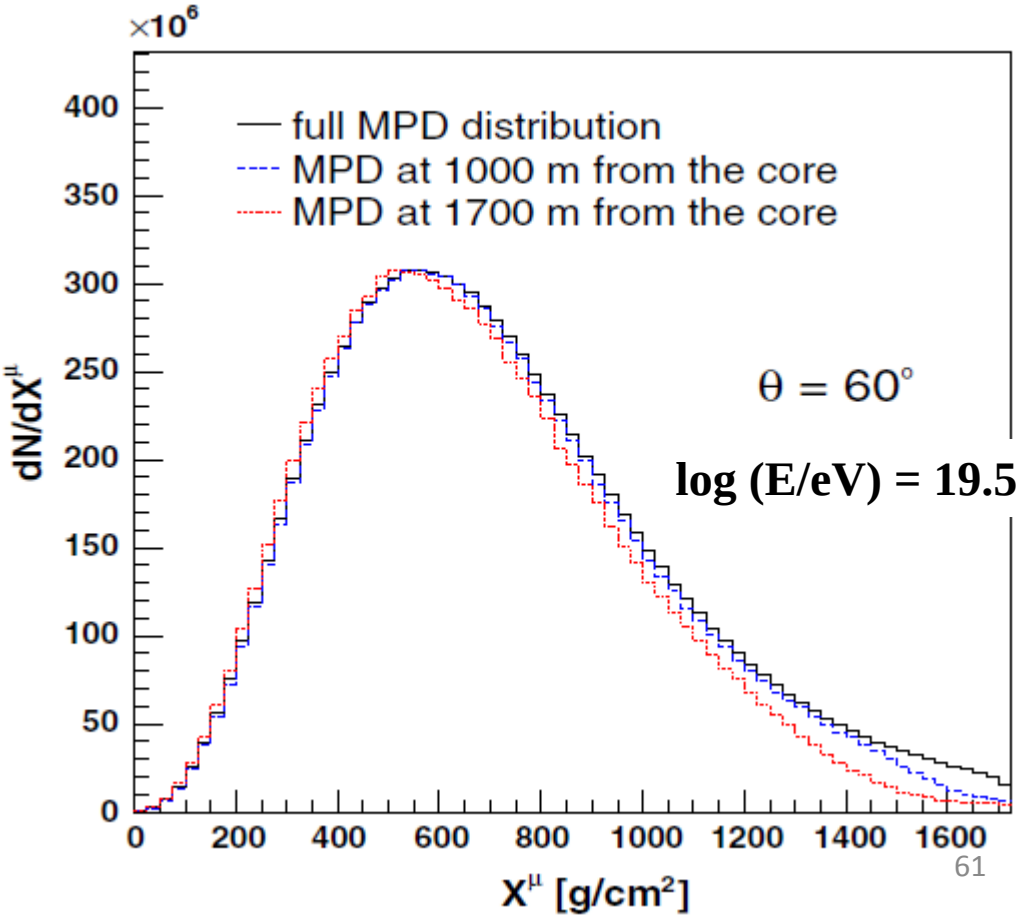

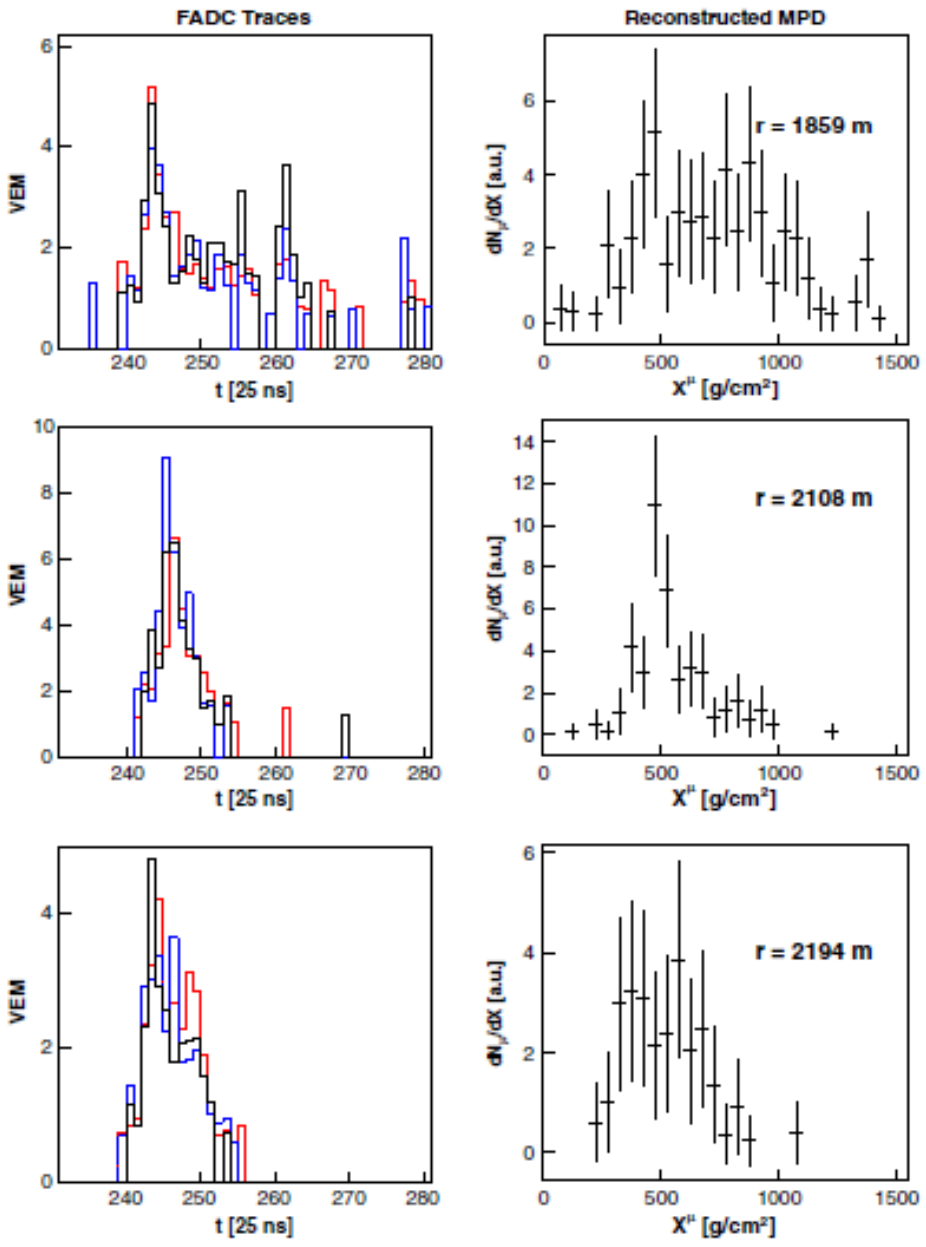
FADC Traces
Reconstructed MPD
VEM
t [25 ns]
dN_μ/dX [a.u.]
X^μ [g/cm²]
r = 1859 m
r = 2108 m
r = 2194 m

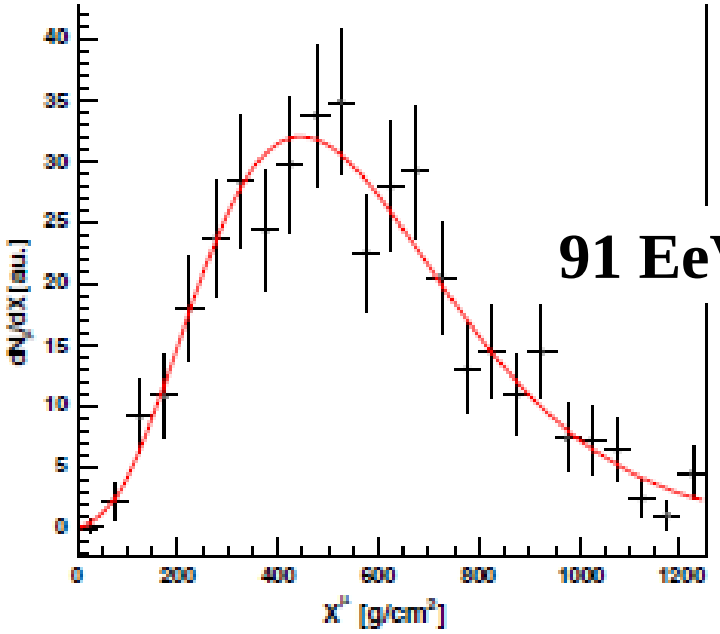
91 EeV
dN_μ/dX [a.u.]
X^μ [g/cm²]

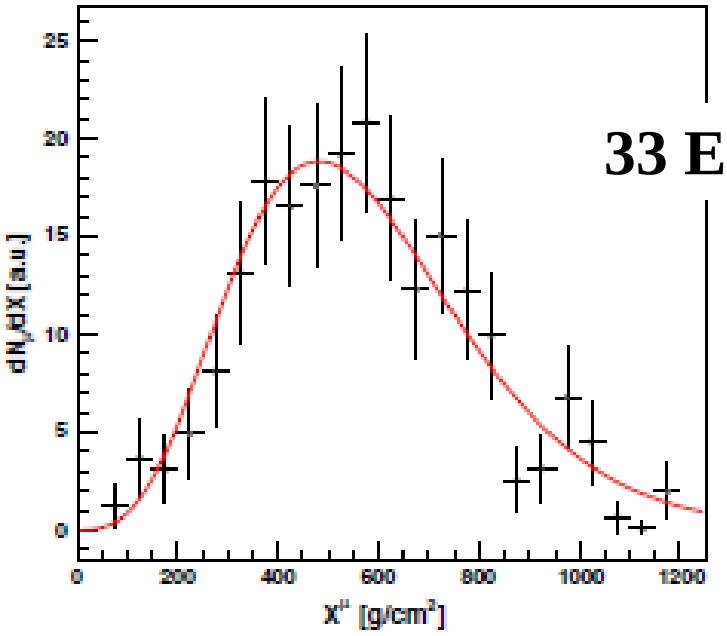
33 EeV
dN_μ/dX [a.u.]
X^μ [g/cm²]

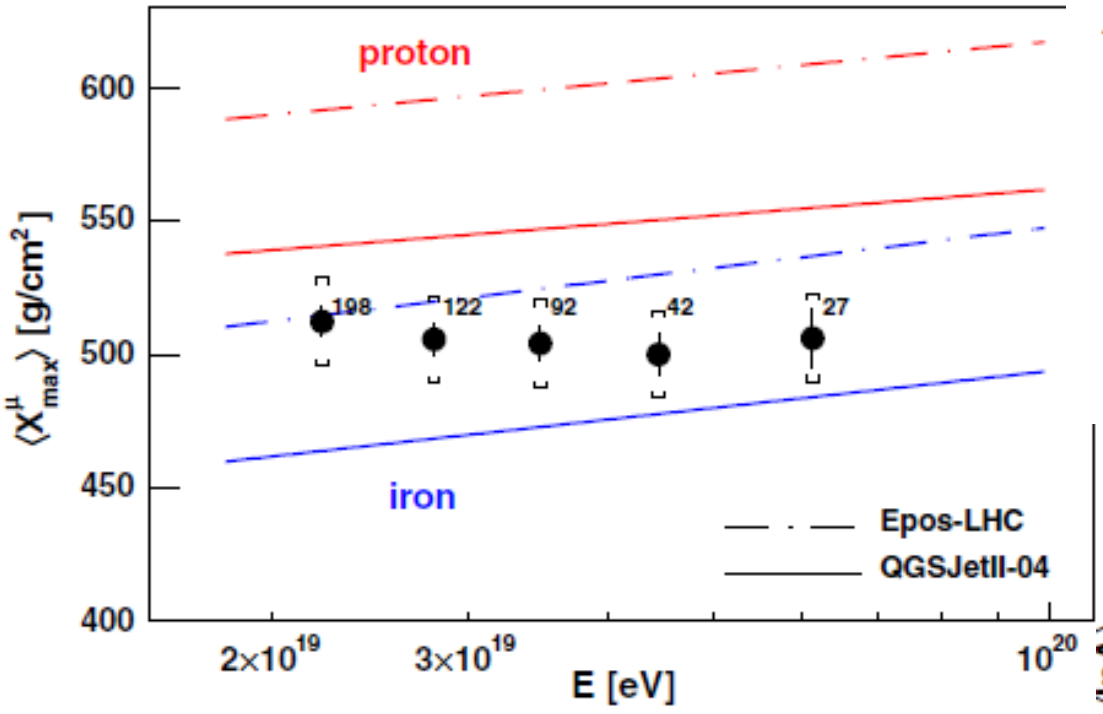

FIG. 8 (color online). $\langle X^{\mu}_{\max} \rangle$ as a function of energy. Th

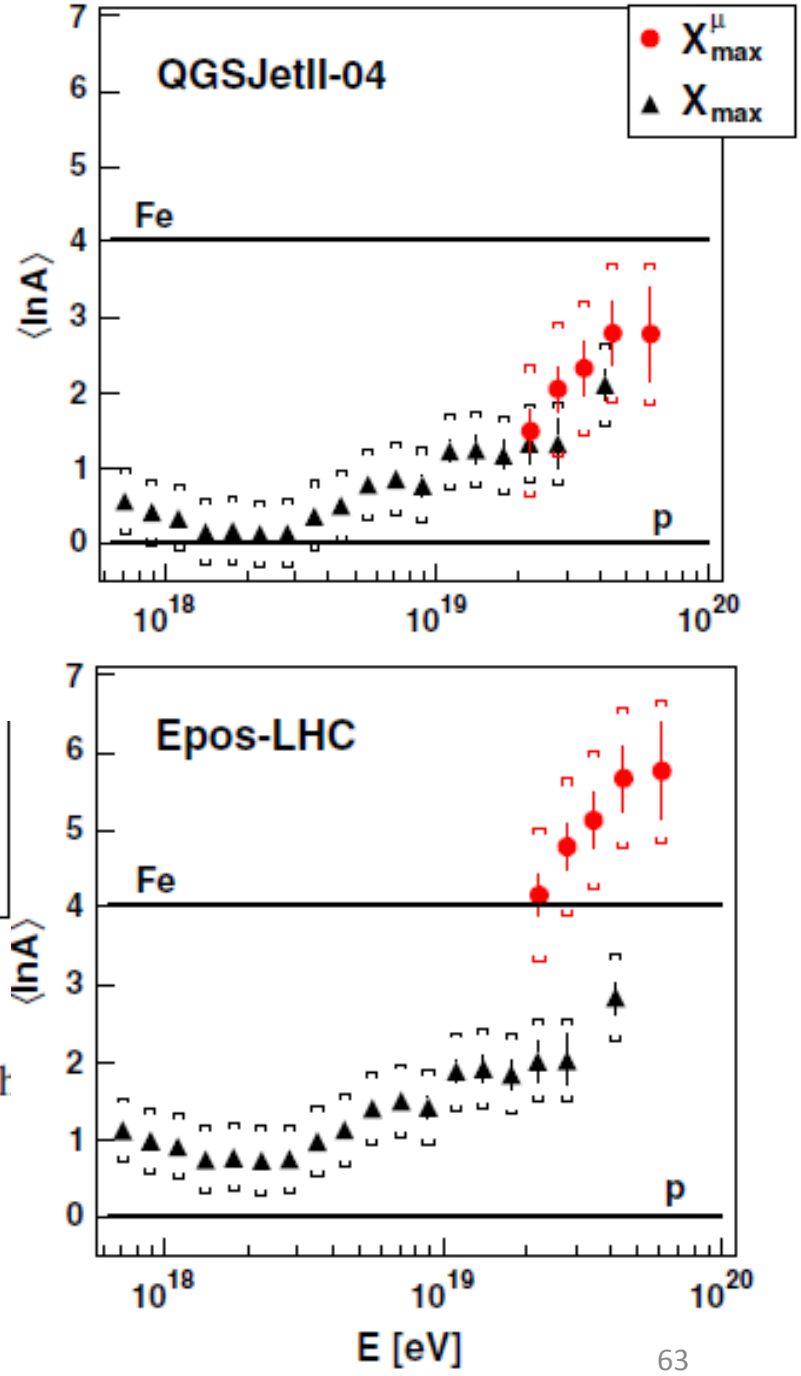

Summary of main results from Auger Observatory

- **Spectrum suppression above ~ 40 EeV**
- **Large scale dipole in arrival distribution above 8 EeV**
- **Large scale anisotropy indicated by phase shift in RA below the knee**
- **Indications of anisotropy above 40 EeV – but hugely more events needed**
- **X_{max} shows (i) distinct change of slope with energy**
  (ii) rms becomes smaller with energy

These changes suggest mass becomes heavier as energy increases

Important limits to fluxes of neutrinos and photons

- **Inconsistencies of muon data (number and depth of maximum) with models**
- **Major question: Is suppression GZK or photodisintegration?**

Maximum energy scenario

Propagation and photodisintegration

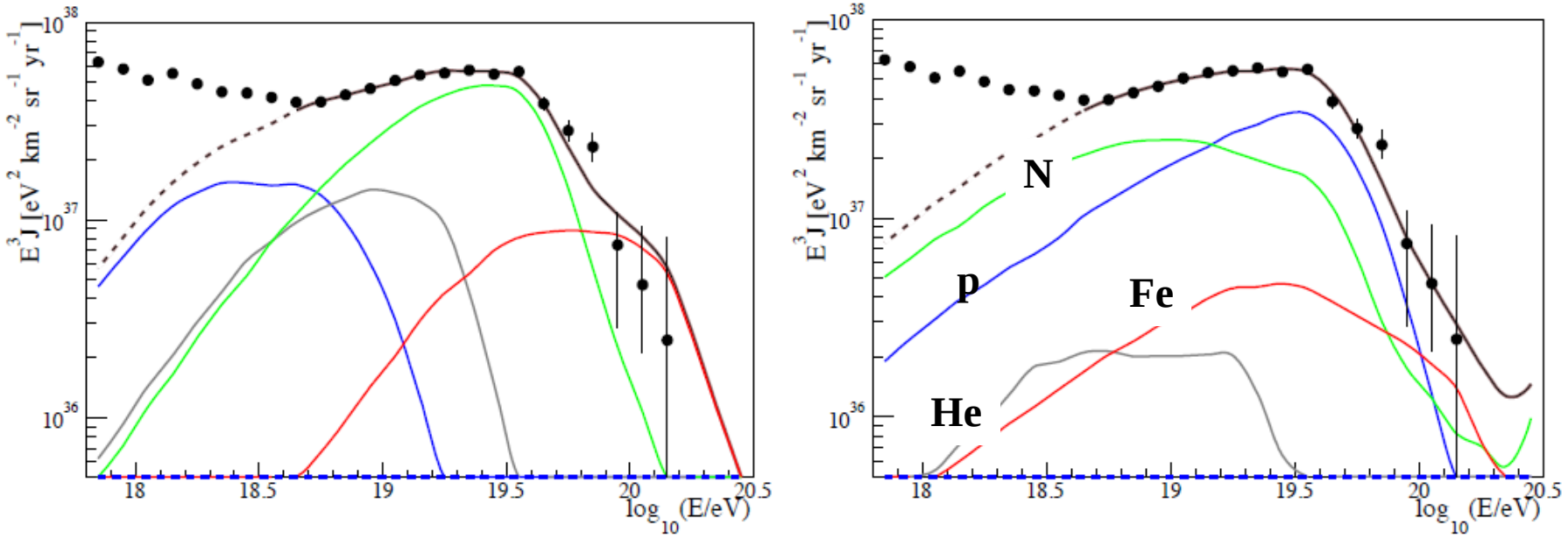

Figure 2.10: Examples of fluxes of different mass groups for describing the Auger spectrum and composition data. Shown are the fluxes of different mass groups that are approximations of the maximum-energy scenario (left panel) and one photo-disintegration scenario (right panel). The colors for the different mass groups are protons – blue, helium – gray, nitrogen – green, and iron – red. The model calculations were done with SimProp [30], very similar results are obtained with CRPropa [29].

To answer this question we need mass information in more detail and at higher energies

This is the main aim of the plans being evaluated now for the next phase of the Observatory

What we plan to do:-

- **FD on-time will be extended to 19% to access higher energies**
- **Radio technique will be developed to get many more data on X_{max} at lower energies**
- **Scintillators will be added above water-Cherenkov detectors to deduce muons with method calibrated with buried muon detectors**

Aim is to identify mass of primary on event-by-event basis

(i) Detection of Showers using Radio antennas

with AERA-24 data (126 HQ events)

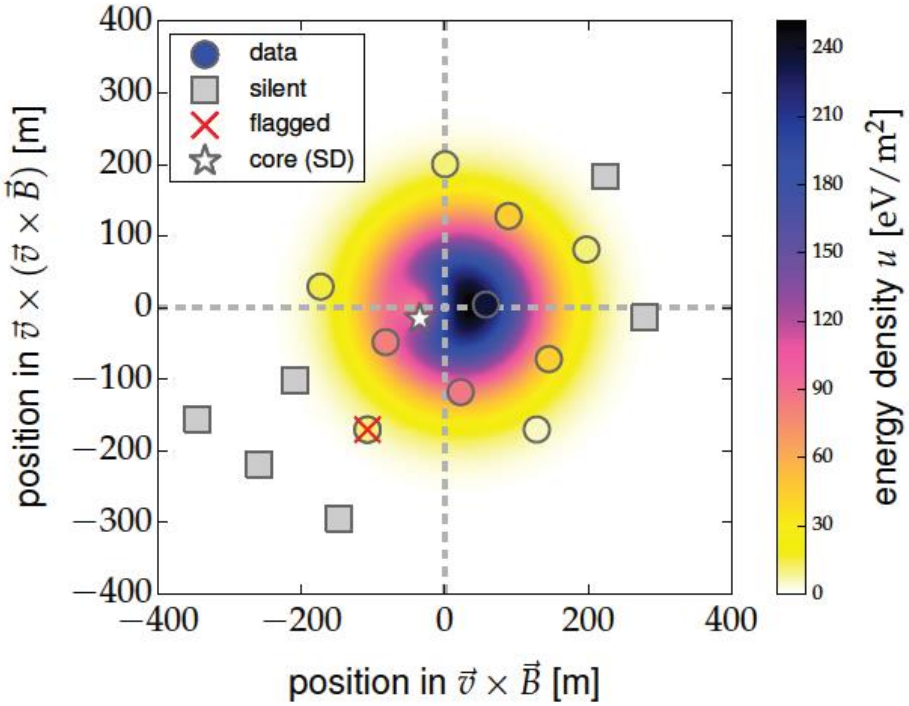

40 – 80 MHz

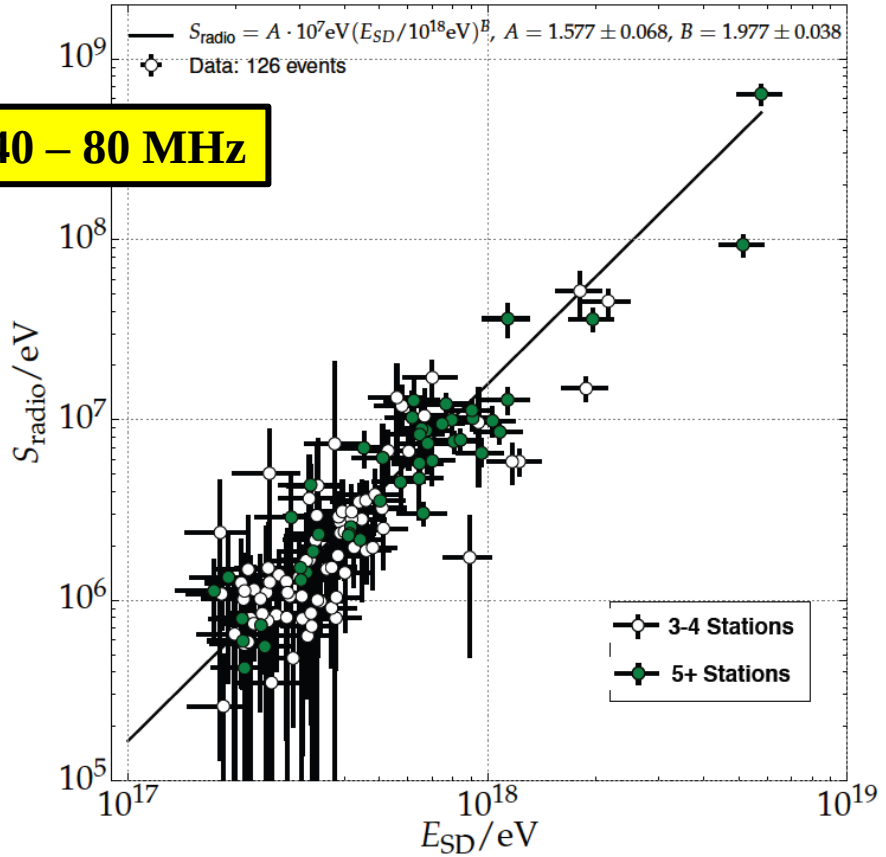

Energy resolution better than 22%

15.7 MeV in 1 EeV shower

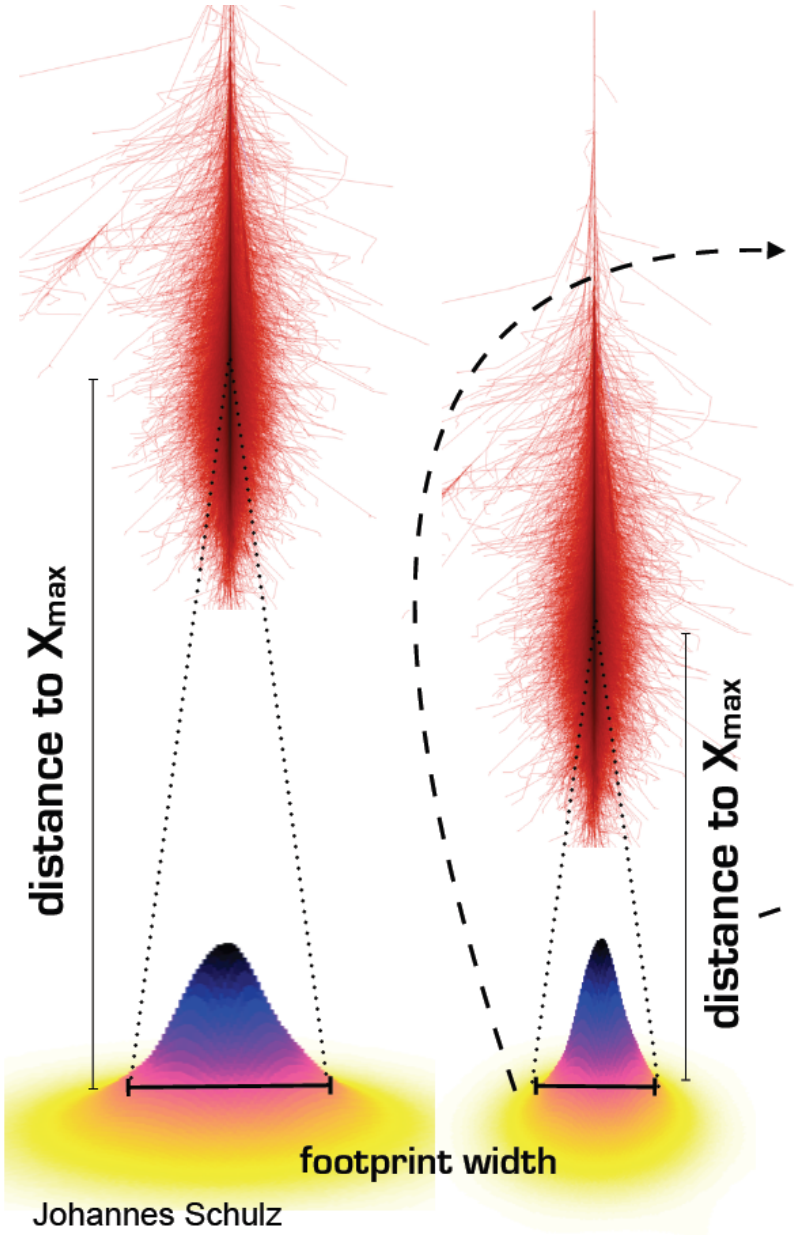

AERA24 **Simulations**:

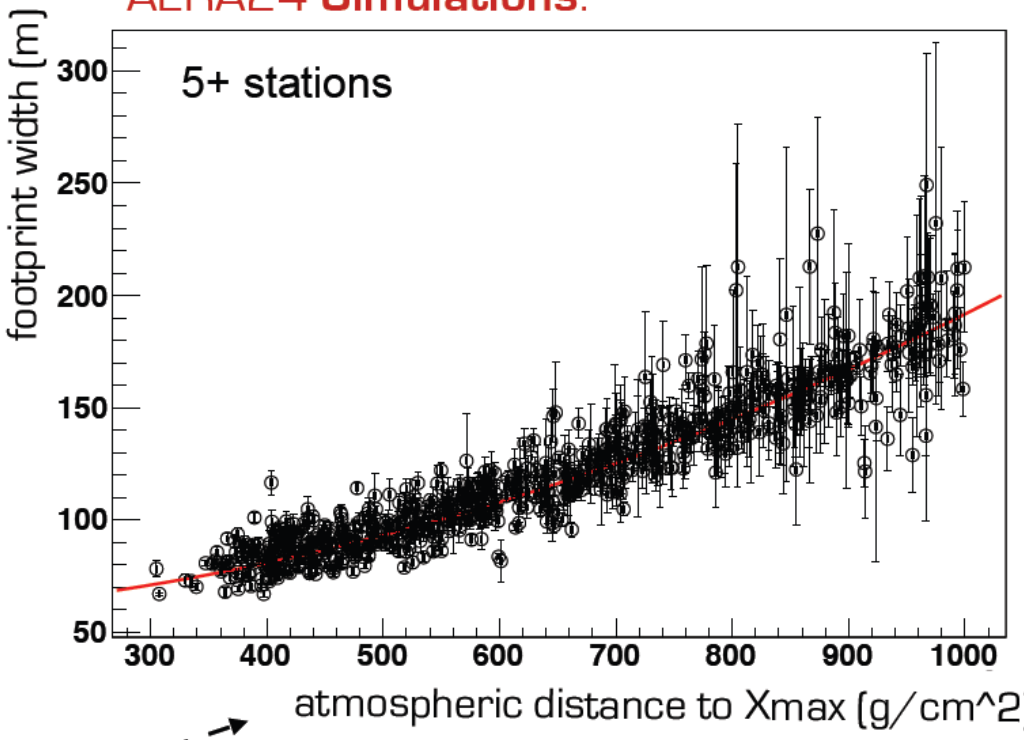

X_{max} = total atmosphere — distance to X_{max}

distance to Xmax resolution ~50 g/cm^2

Method: A. Nelles et al., submitted to JCAP, arXiv1411.7868

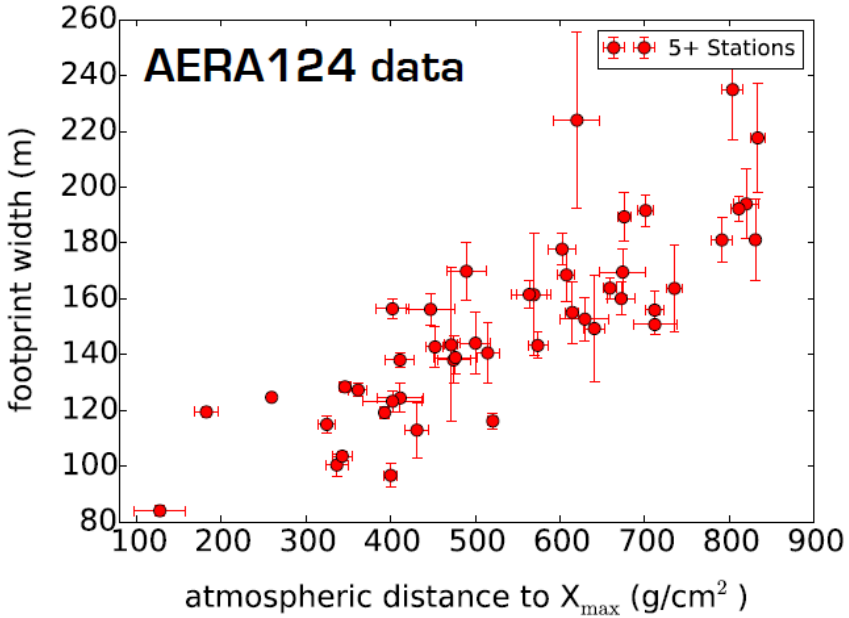

distance to Xmax based on FD measurement

no quality cuts applied

-

definition of radio quality cuts concerning 2D-LDF pending

width of the radio footprint shows sensitivity to Xmax

-

exact dependency and resolution to be determined

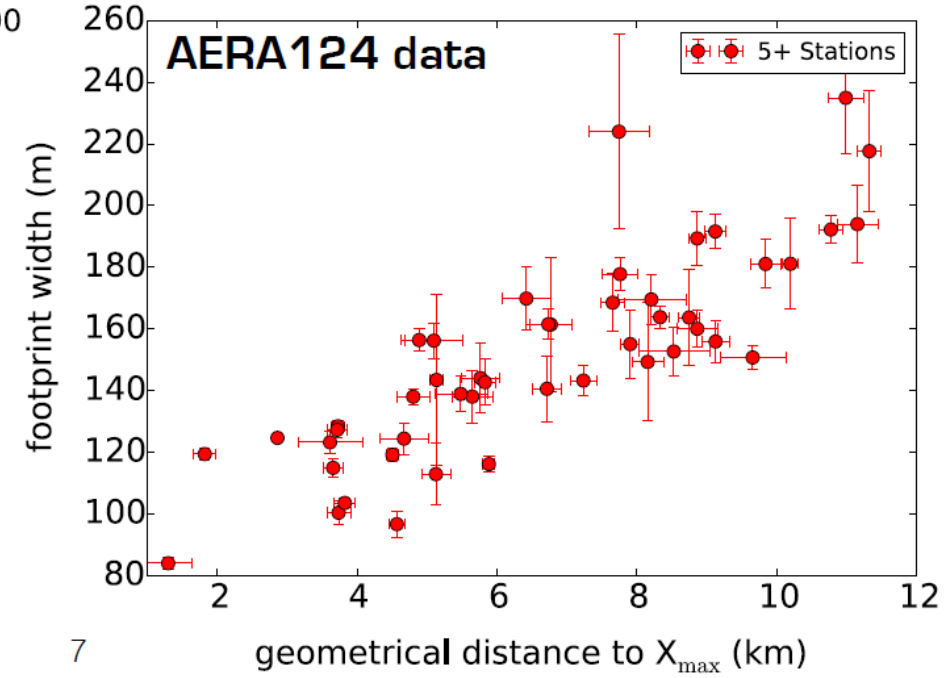

Prospect of X_{max} resolution of ~20 g cm^{-2}

(ii) 4 m^2 Scintillators above Water-Cherenkov detectors

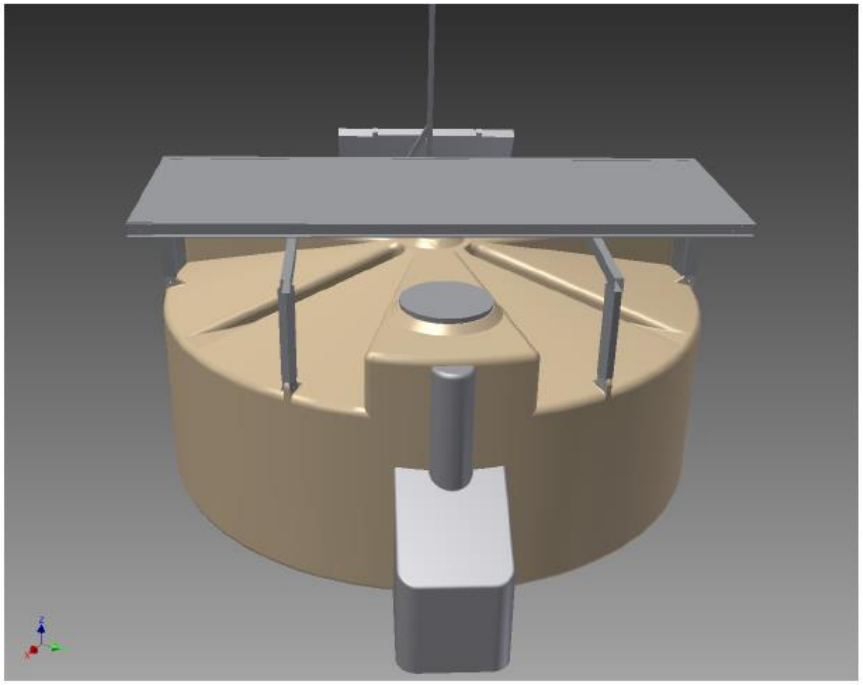

Figure 4.1: 3D view of a water-Cherenkov detector with a scintillator unit on top.

Scintillators respond to muons and electromagnetic component

Water-Cherenkov detectors absorb all of the em component and are fully sensitive to muons

It has been demonstrated with simulations that techniques exist to separate out the muon component

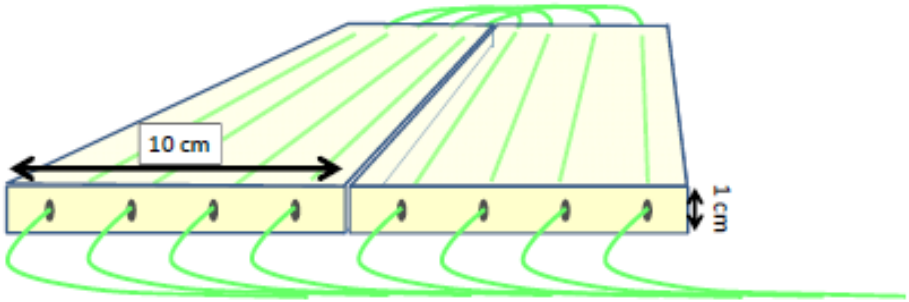

(iii) Buried Muon Detectors (1.3 m below surface)

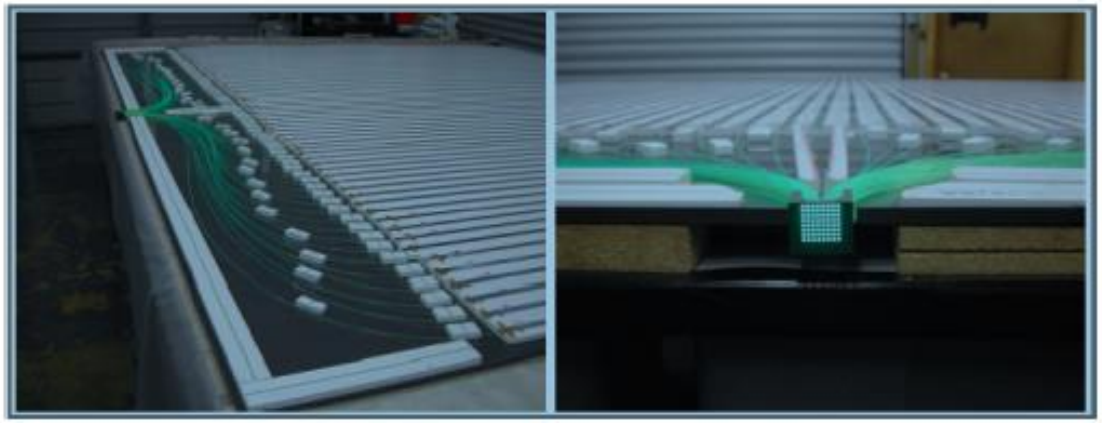

Figure 5.1: Scintillators strips: left: general mounting in the PVC housing, right: detail of the 64-pixel optical connectors.

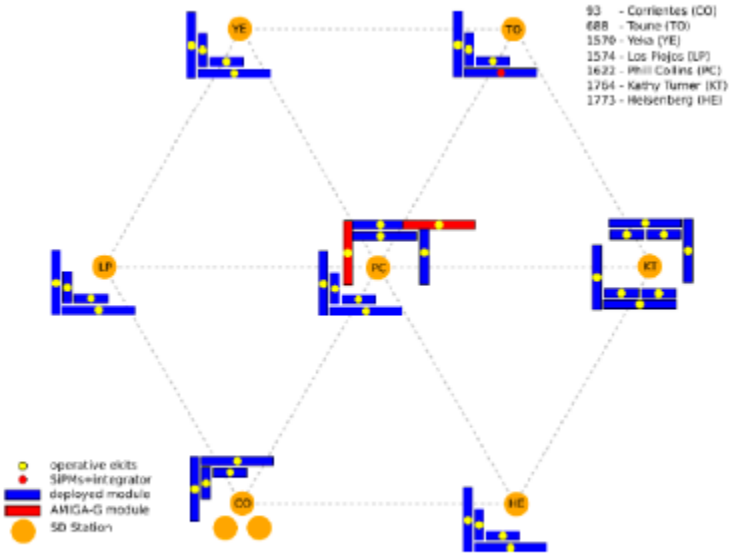

60 x 20 m^2

Figure 5.2: AMIGA unitary cell.

Long-term Future

Auger Observatory is at least one-order of magnitude to small

Planned space projects as very important: is there something interesting to measure beyond the present questions?

Compare SPS and LEP

Young people working together and getting to know each other is necessary for any future World Observatory
Joint Working Groups – great success

How can a giant Observatory be created?

How can we take this concept forward?

Timescale is surely at least 10 years to begin

Back Up Slides

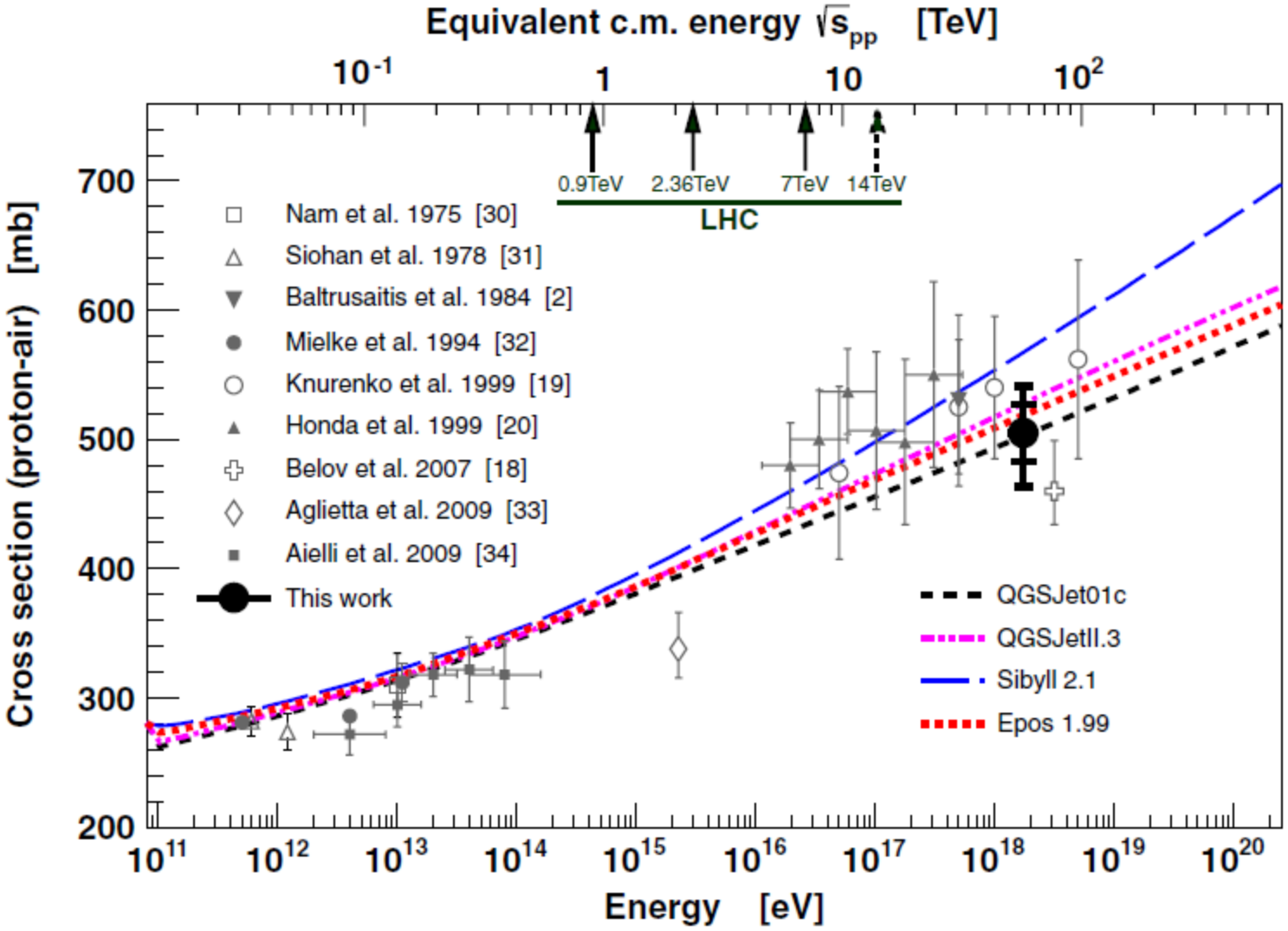
Equivalent c.m. energy $\sqrt{s}_{pp}$ [TeV]
10^{-1}
1
10
10^{2}
0.9TeV
2.36TeV
7TeV
14TeV
LHC
Nam et al. 1975 [30]
Siohan et al. 1978 [31]
Baltrusaitis et al. 1984 [2]
Mielke et al. 1994 [32]
Knurenko et al. 1999 [19]
Honda et al. 1999 [20]
Belov et al. 2007 [18]
Aglietta et al. 2009 [33]
Aielli et al. 2009 [34]
This work
QGSJet01c
QGSJetII.3
Sibyll 2.1
Epos 1.99
Cross section (proton-air) [mb]
700
600
500
400
300
200
10^{11}
10^{12}
10^{13}
10^{14}
10^{15}
10^{16}
10^{17}
10^{18}
10^{19}
10^{20}
Energy [eV]

AGN Correlation Update

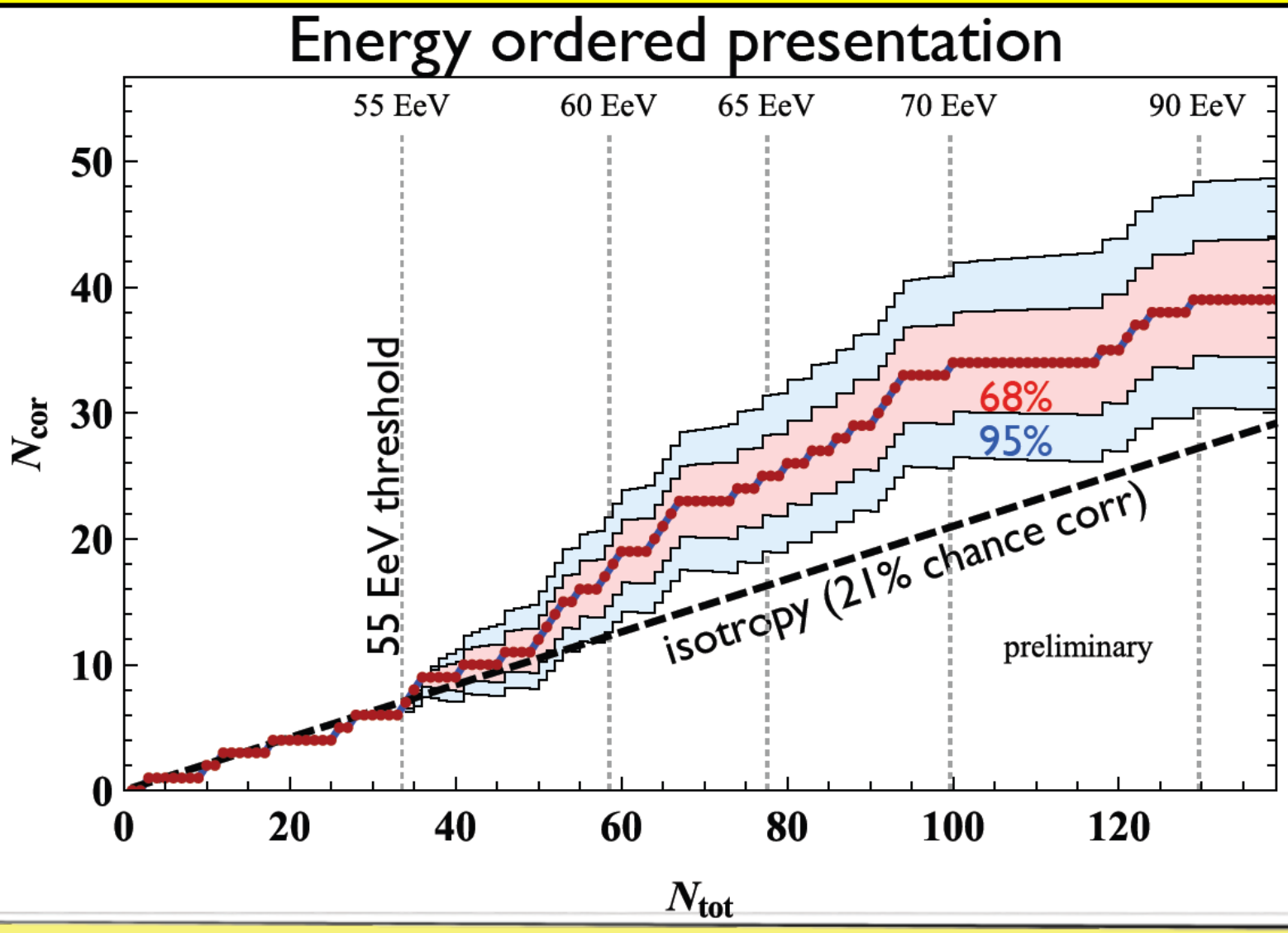

chance probability: 1.4% ; is there an energy dependence?

UHECR Correlation with AGNs

Science: 9 November 2007

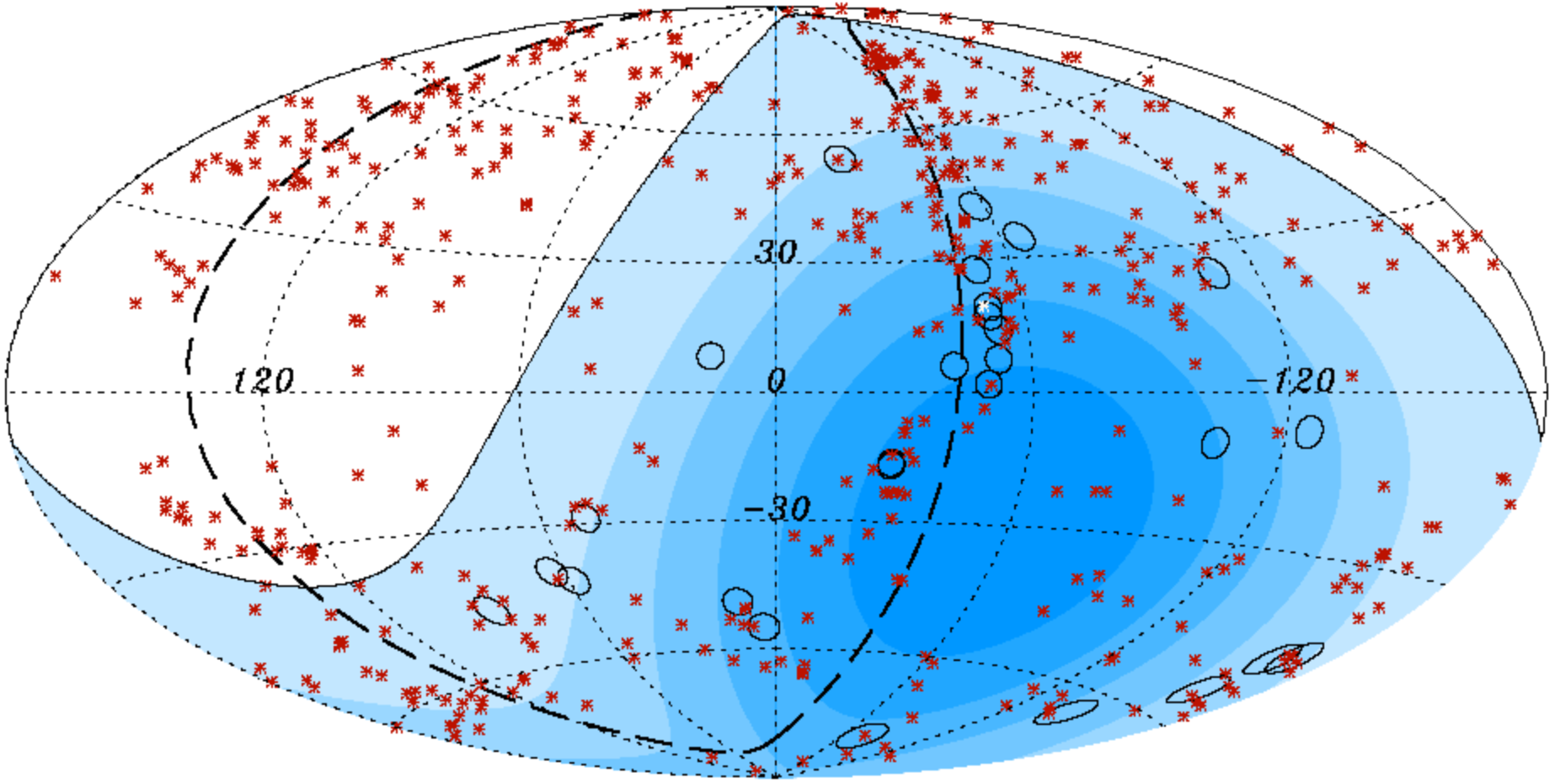

First scan gave ψ < 3.1°, z < 0.018 (75 Mpc) and E > 56 EeV

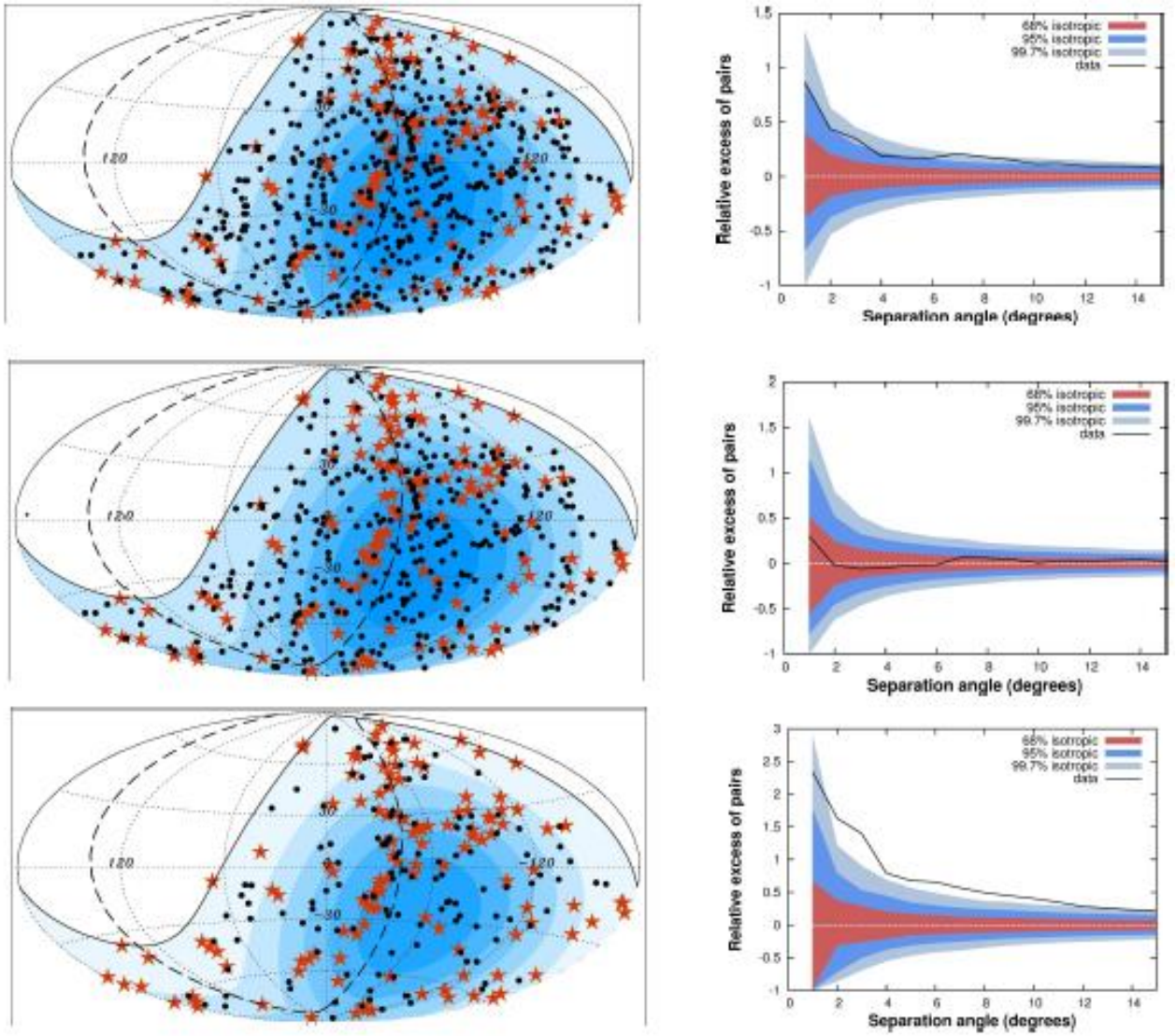

Figure 3.20: Arrival distribution and angular correlation of cosmic rays of the modified Auger dat set with AGNs of the Swift-BAT catalog [138]. Shown are events with $E > 4 \times 10^{19}$ eV. The to row of plots show the complete data set (454 events), the middle row the selection deprived of ligh elements (326 events), and the bottom row the proton-enriched selection (128 events).

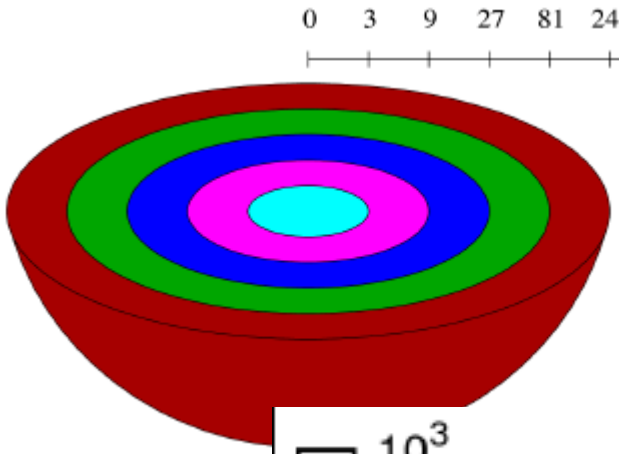

Taylor, arXiv:1107.2055

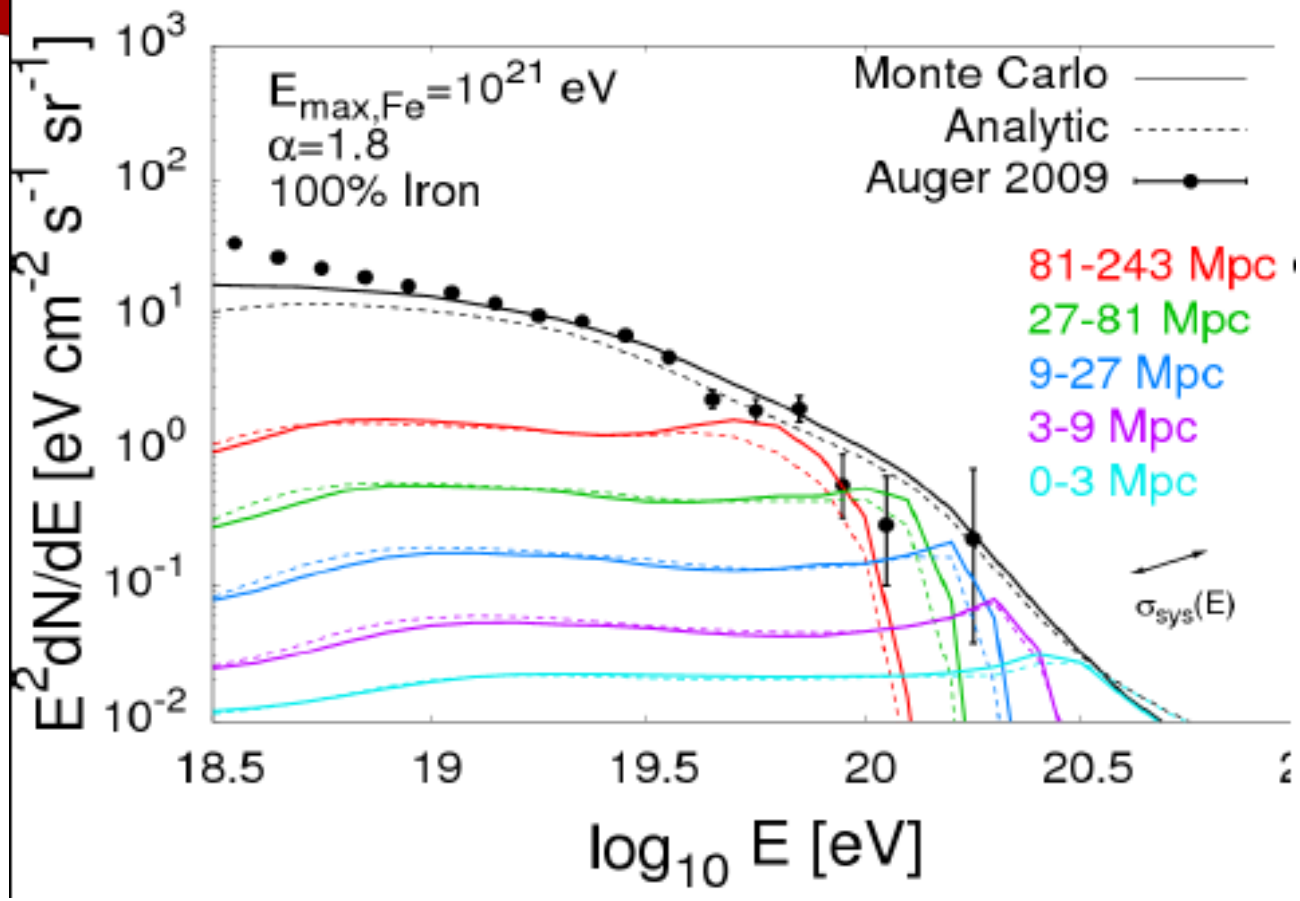

$$\begin{pmatrix} \tilde{S}_{\mathrm{SSD}} \\ \tilde{S}_{\mathrm{WCD}} \end{pmatrix} = \begin{pmatrix} a & b \\ c & d \end{pmatrix} \begin{pmatrix} \tilde{S}_{\mathrm{em}} \\ \tilde{S}_{\mu} \end{pmatrix}, \tag{2.1}$$

where we have defined the total electromagnetic and muonic signals of both detectors as

$$\tilde{S}_{\mathrm{em}} = \tilde{S}_{\mathrm{SSD},\mathrm{em}} + \tilde{S}_{\mathrm{WCD},\mathrm{em}} \qquad \text{and} \qquad \tilde{S}_{\mu} = \tilde{S}_{\mathrm{SSD},\mu} + \tilde{S}_{\mathrm{WCD},\mu}. \tag{2.2}$$

The matrix elements in Eq. (2.1) depend on the specific features of the two detectors and have to be determined by a detailed detector simulation. In first approximation there is no conversion of one shower component into the other within the detectors, implying

$$\tilde{S}_{\mathrm{SSD},\mathrm{em}} + \tilde{S}_{\mathrm{WCD},\mathrm{em}} = a\,\tilde{S}_{\mathrm{em}} + c\,\tilde{S}_{\mathrm{em}} = \tilde{S}_{\mathrm{em}}. \tag{2.3}$$

This leads to $c = 1 - a$ and $d = 1 - b$. The numerical values of a and b will be discussed in Sec. 3.5. Inverting Eq. 2.1 gives

$$\begin{aligned} \tilde{S}_{\mathrm{em}} &= \frac{1}{a-b}\left[(1-b)\,\tilde{S}_{\mathrm{SSD}} - b\,\tilde{S}_{\mathrm{WCD}}\right] \\ \tilde{S}_{\mu} &= \frac{1}{a-b}\left[(1-a)\,\tilde{S}_{\mathrm{SSD}} - a\,\tilde{S}_{\mathrm{WCD}}\right], \end{aligned} \tag{2.4}$$

from which one can obtain, for example, the muonic signal in the water-Cherenkov detector as

$$\tilde{S}_{\mathrm{WCD},\mu} = (1-b)\,\tilde{S}_{\mu} = \frac{1-b}{a-b}\left[(1-a)\,\tilde{S}_{\mathrm{SSD}} - a\,\tilde{S}_{\mathrm{WCD}}\right]. \tag{2.5}$$

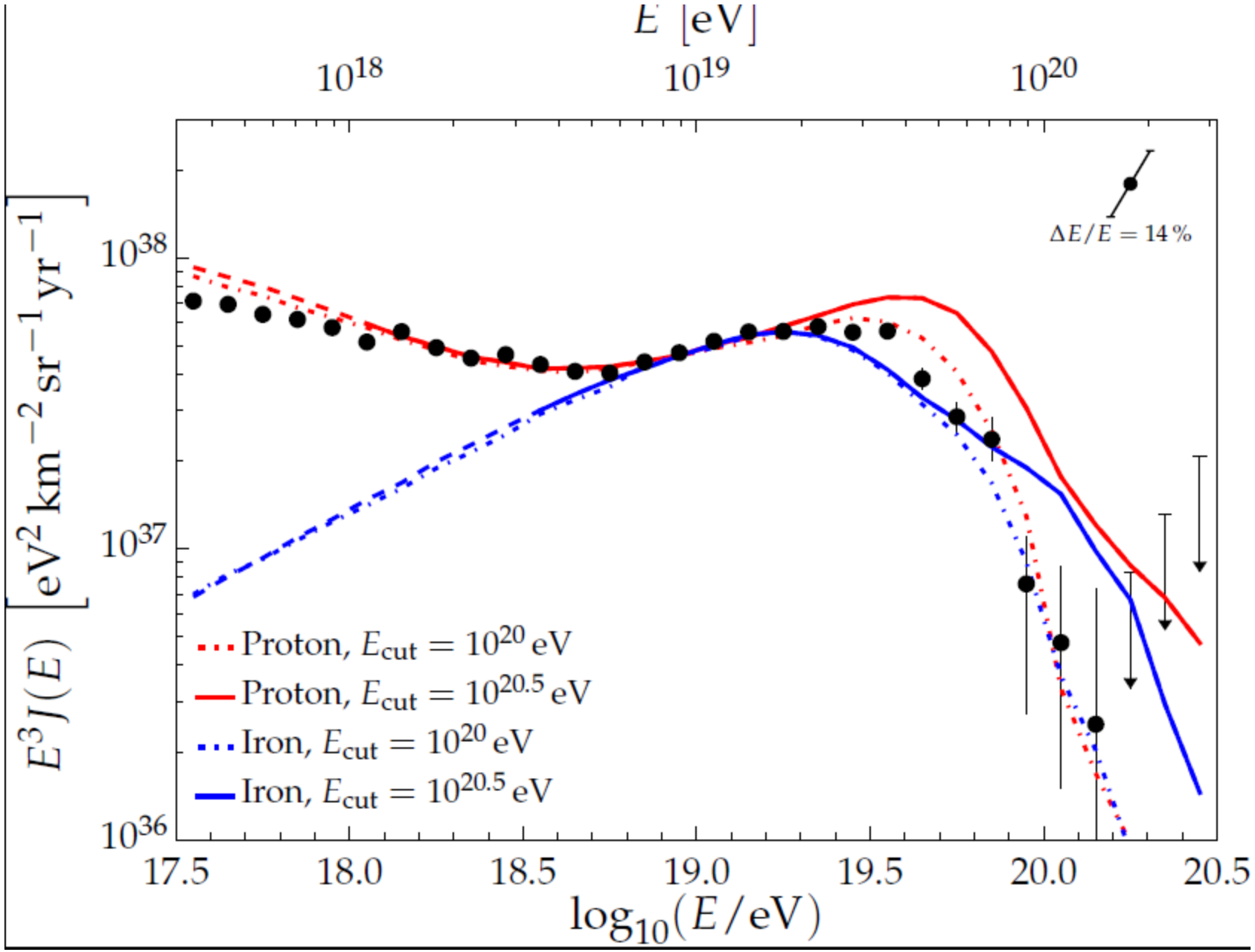
E [eV]
10^{18}
10^{19}
10^{20}
$\Delta E/E = 14\,\%$
$E^3 J(E)$ $\left[\mathrm{eV}^2\,\mathrm{km}^{-2}\,\mathrm{sr}^{-1}\,\mathrm{yr}^{-1}\right]$
10^{38}
10^{37}
10^{36}
Proton, $E_{\mathrm{cut}} = 10^{20}$ eV
Proton, $E_{\mathrm{cut}} = 10^{20.5}$ eV
Iron, $E_{\mathrm{cut}} = 10^{20}$ eV
Iron, $E_{\mathrm{cut}} = 10^{20.5}$ eV
17.5
18.0
18.5
19.0
19.5
20.0
20.5
$\log_{10}(E/\mathrm{eV})$

The phase-first argument of Linsley

ments. If the number of events available in an experiment is such that the RMS value of r is equal to the true value of s, then in a sequence of experiments r will only be significant (say p < 1%) in one experiment out of ten whereas the phase will be within 50 degrees of the true phase in two experiments out of three.

Dependence of Exposure on Declination

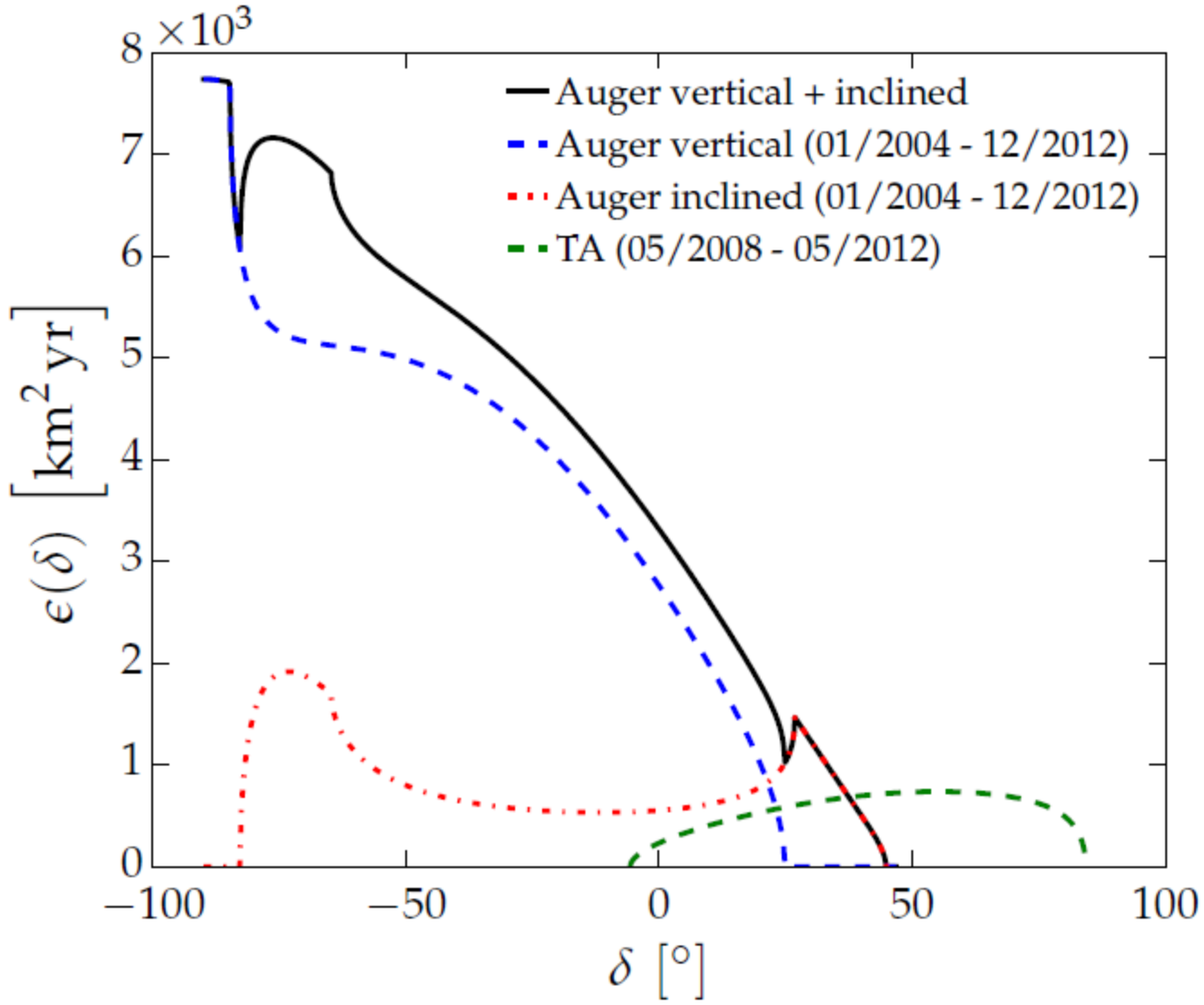

Telecommunication system

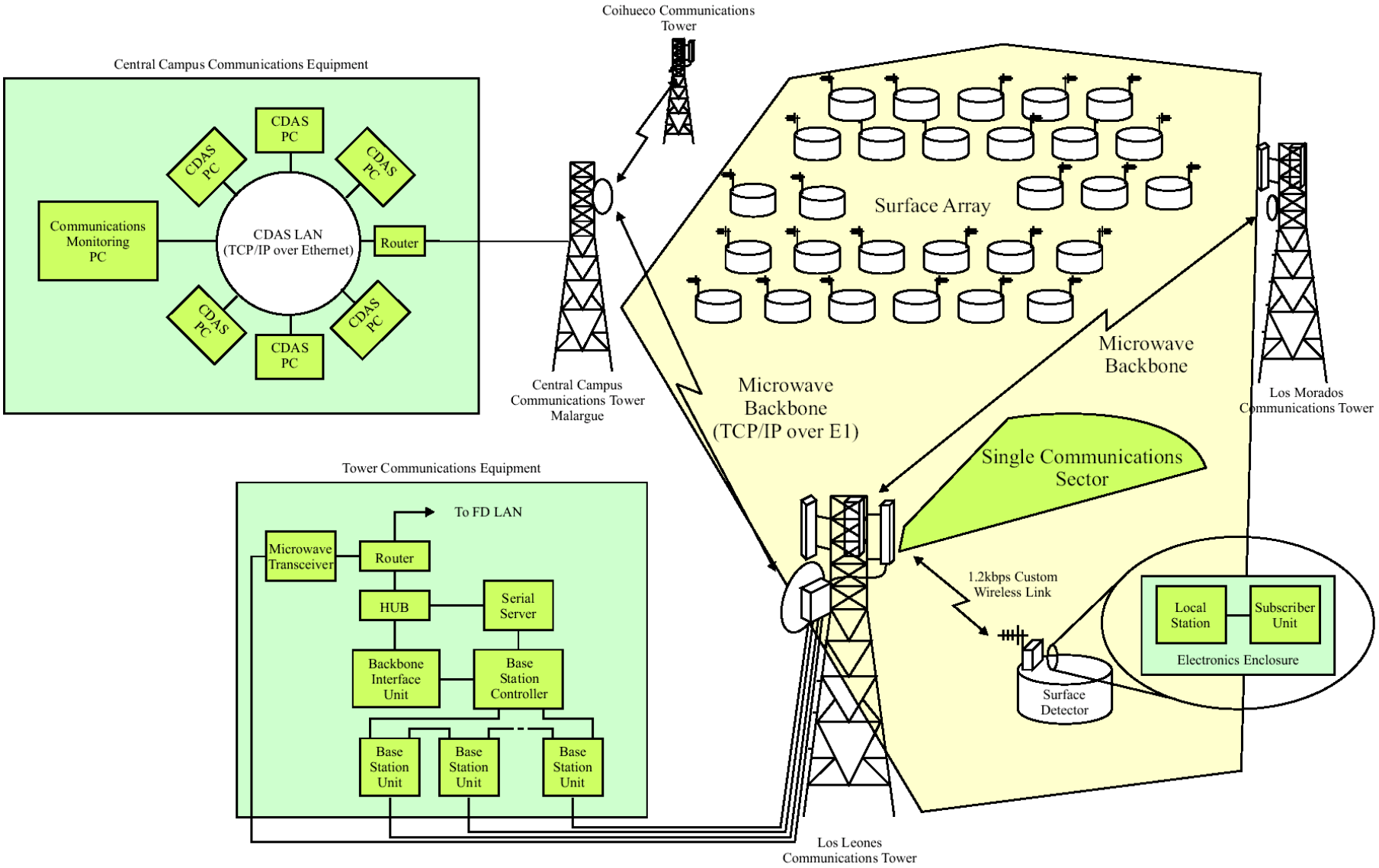

Comparison of characteristics of the Pierre Auger Observatory and the Telescope Array

			Auger	TA
SD	Average latitude		35.3° N	39.4° S
	Average altitude		1,400 m	1,400 m
	Surface area		3,000 km^2	700 km^2
	Lattice		1.5 km hexagon	1.2 km square
	Detector	Type	Cherenkov	Plastic scintillator
		Size	10 $m^2 \times 1.2$ m	$(2\times)$ 3 $m^2 \times 1.2$ cm
		Sampling	25 ns	20 ns
FD	Sites		4	3
	Telescopes	Number	24	36
		Size	13 m^2	6.8 m^2/3 m^2
		Field of view	$28.5° \times 30°$	$16° \times 14°/18° \times 15°$
		Pixels	440	256

Enrique Zas: European Symposium, Kiel 2015

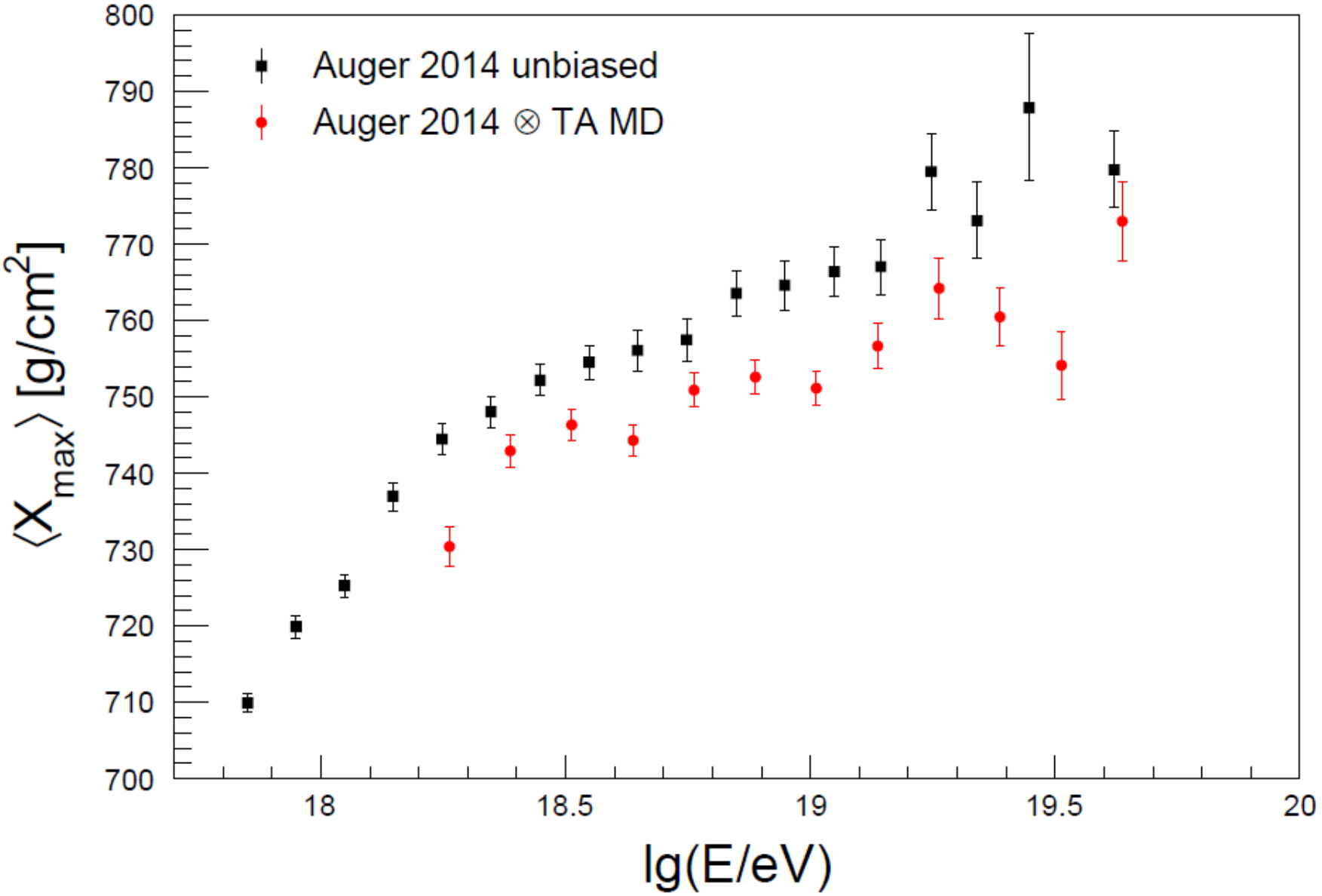
Auger 2014 unbiased
Auger 2014 ⊗ TA MD
⟨X_max⟩ [g/cm²]
lg(E/eV)
800
790
780
770
760
750
740
730
720
710
700
18
18.5
19
19.5
20

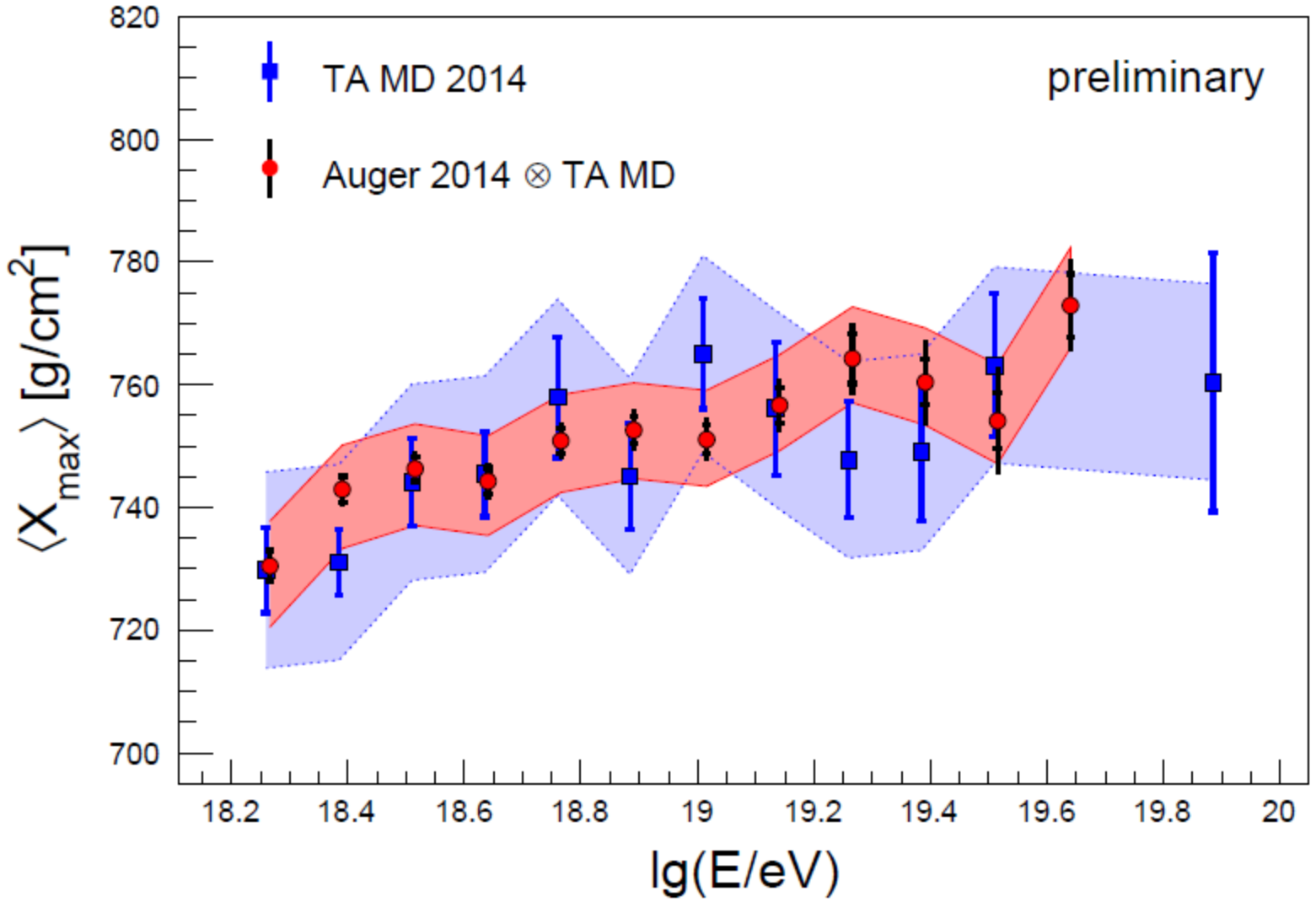
TA MD 2014
Auger 2014 ⊗ TA MD
preliminary
⟨X_max⟩ [g/cm²]
820
800
780
760
740
720
700
18.2
18.4
18.6
18.8
19
19.2
19.4
19.6
19.8
20
lg(E/eV)

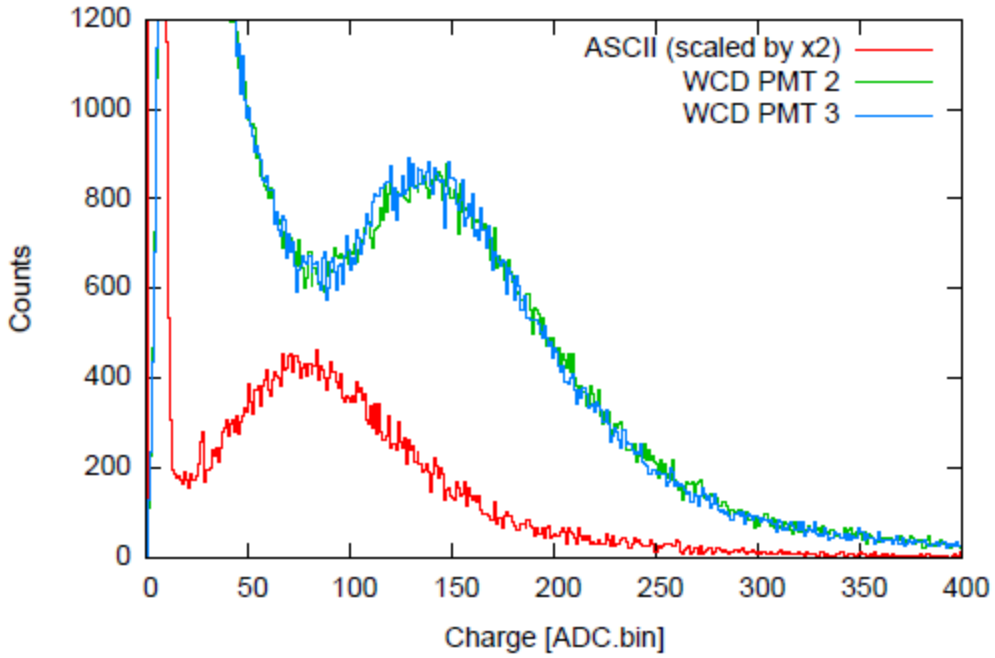

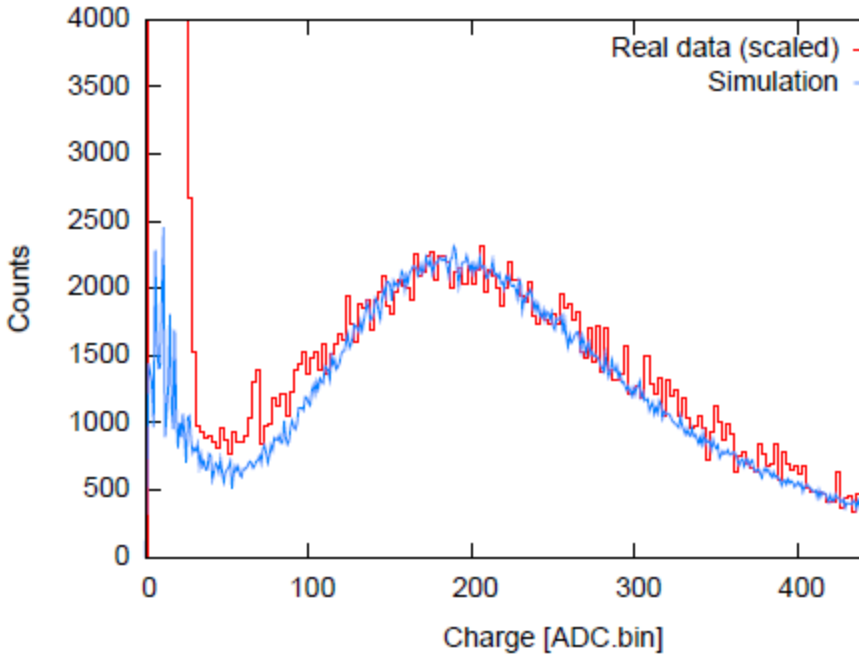

Figure 4.13: MIP histogram of a 2 m^2 prototype running in the pampa, together with VEM cali
histograms of the WCD over which it is installed (left), and comparison to a simplified sim
(right). These histograms correspond to one minute of data taking. Given the clean separatio
MIP from the low energy background, no calibration issue is foreseen.

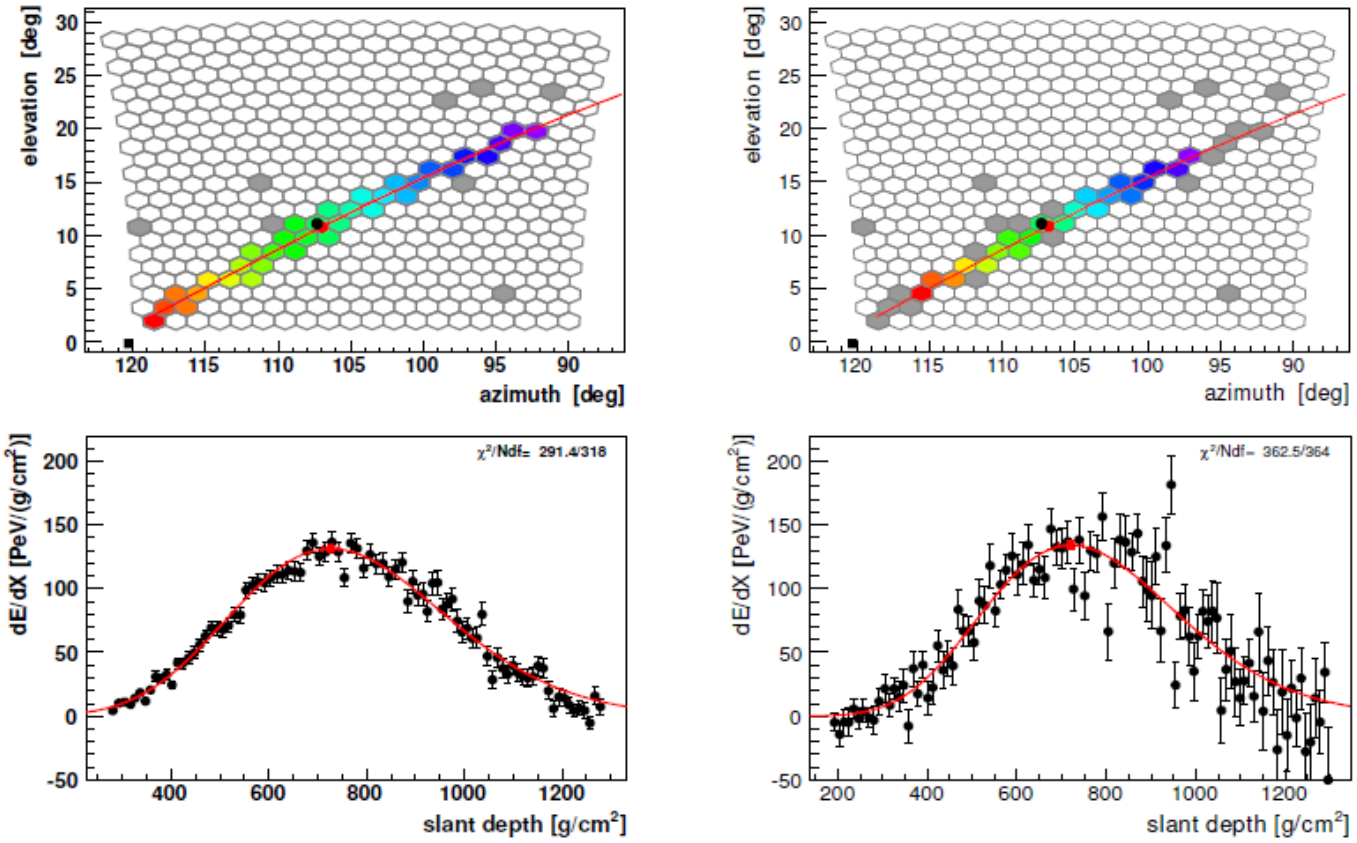

Figure 6.3: A real FD event with reconstructed energy 7×10^{19} eV. In the left panel are measured data (clear sky and no scattered moonlight, a baseline variance of 25 (ADC counts)^2) and in the right panel the same data after adding random noise corresponding to a 40 times higher NSB.

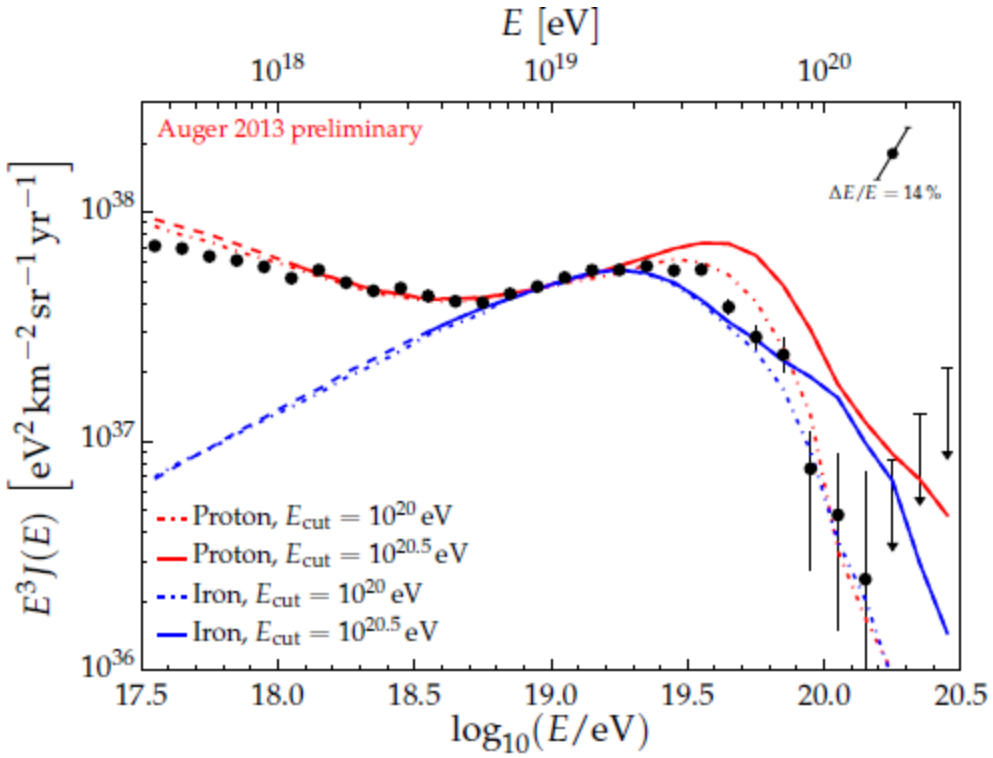
E [eV]
10^18
10^19
10^20
Auger 2013 preliminary
ΔE/E = 14 %
10^38
10^37
10^36
E^3 J(E) [eV^2 km^-2 sr^-1 yr^-1]
Proton, E_cut = 10^20 eV
Proton, E_cut = 10^20.5 eV
Iron, E_cut = 10^20 eV
Iron, E_cut = 10^20.5 eV
17.5
18.0
18.5
19.0
19.5
20.0
20.5
log10(E/eV)